Development of Spherical Ni-Co/MgAlO Bimetallic Catalyst for CO_2 Reforming of CH_4

A Thesis Submitted to the College of Graduate Studies and Research

in Partial Fulfillment of the Requirements for the Degree of

Master of Science

In the Division of Environmental Engineering

University of Saskatchewan

Saskatoon, Saskatchewan, Canada

By

LU TIAN

PERMISSION TO USE

In presenting this thesis in partial fulfillment of the requirements for a Postgraduate degree from the University of Saskatchewan, I agree that the Libraries of the University of Saskatchewan may make it freely available for inspection. I further agree that permission for copying of this thesis in any manner, in whole or in part, for scholarly purpose may be granted by the professor or professors who supervised my thesis work, or, in their absence, by the Graduate Chair of the Division of Environmental Engineering or the Dean of the College of Graduate Studies and Research in which my thesis work was done. It is understood that any copying or publication or use of this thesis or parts thereof for financial gain shall not be allowed without my written permission. It is also understood that due recognition shall be given to me and to the University of Saskatchewan in any scholarly use which may be made of any material in my thesis.

Requests for permission to copy or to make other use of material in this thesis in whole or part should be addressed to:

The Graduate Chair of the Division of Environmental Engineering

University of Saskatchewan

Saskatoon, Saskatchewan

S7N 5C5

ABSTRACT

Carbon dioxide reforming, or drying reforming, of methane can now be used in new applications such as landfill gas utilization where CO_2 and CH_4 need to be converted to a mixture of CO and H_2, called synthesis gas or syn-gas. A novel Ni-Co/$AlMgO_x$ bimetallic powder catalyst was developed in previous research for dry reforming of methane (DRM) process which can eliminate carbon deposition. But it is difficult to apply this loose-powder catalyst in industrial scale.

The procedure of making spherical Ni-Co/$AlMgO_x$ bimetallic catalyst supported on BASF CSS-350 alumina balls (BASF Catalysts LLC) using impregnation method with different impregnation steps and calcination steps is explained in this thesis. For every batch of preparation, the concentration of metal solution was calculated based on different impregnation steps. BET (Brunauer-Emmett-Teller) analysis, compressive strength test, XANES (X-ray Absorption Near-Edge Structure) measurement and ICP-MS (Inductively Coupled Plasma Mass Spectrometry) analysis are conducted to understand the physical and chemical properties of the catalyst. It is found that both impregnation steps and calcination steps have great influence on the performance of the prepared catalyst samples. Among all the catalysts prepared, BF-4-0.25(MgNiCo)-C, which was made by using 4 impregnation-calcination cycles, shows the best activity and stability for 160 h time-on stream (TOS) under the reaction condition of 0.10 g catalyst loading, 750 ^oC, ambient pressure, GHSV=100,000 ml/g_c·h, and $CH_4/CO_2/N_2$ = 1/1/1. The CH_4 conversion started at 66.7% and slowly dropped to 52.8% after 160 hours.

BF-4-0.25(MgNiCo)-C spherical catalyst shows lower reaction rate compared to the loose powder format but shows compatible or higher activity to other two reported catalysts in similar compositions. Most importantly, it is a shaped catalyst ready for industrial use.

Key words

Dry reforming, Spherical catalyst, Alumina ball support, Impregnation, Ni, Co

ACKNOWLEDGEMENTS

I wish to give my sincere gratitude to Dr. Hui Wang, my supervisor, who provides me the precious opportunity to study at the University of Saskatchewan, and always gives me unwavering support, help me improve myself.

I want to thank my advisory committee members, Dr. Aaron Phoenix and Dr. Mehdi Nemati, for their many valuable advices to my study and research, which are very helpful and I really appreciate.

My thanks also go to my fellow students and staff in the Chemical & Biological Engineering department and the Environmental Engineering division: Mohsen Shakouri, Sandeep Badoga, Jiancheng Wang, Armin Moniri and Philip Boahene, Jan Compain, Kelly Bader, Jean Horosko, Richard Blondin, Dragan Cekic, Heli Eunike, Rlee Prokopishyn, for their patient help during my research.

I am especially grateful to my parents, Mr. Hong Tian and Mrs. Jiang Yu who has given me unquestioning trust and support. Without them, I would have never been to where I am now.

TABLE OF CONTENTS

LIST OF TABLES

LIST OF FIGURES

ABBREVIATIONS

BET: An analysis technique for the measurement of the specific surface area and porous structure of a solid material based on Brunauer-Emmett-Teller theory

DRM: Dry Reforming of Methane

GHGs: Greenhouse gases

IPCC: Intergovernmental Panel on Climate Change

ICP-MS: Inductively-coupled plasma mass spectrometry

LOI: Loss on ignition

MFC: Mass flow controller

NEXAFS: Near-edge X-ray absorption fine structure

RWGS: Reverse water-gas shift reaction

SA: Surface area (m^2/g)

SMSI: Strong metal-support interaction

SRC: Saskatchewan Research Council

TCD: Thermal conductivity detector

TEM: Transmission electron microscopy

XANES: X-ray absorption near-edge Structure

XPS: X-ray photoelectron spectroscopy

XRD: X-ray diffraction

NOMENCLATURE

$\mathring{A}$: Angstrom (10^{-10} m)

ΔH^0 : Reaction enthalpy (kJ/mol)

F_I : Inlet flow rate of respective reactant (mL/min)

F_O : Outlet flow rate of respective reactant (mL/min)

$F_{CH_4,I}$: Inlet flow rate of CH_4 (mL/min)

$F_{CH_4,O}$: Outlet flow rate of CH_4 (mL/min)

$F_{CO,I}$: Inlet flow rate of CO (mL/min)

$F_{CO,O}$: Outlet flow rate of CO (mL/min)

$F_{CO_2,I}$: Inlet flow rate of CO_2 (mL/min)

$F_{CO_2,O}$: Outlet flow rate of CO_2 (mL/min)

$F_{H_2,O}$: Outlet flow rate of H_2 (mL/min)

S_{H_2} : Selectivity of H_2

S_{CO} : Selectivity of CO

$-r_{CH_4}$: Reaction rate of CH_4 (mmol/g_{cat}/s).

W_{Cat} : The weight of catalyst (g_{cat})

CHAPTER 1 INTRODUCTION

1.1 Background of the Project

Climate change is one of the greatest or the most challenging environmental threats the world is facing in this century. Human activities have influenced the chemical composition of the atmosphere through the emissions of significant quantities of greenhouse gases (GHGs); and increasing concentrations of GHGs are likely to accelerate the rate of climate change. The average surface temperature of the earth has already increased by about 0.6 ^{o}C during the 20th century. Evidence shows that most of the global warming which has occurred over the last 50 years is attributable to human activities (UNEP and UN Framework Convention on Climate Change, 2001). The Intergovernmental Panel on Climate Change (IPCC) in its Third Assessment Report (published in 2001) mentioned that the global average surface temperatures will rise by about 1.4 to 5.8 ^{o}C by the year 2100. This change would be larger than any climate change experienced over the last 10,000 years (IPCC, 2001; Climate Change, 2001).

Carbon dioxide (CO_2) has been regarded as the most significant greenhouse gas coming from anthropological activities. Due to a great quantity of fossil fuels consumed worldwide in the past century, there is a dramatic increase of CO_2 concentration in the atmosphere (Dyrssen and Turner, 1994). Although the precise correlations are uncertain, there are several different indicators showing that greenhouse gas emissions are causing global climate problems. They include the

increase of mean global temperature rise with atmospheric methane (CH_4) and CO_2 concentrations and increasing volatility of global weather patterns (Hileman, 1997).

As a result, there has been increased research interest of CH_4 and CO_2 disposal, removal, utilization to minimize the influence of these gases to the atmosphere. The study of the reaction between CO_2 and CH_4 to produce synthesis gas, which can be used in chemical energy transmission systems (Chubb, 1980; McCrary *et al*., 1982; Fish and Hawn, 1987) or utilized in the Fischer-Tropsch reaction to produce liquid hydrocarbons (Ross *et al*., 1996) has already attracted much attention in the last few decades. CH_4 reforming with CO_2, rather than H_2O, is attractive because it can convert two major undesirable greenhouse gases into valuable chemicals. A principal advantage of syn-gas production from CO_2 reforming is the low H_2/CO ratio obtained, which is suitable for further syntheses of valuable hydrocarbons (Hu and Ruckemstein, 2004; Ross, 2005) and it is an ideal feedstock for the Fischer-Tropsch synthesis of long-chain hydrocarbons (Gadalla and Bower, 1988).

Although DRM has shown great advantages in both economic and environmental aspects, there are problems to be solved before this process can be industrialized. The major problem is that there has not been a catalyst which can be used in an industrial scale so far.

DRM is a strong endothermic reaction and very high temperature needs to be provided to obtain an acceptable conversion. A catalyst is essential for this reaction, because with its existence, the

reaction rate can be economically justifiable (Sun, 2005). The catalysts used in a DRM process can be all type VIII transition metals except Os. Noble metals and the non-noble metal Ni have been studied extensively for this reaction (Ertl *et al.,* 2008). It has been found that supported Rh, Ru, Pd, Pt, and Ir catalysts can provide stable operations for carbon dioxide reforming of methane with low carbon formation or deposition on the catalysts during the reaction (Bradford and Vannice, 1999). However, it is more realistic to develop non-noble metal-based catalysts to reduce the cost from an industrial standpoint.

Due to its low cost and availability, Ni has drawn significant research attention (Rostrup-Nielsen, 1997). The problem for Ni catalysts is that they suffer severe catalyst deactivation due to sintering, metal oxidation (Slagtern *et al*., 1997), and especially significant coke formation (Bradford and Vannice, 1999; Rostrup-Nielsen, 1997; Ashcroft *et al*., 1991).

In last decade, lots of nickel-based catalysts have been reported. Among them, the Ni-Co/Al_2O_3-MgO bimetallic catalyst developed in Dr. H. Wang's group at University of Saskatchewan has shown stable and high active performance (Zhang *et al.*, 2007). The catalyst in loose-powder form prepared by co-precipitation maintained excellent stability with no significant deactivation in a 2000 h TOS test for the dry reforming reaction. However, it is unrealistic to use loose-powder catalyst at an industrial scale. Precipitated catalysts and supports for impregnation need to be formed into suitably sized particles for use in the reactor (Chorkendorff *et al*., 2007). The particle size of the loose-powder is in the range of micrometer to millimeter. Operations in

packed-bed or fluidized-bed reactors of catalysts in this size would result in difficulties such as tremendous pressure drop or entrainment. Hence, catalysts need to be shaped in larger bodies of sufficient mechanical strength to allow convenient handling and proper operation.

1.2 Scope and Outline of the Work

To find a procedure to make shaped Ni-Co/MgAlO bimetallic catalyst for CO_2 reforming of CH_4 using the formula developed by Zhang *et al.*(2007), the target is that the shaped catalyst can maintain good catalytic performance as the loose-powder catalyst does but can have mechanical strength to be used in industrial scale. The hypothesis for this project is that the solution of Ni, Co, and Mg may form a layer on the alumina ball surface through proper procedures of impregnation and solid reaction in calcinations and the layer is of similar compositions and properties to the powder catalyst. The work of this project comprises of two major parts: development of the preparation procedure of the shaped catalyst, and evaluation of the shaped catalyst with DRM process. In the catalyst preparation part, the factors which influence the surface area and pore structures are to be optimized. The results will provide reference for future preparation of shaped Ni-Co/Al_2O_3-MgO bimetallic catalyst. Instrumental characterizations which could help understand the correlations between influential factors and catalytic performance will be conducted. In the catalyst evaluation part, the factors which influence the performance of catalysts will be evaluated. Based on the experimental results, in order to improve the performance of catalyst, some modifications to the catalyst preparation will be

conducted.

1.3 Thesis Organization

This thesis consists of 5 chapters, including the literature review, experimental procedures, results and discussion, conclusions and recommendations. Following this chapter, chapter 2 discusses the fundamentals of different types of shaped catalysts, the method of catalyst preparation, reasoning out the objectives of this research. Chapter 3 explains the experimental procedures and instrumental analysis used in this research, including equipment, chemicals and other materials. Chapter 4 presents the experimental results, gives the respective discussion and leads to conclusions. Chapter 5 briefs the research conclusions drawn from Chapter 4, and also provides recommendations for the future research.

CHAPTER 2 LITERATURE REVIEW

2.1 Reaction Chemistry

The equilibrium of DRM reaction (ΔH^0 is the enthalpy of reaction) (Sun *et al*., 2005),

$CH_4 + CO_2 \rightarrow 2H_2 + 2CO$ (ΔH^0=247.3 kJ/mol) (2.1)

is influenced by the reverse water-gas shift (RWGS) reaction that is co-occurring

$CO_2 + H_2 \rightarrow CO + H_2O$ (ΔH^0=41.17 kJ/mol) (2.2)

Due to the RWGS reaction, H_2/CO ratio is less than unity and the conversion of CO_2 is always greater than that of CH_4.

In addition to the DRM and RWGS reactions, there are two more side reactions which occur simultaneously.

The CH_4 decomposition

$CH_4 \rightarrow C(s) + 2H_2$ (ΔH^0=74.85 kJ/mol) (2.3)

and CO disproportionation

$2CO \rightarrow CO_2 + C(s)$ (ΔH^0= -173.46 kJ/mol) (2.4)

These two reactions are directly responsible for the carbon deposition on the catalyst. If the reaction temperature range is from 800~900 K, the reaction is more preferential to carbon depositions than to DRM (Zhang *et al*., 2007). Therefore, a catalyst which can inhibit the carbon formation and improve the DRM reaction rate appears to be necessary.

2.2 Catalyst Preparation Methods

Most catalysts are either a finely dispersed metal on a support such as alumina or silica, or a compound on a support or unsupported. There are two types of processes commonly used for making catalysts, generally termed the precipitation method and the impregnation method.

2.2.1 *Precipitation Method*

In a common procedure, an aqueous metal salt solution is contacted with an aqueous alkali, ammonium hydroxide or ammonium carbonate, to cause the precipitation of an insoluble metal hydroxide or carbonate, followed by filtration, washing, drying, and calcination.

2.2.2 *Impregnation Method*

Impregnation is an easier method of making a catalyst compared with co-precipitation method since it requires less equipment: the filtering and forming steps are eliminated and washing may not be needed. A support, usually porous solid, is contacted with a solution, usually aqueous, of one or more suitable metallic compounds. The size and shape of the catalyst particles are the same as the support. The impregnated support is then dried and calcined to form the catalyst. Fig. 2.1 shows the procedure of impregnation method.

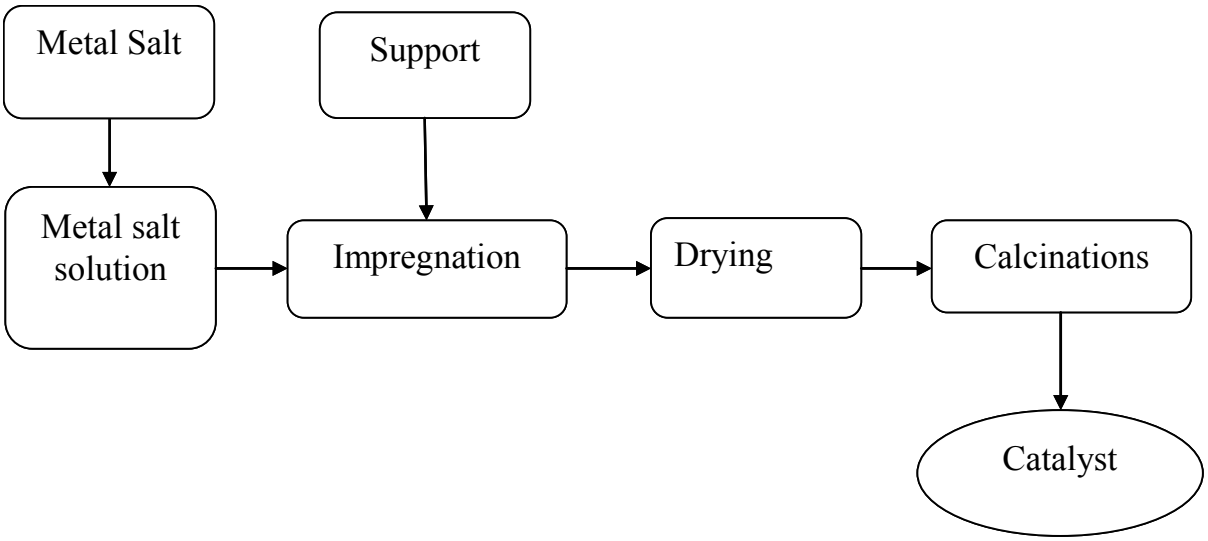

Figure 2.1 Procedure of impregnation catalyst preparation method.

2.3 Ni-Co/AlMgO loose powder catalyst prepared by co-precipitation method

Zhang *et al*. (2007) reported that Ni-Co/Al_2O_3-MgO bimetallic catalysts gave stable and highly active performances. Ni-Co/Al_2O_3-MgO bimetallic loose-powder catalyst is prepared by co-precipitation. It showed excellent stability with no significant deactivation in long-term activity test for the dry reforming reaction. There are several reasons that lead to the good performance of this bimetallic loose-powder catalyst. The co-precipitation preparation method as well as high-temperature calcination converted the catalyst into stable $Ni_xMg_{1-x}Al_2O_4$ and $Co_xMg_{1-x}Al_2O_4$ spinal-like framework structures due to strong metal-support interactions (SMSI). This method also resulted in small metal particle sizes after the precipitate was reduced. The formation of Ni-Co alloy during the catalyst reduction effectively suppressed the carbon formation in comparison with that on Ni sites alone.

As the experiments showed, these Ni-Co/AlMgO loose-powder bimetallic catalysts can provide not only very good carbon resistance in a 2000 h stability test, but also high activity.

Zhang *et al*. (2007) also pointed out that high reaction temperatures (*i.e*., 750 ^oC and above) are more favorable to increasing the equilibrium conversion of the target reaction (Eq. (2.1)) than that of the side reactions.

2.4 Shaped Catalysts

Industrial reactors require shaped catalyst to minimize pressure drops and plugging. Powders can leach into product streams (Ertl *et al*., 2008). Consequently, catalytic materials are shaped before using in a reactor.

Shaping is considered another unit operation proper to the field of ceramics engineering (Richerson, 1992). There are two major methods which are widely used: one is to introduce shaping agents in the powder catalyst to form shaped catalyst, the other is to impregnate powder catalyst components on a structured support.

Shaping agents comprise several substances classified as binders, lubricants, plasticizers, and compaction agents (Richerson, 1992). These substances can be either organic or inorganic in nature. Among them, the most commonly used are organic and inorganic acids (e.g. stearic acid, oleic acid, naphthenic acid, boric acid), oils, paraffins, stearates, polymers, clays, and graphite (Richerson, 1992). Inorganic agents cannot be removed from the formed catalytic material once they have been added (Richerson, 1992). In catalysis science, studies involving shaping are often aiming at obtaining a good recipe whereby the added shaping agents have no marked negative impact on the performance of the formed catalysts and can provide the mechanical resistance of the formed bodies. Previous research on this subject has been mostly conducted on zeolite-based catalysts because of their wide industrial utilization (Choudhary *et al*., 1997; Boix *et al*., 2004). It

has been shown, for example, that the impact of clay binders on the acid properties of zeolite powders can alter their catalytic activity and selectivity (Choudhary *et al*., 1997; Dorado *et al*., 2001; Jasra *et al*., 2003). Other studies (Avila *et al*., 1993; Zakeri *et al*., 2010) have analyzed the effect of binders on the properties of mixed oxides and supported metallic catalysts. Avila *et al*. (1993) determined that binders such as phosphoric acid and sepiolite can act on the catalytic and physicochemical properties of TiO_2-supported V_2O_5 in different manners because they bind the catalyst particles by different mechanisms. Zakeri *et al*. (2010) analyzed the effects of using colloidal silica and ethyl silicate for shaping Co-Mn/TiO_2 catalysts for the Fischer-Tropsch reaction. Both substances were reported modify the selectivity of the catalysts after shaping. The cited works (Choudhary *et al*., 1997; Zakeri *et al*., 2010) thus evidence that, apart from improving the mechanical resistance of the catalysts, the addition of shaping agents to catalytic powders can modify their functionalities.

On the other hand, structured support can provide uniform size, physical integrity, smooth surface, controlled surface chemistry and controlled pore structure (BASF., 2012). Hunter *et al*. (1959) claimed a patent of the method for manufacture catalyst of cobalt molybdate type supported on a support, such as alumina. This invention particularly resides in a satisfactory manner for simply and effectively impregnating catalyst supports with cobalt molybdate to attain desirable and active catalysts. Burmeister *et al*. (1966) reported an invention relates to a process and apparatus for uniform and reproducible impregnation of fixed bed catalyst supports in the form of loose particles with a desired shell volume, by applying atomized impregnating solutions

of precursors of the catalytically active components onto the catalyst supports, which are in the form of extruded strands, granulates, or pellets, that are circulated in a tank.

There are different formats which can be used in catalyst manufacture to make shaped particles from loose powder. Two types of catalyst shape which are most commonly used in industry will be introduced.

2.4.1 *Pellets*

A common form of catalyst is pellet, produced either by extrusion or by tableting (pelletizing). Pellets are used when a high mechanical strength is required.

It is produced by compressing of the supported power and several binders and lubricants in a press. Extrusion produces low-density high-porosity pellets containing many macropores. Extruded pellets below 1 mm diameter are obtainable from pastes of fine powders or gels, by using either ring-roll or auger-type extruders. In the ring-roll method, the mix is fed to a rotating cylinder drilled with numerous holes of a given size. Instead the cylinder one or more compression rolls press the mix and a rotating knife cuts off the extrudate to form pellets.

However, it has been shown that mixed oxides and oxide-supported metal catalysts are typical materials with a brittle failure mode and that their mechanical failure is due to brittle fracture (Li

et al., 1989; Li *et al*.,1999; Li *et al*., 2000). The pellets experience very little plastic deformation and a small elastic deformation before the fracture happens.

2.4.2 *Supported Catalyst*

Supported catalysts are used for a wide variety of reactions, and are the most frequently used types of catalysts. The porous support, typically alumina or silica, which is designed to disperse the active component (Ni, Pt, Pd, Co, etc.) also provides thermal and mechanical stability, and reduces the amount of the (often expensive) active component (Ertl *et al*., 1999). The preparation of supported catalysts generally involves three steps: (1) deposition (precipitation and/or adsorption) of the active agent, called the precursor, on the porous support, (2) removal of the liquid solvent, i.e., drying, and (3) transformation of the precursor into its desired form by calcination (Lee & Aris,1985; Komiyama,1985). Frequently, pretreatment in the reactor is required to obtain the active form of the catalyst, e.g., reduction by H_2 or CO. Deposition of the active component (metal) is typically done by impregnation, often involving aqueous solutions (Lee & Aris, 1985; Ertl *et al*., 1999). If the support surface is hydrophobic or if hydrolysis of the support must be avoided, a non-aqueous solution is used (Lee & Aris, 1985). During the impregnation step, the support is immersed in a solution of the inert precursor. In the case of capillary impregnation, the support is initially dry, while during impregnation the support is initially filled with the liquid solvent (Neimark, Kheifez, & Fenelonov, 1981; Komiyama, 1985; Lee & Aris, 1985; Gavriilidis, Varma, & Morbidelli, 1993; Ertl *et al*., 1999).

The utilization of supported catalysts in the chemical industry has been considered for years. Conventional fixed-bed reactors have some obvious disadvantages such as maldistributions of various kinds (including a non-uniform access of reactants to the catalytic surface), high pressure drop in the bed, etc. Structured catalysts are promising as far as elimination of these drawbacks is concerned.

Flytzani-Stephanopoulos and Voecks (1980) investigated steam reforming of n-hexane in Ni catalysts supported by cordierite and Kanthal supports washcoated with γ-alumina. Results have shown that the ceramic support was not stable when used throughout the entire bed. A rapid disintegration of the solid was observed at conditions common in steam reformers. This instability was probably caused by damaging of the washcoat and by subsequent extraction of the support silica by steam.

Nickel on ceramic or, mostly, metallic supports washcoated with alumina was subjected to study by Jarvi *et al.* (1980) and Sughrue *et al*. (1982). The activity of monolithic catalysts measured at a low conversion range was found to be 2 to 5 times than that of spherical or extruded catalysts. It has been provided that diffusion resistance in monolithic catalysts was less than in pellets. At high conversions and high space velocities, the monolithic catalyst showed a 20-100% higher an activity which was attributed to the low pore mass transfer resistance.

Boersma *et al*. (1978; 1980) studied ethane combustion in the presence of a platinum catalyst.

They compared the performance of empty and packed tubular wall reactors for undeveloped, developing, and fully developed flow. A good agreement between theoretically calculated and measured profiles was found.

Generally, supported catalysts provide low pressure drop, large geometrical surface area, good mechanical properties and thermal stability.

2.5 Knowledge Gap

In 2010, a patent was awarded to the technology of making the loose-powder Ni-Co/AlMgO bimetallic catalyst which was developed in our previous research. How to make the loose-powder into a shaped catalyst still remains unknown. However, this technology is needed when commercializing the catalytic CO_2 reforming of CH_4.

2.6 Catalyst Design Idea

As discussed, it is important to have a shaped catalyst to be utilized in the commercial scale because it can last longer as well as maintain a more stable structure than the loose-powder catalyst.

Commercial alumina ball is a common material used as support for catalysts. Its mechanical

strength is designed and tested for the use in commercial scales. Because Al is a component in the Ni-Co/Al_2O_3-MgO loose-powder catalyst, so the alumina support itself may not bring uncertainty to the shaped catalyst. loading the other three metals, Ni, Co, Mg, onto the surface of alumina balls by impregnating followed by calcination, it is hoped that a layer be formed that has the same structure and properties as the loose-powder catalyst does.

2.7 Objectives of the Work

This thesis work is to prepare a shaped Ni-Co/MgAlO bimetallic catalyst for CO_2 reforming of CH_4 using impregnation method with commercially available alumina support in the form of spherical balls. Thus, a commercial product, BASF-CSS-350 alumina ball (BASF Catalysts LLC), was selected to be the support. The main component of this spherical support is Al_2O_3, which is, as mentioned before, the major support component of the loose-powder catalyst. The assumption is that with a target metal loading, which is calculated based on the metal content of powder catalyst, the metal solution will form a thin layer on the surface of support which has the same catalytic properties as the loose-powder. In addition, the catalyst will have good mechanical strength.

The research work is planned as follow: to impregnate the metal solution on the spherical support, and investigate the influence of impregnation steps and calcination steps on the catalyst performance and properties; to use instrumental analysis such as ICP, BET, XANES to

characterize both surface and bulk properties; and to find the optimal catalyst preparation condition by evaluate the catalyst performance.

CHAPTER 3 EXPERIMENTAL DESCRIPTIONS

3.1 Catalyst Preparation

The spherical bimetallic Ni-Co/$AlMgO_x$ catalysts were prepared by impregnation method, using nickel nitrate (98% purity; Alfa), cobalt nitrate (99% purity; Alfa), magnesium nitrate (>98%, EMD, Gibbstown, NJ), and aluminum nitrate (>98%, EMD, Gibbstown, NJ) to prepare the solution and then impregnating it on the BASF-CSS-350 alumina balls (BASF Catalysts LLC). X means the chemical valence state of the metal oxides. Alumina is one of a frequently used support material which has high melting and decomposition temperatures (Marjolein *et al*., 2001). With this support, other important physical features like specific surface area, pore size distribution, pore volume and mechanical strength can be established. Table 3.1 shows the chemical composition (wt %) and physical properties of BASF-CSS-350 alumina balls. The major component of BASF-CSS-350 is aluminum oxides, which is an ideal candidate for support because it will not introduce new material to the catalyst to be made and bring uncertainty to the catalyst performance.

For every batch of preparation, the concentration of metal solution was calculated based on different impregnation steps. Ten different catalyst samples were prepared, of which the target metal loading (the metal load defined as weight percent of elemental metal in the catalyst) varied from Mg 1.3 ~ 5.3 wt%, Ni 0.6 ~ 2.4 wt%, Co 0.6 ~ 2.4 wt%.

Table 3.1 Chemical composition (wt %) and physical properties of BASF-CSS350 alumina balls*.

Chemical composition	wt %	Physical properties	
Al_2O_3**	99.6	Surface area, m^2/g	350
SiO_2	0.02	Pore volume, mL/g	0.55
Na_2O	0.35	Abrasion loss, wt %	0.1
LOI (Loss on ignition 2250-1000^o)	5.0	Bulk density, lbs/ft^3	46
		Attrition, wt %	1.0
		Macroporosity, mL/g	0.10

* Chemical composition (wt %) and physical properties of BASF-CSS350 alumina balls are all based on the document provided by BASF, and the units are followed by this document.

** Calcined basis (BASF Catalysts LLC).

The catalyst preparation procedure is described below. Required amounts of $Ni(NO_3)_2 \cdot 6H_2O$, $Co(NO_3)_2 \cdot 6H_2O$ and $Mg(NO_3)_2 \cdot 6H_2O$ were dissolved in certain volume of water (Development procedure and the recipe of each catalyst are shown in Appendix A). After stirring, followed by equal volume impregnation step (titration volume is the same as the amount alumina balls can uptake): titrate the metal solution on the spherical support evenly, then dried in the air for 4 hours, and dried in the oven at 120 ^{o}C over night. This procedure may be repeated until the calculated amount of metal compound taken up by the support material corresponds to the desired metal content of the catalyst. The metal content of the catalyst can then be controlled in a simple fashion via the amount of the liquid taken up and the metal concentration of the solution.

For some catalysts, the impregnation procedure was repeated for 1~3 times then the whole procedure was finished by calcination step, while for other catalysts, each impregnation procedure was followed by one calcination step. The condition of calcination step is 800 ^{o}C for 6 hours without inert gas protection. Multiple impregnation steps and calcination steps were applied to different prepared samples (See details in Appendix A).

The prepared catalysts were designated as BF-x-y (aMgbNicCo). BF stands for the manufacturer of the alumina support, BASF Catalysts LLC. x means the number of impregnation steps conducted, and y represents the proportion of metal loading in single impregnation step of the total target metal loading. When there is a -C in the end of the name, it means that after each impregnation step, the samples were dried overnight at 120 ^{o}C and subsequently calcined in air at

800 ^{o}C for 4 h. Otherwise, there was only one calcination step followed by the last impregnation step. Table 3.2 shows the name and preparation information for each catalyst.

BF-1-MgNiCo was developed first, The target loading weight percentage of the active metal (Ni, Co) was exactly the same as the loose-powder catalyst (3.9% for each of Ni and Co). All the metals were loaded onto the alumina balls in one impregnation step. (This amount of Ni, Co, Mg metal loading in BF-1-MgNiCo were regarded as reference to other catalyst samples. The number that y represents is that portion of this amount.)

BF-1-MgNiCo-Buffer was developed because it was believed the pH of the metal solution used in co-precipitation has strong effect on catalyst properties. When making the loose powder catalyst in precipitation pH was controlled between 8.5~8.7, the pH of the metal solution in making BF-1-MgNiCo was around 3.8. By adding the buffer, it was hoped that the resultant catalyst has closer properties with the loose-powder catalyst. It can also provide the information of how pH affects the performance of catalyst.

BF-Mg-MgNiCo and BF-2-(Mg0.5Ni0.5Co) were designed due to the mole ratio of Mg to Al is much larger in loose powder catalyst than that in BF-1-MgNiCo. Thus, Mg content was doubled in hope that the composition of the surface layer of this shaped catalyst be as close as

Table 3.2 Preparation procedures of the catalyst samples.

Catalyst	Impregnation step	Calcination step
BF-1-MgNiCo	1	1
BF-1-MgNiCo-Buffer	1	1
BF-2-Mg-MgNiCo	2	1
BF-2-(Mg0.5Ni0.5Co)	2	1
BF-2-0.5 (MgNiCo)	2	1
BF-4-0.25(MgNiCo)	4	1
BF-1-0.25(MgNiCo)-C	1	1
BF-2-0.25(MgNiCo)-C	2	2
BF-3-0.25(MgNiCo)-C	3	3
BF-4-0.25(MgNiCo)-C	4	4

possible to that of the loose-powder catalyst. The only difference between BF-Mg-MgNiCo and BF-2-(Mg0.5Ni0.5Co) is that for BF-Mg-MgNiCo only Mg was loaded on the support in the first impregnation step. For the second impregnation, Mg, Ni and Co were loaded at the same time. For BF-2-(Mg0.5Ni0.5Co), two impregnation steps were conducted with the same concentration of the metal solution, also aiming at the doubled Mg content in the catalyst.

Inspired by the procedure to make the catalyst samples BF-Mg-MgNiCo and BF-2-(Mg0.5Ni0.5Co), catalysts BF-2-0.5(MgNiCo) and BF-4-0.25(MgNiCo), for which the total impregnation steps are 2 and 4, respectively, were designed to investigate the influence of impregnation steps on the performance of catalyst.

To determine how calcination steps will affect the performance of catalyst, BF-4-0.25(MgNiCo)-C was developed to be compared with BF-4-0.25(MgNiCo). The former catalyst was made by conducting the impregnation-calcination step for 4 separate times, each step targeting to load one quarter of final the metal (Ni, Co, and Mg) content.

During the process of making BF-4-0.25(MgNiCo)-C, BF-1-0.25(MgNiCo)-C, BF-2-0.25(MgNiCo)-C, BF-3-0.25(MgNiCo)-C were also developed. These samples are used for determining the influence of metal content to the catalytic performance.

3.2 Catalyst Characterization Techniques

In order to understand the changes in chemical and physical properties and material structures of the catalysts during the preparation and reaction, the following instrumental analyses were applied.

3.2.1 *ICP-MS Analysis*

ICP-MS analysis was conducted to determine if the metal was successfully loaded on the support by comparing the actual metal content (Ni, Co, Mg) to the target metal content.

The analysis was done by Geoanalytical Laboratories, SRC (Saskatchewan Research Council) using an Inductively Coupled Plasma Mass (ICP-MS) system which provides high-precision, in situ trace element analysis. Inductively coupled plasma mass spectrometry (ICP-MS) is a type of mass spectrometry which is capable of detecting metals and several non-metals at concentrations as low as one part in 10^{12} (part per trillion). This is achieved by ionizing the sample with inductively coupled plasma and then using a mass spectrometer to separate and quantify those ions.

3.2.2 *BET Analysis*

The BET surface area (SA) and pore distribution were measured to see how different processes influence the structure of prepared catalysts.

It was measured by N_2 adsorption at the temperature of 77 K using Micromeritics ASAP 2000 (Micrometrics, USA). Around 0.2 g catalyst was used for each analysis. The degassing temperature was 473 K to remove the moisture and other absorbed gases from the catalyst surface. The sample tube was evacuated to 20μm Hg during the analysis.

3.2.3 *Compressive Strength Test*

Compressive strength of the catalysts was tested to confirm if the compressive strength would change significantly after the Ni, Co, and Mg have been loaded by comparing with that of the alumina virgin balls (BASF CSS-350). It was measured with Instron 5566 electro-mechanical test system to evaluate the compressive strength of the alumina balls and the catalysts. Fig. 3.1 shows the Instron 5566 electro-mechanical test system. Each alumina ball specimen was positioned at the center of the lower compression platen such that the long axis of the specimen was aligned with the load string. A smaller diameter platen at the crosshead allowed for easier specimen centering and viewing of the specimen during the test. A total of ten specimens were tested and compressive load values were recorded.

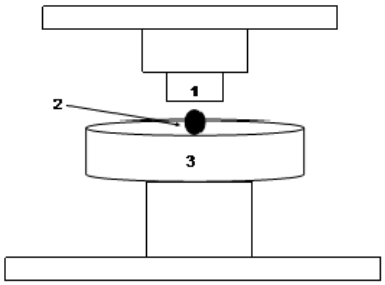

Figure 3.1 Schematic diagram of Instron 5566 electro mechanical test system: 1 - diameter platen; 2 – catalyst sample specimen; 3 - lower compression platen.

3.3 X-ray Absorption Near Edge Structure Analysis

X-ray Absorption Near-Edge Structure (XANES) is measured to see the reduction extent of all the catalyst samples since NiO and CoO are not active sites for the DRM process. To have catalytic activity, the catalyst used for this reaction has to be reduced in H_2 atmosphere before reaction such that the NiO and CoO will be partially reduced to Ni and Co. XANES can provide information about the reduction extend in both qualitative and quantitative aspects.

XANES, also known as Near edge X-ray absorption fine structure (NEXAFS), is a type of absorption spectroscopy. XANES data indicate the absorption peaks due to the photoabsorption cross section in the X-ray Absorption Spectra (XAS) observed in the energy region. Synchrotron XANES for the catalyst samples were conducted in the CLS (Canadian Light Source). A medium energy, bending magnet based beamline, Soft X-ray Microcharacterization Beamline, was used for XANES analysis for Ni and Co. The followings are the operation conditions: energy range 1.7-10 keV, wavelength 7.3 - 1.3 Å, resolution Δ E / E @ E 3.3 × 10-4 Insb (111), 1 × 10-4 Si (111). Flux (γ /s/0.1%BW) @ 100 mA >1 × 1011, spot size (Horizontal × Vertical) 300 μm × 300 μm. The samples were prepared in a reactor using sample shooter. The shooter was placed in the center of a quartz tube reactor and a thermocouple was placed above the sample disc. Reduction was conducted for 4 hours in 5% H_2/N_2. A catalyst sample was scanned twice, each before and after reduction.

3.4 Catalyst Evaluation

3.4.1 *Reactor System*

The schematic diagram of the reactor system is shown in Fig. 3.2. The feed gases are supplied from cylinders and the flow rate of each gas is controlled by a mass flow controller (MFC) (Brooks Instrument Inc., USA). The feedstock is mixed in a mixer before entering the reactor. Mixer and furnace are enclosed in a bench top reactor system (BTSR-jr, Autoclave Engineers, USA). The temperature of the pre-heater is controlled by a temperature controller (2416, EURITHERM, USA) which has 8 segments. The temperature of the catalyst bed is read out by an indicator (2132, EURITHERM, USA). A quartz tube with an inner diameter of 6 mm, external diameter of 9.5 mm and length of 255 mm (Autoclave Engineers, USA) is used as the reactor. Both ends of the tube were connected with the inlet and outlet tubes, respectively, using Swageloc fittings and graphite ferrules (Autoclave Engineers, USA). A 6890 N gas chromatograph (GC) (Agilent Technologies, USA).

3.4.2 *Reaction Condition*

0.10 g powder catalyst, from grinding, diluted with 0.20 g quartz sand was packed in the reactor for each run. The catalyst bed with a length of about 1.0 cm was supported by quartz wool. The position of catalyst bed was fixed for each run to ensure it was located in the isothermal section.

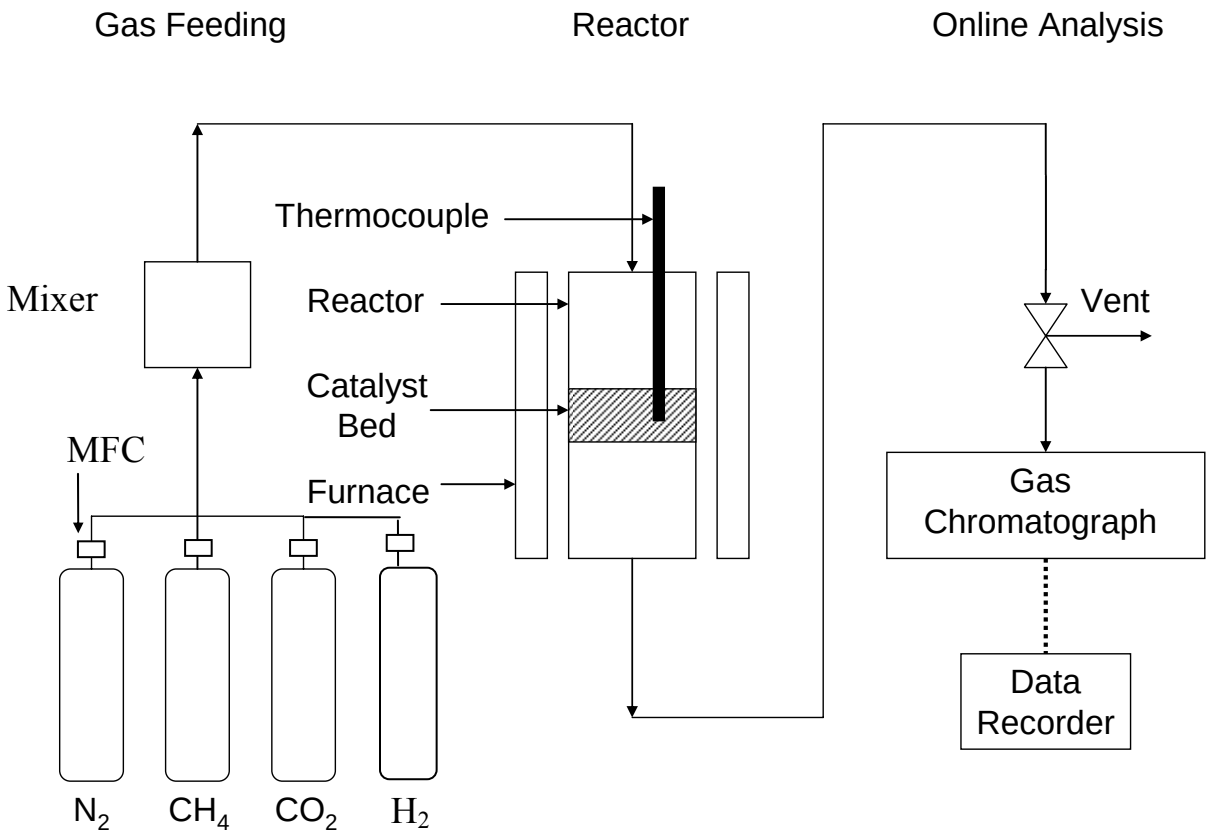

Figure 3.2 The scheme of reactor system.

A thermocouple was inserted from the top of the tube on the surface of the catalyst bed. The reaction was operated under atmospheric pressure at 750 ^{o}C. Before the DRM reaction, the catalyst was reduced in situ with a mixture of H_2/N_2 at the ratio 1:4 at 800 ^{o}C for 4 hours. The furnace temperature then was reduced to 750 ^{o}C for the reaction. The feed gases, with the ratio of CH_4:CO_2:N_2 in 1:1:1 were introduced at a flow rate of 10 L/h. All the gases were supplied by PRAXAIR (PRAXAIR Canada Inc., Mississauga, ON) and the purities of CH_4, CO_2, N_2, H_2, were 99.2%, 99.9+%, 99.9+%, and 99.9%, respectively.

In GC analysis, a GS-GASPRO capillary column (J&W Scientific) with 60 mm in length and 0.32 mm in inner diameter was employed to separate the effluent components. Helium (ultra high purity 5.0, Canada Inc.) was used as the carrier gas. The product gas was analyzed by an on-line Agilent 6890N GC, equipped with TCD and a GS-GASPRO capillary column (J&W Scientific) of 60 m in length and 0.32 mm of inner diameter using GC ChemStation software. Helium (Ultra high purity 5.0, PRAXAIR Canada Inc.) was used as carrier gas. In order to separate CO from N_2 peak, the column needs to work at low temperature. The on-line analysis is controlled by HP ChemStation. The method for GC analysis was as follows: The oven temperature was kept at 40 ^{o}C for 3 minutes before ramping it to 60 ^{o}C at a rate of 10 ^{o}C/min, and then the oven was kept at 60 ^{o}C for 1 minute. After that the oven reached to 125 ^{o}C at the rate of 35 ^{o}C/min, kept for 5.5 min. The GC signals were calibrated prior to the analysis of product gases. The calibrations are shown in Appendix A and the flow rate mentioned in here is the flow rate in standard temperature pressure, 101.3 kPa. The raw data of each run are given in

Appendix B. The followings are the equations employed for calculations:

Conversion of respective reactant is defined as

$$X_{CO_2} = \frac{F_{CO_2,I} - F_{CO_2,O}}{F_{CO_2,I}} \tag{3.1}$$

$$X_{CH_4} = \frac{F_{CH_4,I} - F_{CH_4,O}}{F_{CH_4,I}} \tag{3.2}$$

where, $F_{i,I}$ stands for inlet flow rate of respective reactant (mL/min) and $F_{i,O}$ is the outlet flow rate of respective reactant (mL/min). CO_2 conversion and CH_4 conversion were calculated based on the above equations. The actual inlet flow rates of these gases were obtained from MFC and outlet flow rate was calculated from GC signal, N_2 flow rate is used as reference in the calculation due to it is inert gas in this reaction (see details in appendix B).

Equations for the selectivity are given as follows:

$$S_{H_2} = \frac{F_{H_2,O}}{2 \times (F_{CH_4,I} - F_{CH_4,O})} \tag{3.3}$$

$$S_{CO} = \frac{F_{CO,O}}{(F_{CH_4,I} - F_{CH_4,O}) + (F_{CO_2,I} - F_{CO_2,O})} \tag{3.4}$$

$$H_2 / CO = \frac{S_{H_2}}{S_{CO}} \tag{3.5}$$

where, $F_{CH_4,I}$ is the inlet flow rate of CH_4 (mL/min) and $F_{CH_4,O}$ is the outlet flow rate of CH_4 (mL/min). $F_{CO,O}$ stands for outlet flow rate of CO (mL/min) while $F_{CO_2,I}$ means inlet flow rate of CO_2 (mL/min). $F_{CO_2,O}$ and $F_{H_2,O}$ are outlet flow rate of CO_2 (mL/min) and outlet flow rate of

H_2 (mL/min), respectively. S_{H_2} means the selectivity of H_2 and S_{CO} is the selectivity of CO.

H_2 selectivity and CO selectivity were calculated based on Equations 3.3 and 3.4. The actual inlet flow rates of these gases were obtained from MFC and outlet flow rate was calculated from GC results (See raw data in Appendix A). H_2/CO ratio was calculated based on Equation 3.5.

CHAPTER 4 RESULTS AND DISCUSSION

4.1 Catalyst Preparation and Characterization

4.1.1 *Effect of Impregnation Steps and Calcination Steps on Catalyst Composition*

As designed, the first group of catalysts, BF-1-MgNiCo, BF-1-MgNiCo-Buffer, BF-2-0.5(MgNiCo), BF-4-0.25(MgNiCo) and BF-4-0.25(MgNiCo)-C have theoretically been loaded with the same metal (Ni, Co and Mg) contents, but the metal loading procedures changed. BF-1-MgNiCo were made using the single step of impregnation followed by one step of calcination based on the weight composition of Al, 84 %, Mg, 8.3 %, Ni, 3.9 % and Co, 3.9 %. The metal content of this catalyst was used as the reference. In making BF-1-MgNiCo-Buffer, the only difference was that buffer solution (0.26 % sodium carbonate, 0.2 % sodium bicarbonate) was used to dissolve the three metal nitrate salts. BF-4-0.25(MgNiCo) was made by 4 times of impregnation with the solution of 1/4 metal nitrate salts (based on BF-1-MgNiCo), each after the previous drying at 120 ^{o}C overnight, followed by one-step calcination. BF-4-0.25(MgNiCo)-C was made by 4 steps, each consisting impregnation of the solution of 1/4 metal nitrate salts, drying, and calcination,

The second group of catalysts, BF-2-Mg-MgNiCo and BF-2-(Mg0.5Ni0.5Co), should have twice Mg content than the first group. BF-2-Mg-MgNiCo was made by two steps of impregnation. The

first step only impregnated Mg for 8.3 wt%; then the second step impregnated the MgNiCo nitrate solution. In preparing BF-2-(Mg0.5Ni0.5Co), two steps of impregnation were used, but the solution contains half of Ni and Co compared with the reference catalyst.

In comparison with the first group, the third group of BF-1-0.25(MgNiCo)-C, BF-2-0.25(MgNiCo)-C, BF-3-0.25(MgNiCo)-C and BF-4-0.25(MgNiCo)-C, varied the metal contents from 1/4, 2/4, 3/4 and 4/4. A solution containing 1/4 of Mg, Ni and Co nitrate salts was prepared. Every each impregnation was followed by drying and calcination. The procedure was repeated different times so that the catalysts of this group contains different amounts of Mg, Ni, and Co. The impregnation was conducted at the room temperature (~23 ^{o}C). The impregnated balls was first dried at the room temperature for 4 h and then transferred into an oven at 120 ^{o}C for overnight (10 h). The calcination was conducted in the air at 800 ^{o}C for 6 h.

The actual metal contents (Al, Mg, Ni, Co) of the catalysts were measured using ICP-MS. Table 4.1 shows the metal content based on calculation and the ICP-MS measurement. The actual Mg, Ni, Co contents of all prepared catalyst samples are less than the expected values obtained based on calculation. To find out how impregnation steps affect catalyst metal loading, the results of first group were compared. In the first group of catalysts, BF-1-MgNiCo, BF-2-0.5(MgNiCo) and BF-4-0.25(MgNiCo), the metal loading (Mg, Ni, Co) shows a slight increasing tendency, which means that multiple impregnation steps can improve the loaded

Table 4.1 Expected and actual metal composition of prepared catalyst samples.

	Expected, wt %				Actual (ICP-MS results), wt%			
Catalyst name	Al	Mg	Co	Ni	Al	Mg	Co	Ni
BF-1-MgNiCo	84.0	8.2	3.9	3.9	86.8	7.2	3.2	2.8
BF-1-MgNiCo-Buffer	84.0	8.2	3.9	3.9	85.3	8.3	3.5	2.9
BF-2-Mg-MgNiCo	77.5	15.3	3.6	3.6	78.4	15.9	3.0	2.7
BF-2-(Mg0.5Ni0.5Co)	77.5	15.3	3.6	3.6	86.0	10.1	2.1	1.8
BF-2-0.5 (MgNiCo)	84.0	8.2	3.9	3.9	85.4	7.8	3.6	3.2
BF-4-0.25(MgNiCo)	84.0	8.2	3.9	3.9	85.3	8.3	3.4	3.0
BF-1-0.25(MgNiCo)-C	95.4	2.4	1.1	1.1	95.4	2.5	1.0	1.1
BF-2-0.25(MgNiCo)-C	91.3	4.5	2.1	2.1	90.8	4.9	2.0	2.3
BF-3-0.25(MgNiCo)-C	87.5	6.5	3.0	3.0	88.0	7.0	2.8	2.2
BF-4-0.25(MgNiCo)-C	84.0	8.2	3.9	3.9	84.5	8.7	3.8	3.0

metal amount. On the other hand, the influence of calcination steps was determined by comparing BF-4-0.25(MgNiCo) with BF-4-0.25(MgNiCo)-C.

The result shows that BF-4-0.25(MgNiCo)-C has more metal loaded, which means that multiple calcination steps can also improve the metal loading amount. BF-1-0.25(MgNiCo)-C, BF-2-0.25(MgNiCo)-C, BF-3-0.25(MgNiCo)-C and BF-4-0.25(MgNiCo)-C generally show an increase of Mg, Ni and Co content from 1/4, 2/4, 3/4 and 4/4 compared to the reference catalyst, which in agreement with the calculated value.

In conclusion, BF-4-0.25(MgNiCo)-C shows the highest Mg, Ni, Co metal content, meaning that multiple impregnation steps and multiple calcination steps can improve the metal loading amount on the support to some extend. And for all the catalyst samples, the ICP-MS results are generally in agreement with the expected values, which mean although the procedures to make those samples are varying, the metal solution are all successfully impregnated on the alumina support.

4.1.2 *Effect of Impregnation Steps and Calcination Steps on Catalyst Surface Area and Pore Structure*

Specific surface area, average pore diameter, and pore volume of catalysts made with different impregnation steps or calcination steps were measured by N_2 adsorption (or BET method). The results are presented in Table 4.2.

For the first group, BF-1-MgNiCo, BF-1-MgNiCo-Buffer, BF-2-0.5(MgNiCo), BF-4-0.25(MgNiCo) and BF-4-0.25(MgNiCo)-C, of which the loading of Mg, Ni and Co are supposed to be the same, BF-1-MgNiCo, BF-2-0.5(MgNiCo) and BF-4-0.25(MgNiCo) appear to have similar BET properties. The surface area is between 124 and 131 m^2/g, the average pore diameter is between 117 and 128 Å, and the pore volume between 0.36 and 0.42 mL/g. When they were made, they experienced one-step calcination though the metals Mg, Ni and Co were loaded by various impregnation steps. However, BF-4-0.25(MgNiCo), subjected to one-step calcination, and BF-4-0.25(MgNiCo)-C, subjected to four times of calcinations, have different BET properties (124 vs. 84 m^2/g in specific area, 117 vs. 146 Å in pore size, and 0.36 vs. 0.31 mL/g in pore volume). In catalyst preparation, it has been well established that the calcination step is the most significant one that affects BET properties. Yun *et al*. (2012) reported that for the vanadium phosphate catalyst they investigated, the BET surface area for the catalyst samples VPO6, VPO24 and VPO48, which were calcined for 6 h, 24 h, 48 h respectively, are 11, 10 and 7 m^2/g. The results show that the increasing calcinations duration led to a decrease in total surface area.

The second group of catalysts, BF-2-Mg-MgNiCo and BF-2-(Mg0.5Ni0.5Co), show the similar average pore diameter and pore volume but BF-2-Mg-MgNiCo has a smaller surface area.

Table 4.2 BET properties of the prepared catalysts.

Catalyst Name	Surface area (m^2/g)	Average pore diameter (Å)	Pore volume (mL/g)
BF-1-MgNiCo	131	128	0.42
BF-1-MgNiCo-Buffer	126	117	0.35
BF-2-Mg-MgNiCo	99	129	0.32
BF-2-2(Mg0.5Ni0.5Co)	114	122	0.33
BF-2-0.5(MgNiCo)	120	128	0.36
BF-4-0.25(MgNiCo)	124	117	0.36
BF-1-0.25(MgNiCo)-C	138	124	0.43
BF-2-0.25(MgNiCo)-C	122	137	0.39
BF-3-0.25(MgNiCo)-C	102	150	0.38
BF-4-0.25(MgNiCo)-C	84	146	0.31
BASF-CSS-350	345	49	0.42

For group three, BF-1-0.25(MgNiCo)-C, BF-2-0.25(MgNiCo)-C BF-3-0.25(MgNiCo)-C, BF-4-0.25(MgNiCo)-C show a decreasing tendency of BET surface area and pore volume.

Comparing the surface area of alumina support and that of the prepared catalysts shown in Table 4.2, BET surface area of all the prepared catalysts was observed much lower than that of the BASF alumina support (around 100 m^2/g vs. 345 m^2/g). The difference of the specific surface area among all the catalyst samples is as large as 54 m^2/g. And the average pore diameter increased dramatically. There may be three reasons for these changes. Firstly, the main reason is that during calcination step, not only do the loaded metal salts turn to metal oxides but also the support is restructured. According to Yao *et al*., during the high temperature calcination step, γ-Al_2O_3, of which the surface area is 150-350 m^2/g, will partially transform to α-Al_2O_3, of which the surface area is less than 3 m^2/g. Secondly, the increase of pore diameter may be caused by the loaded metal particles blocking some of the mesopore channels (diameter of pores between 2 nm to 50 nm), Figs. 4.1 and 4.2 show the pore diameter distribution of the virgin Al_2O_3 ball and BF-1-MgNiCo, respectively. It can be observed that most of the pores of Al_2O_3 virgin ball are around 50 Å in diameter while of catalyst BF-1-MgNiCo are two groups of pores seen around 50Å and 150 Å. Nguyen *et al*. (2002) reported that the increase in pore size could be ascribed to the $LaCoO_3$ loaded inside the mesopore channels of the support. Thirdly, the metal nitrate solution was acidic (pH 3.72), which can lead to the merging of micropores.

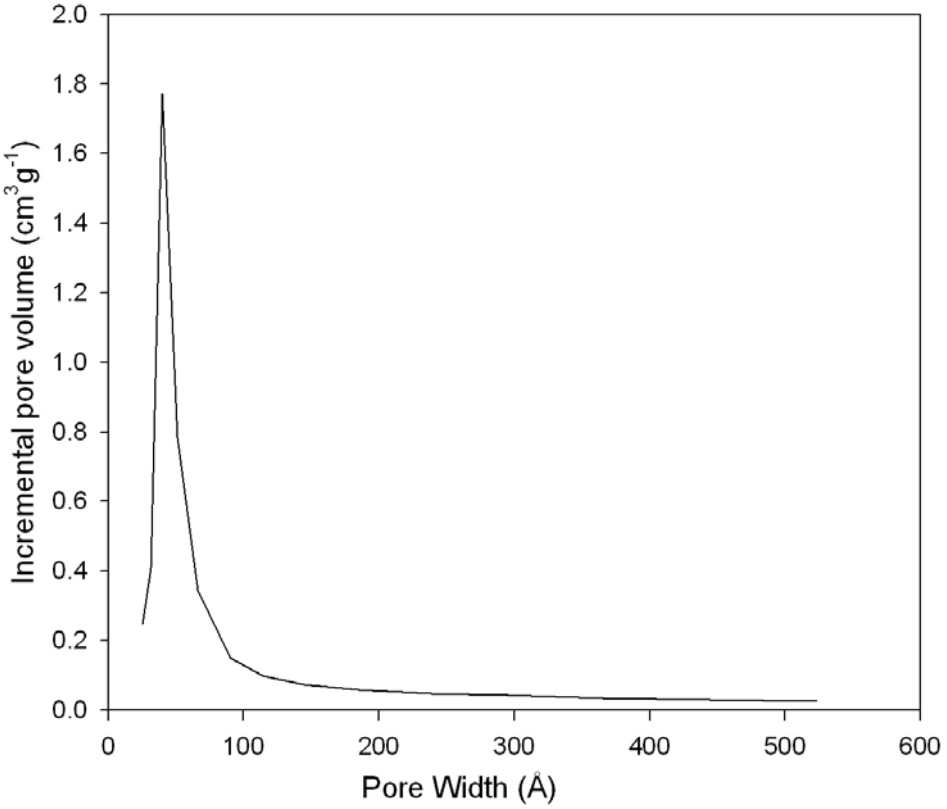

Figure 4.1 Pore volume distribution curve for the BASF CSS 350 Al_2O_3 balls.

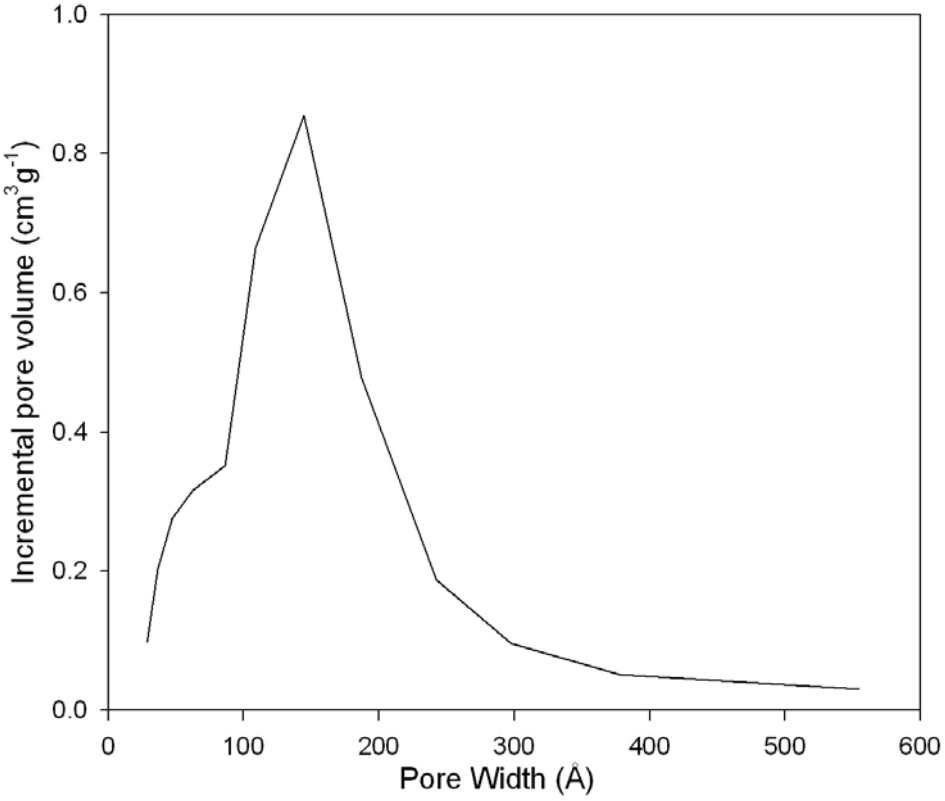

Figure 4.2 Pore volume distribution curve for BF-1-MgNiCo.

In conclusion, the step of loading the metal solution on support is the major reason of the severe surface area decrease when alumina support was prepared into catalysts. Calcination step is the dominate factor to the change in textural properties of supported catalysts. Multiple calcinations can attribute to the reduction of surface area and pore volume.

4.1.3 *Effect of Impregnation Steps and Calcination Steps on Catalyst Compressive Strength*

Compressive strength of the catalyst balls and the BASF virgin ball was measured with Instron 5566 electro mechanical test system. The compressive strength was measured 10 times for each sample, the average compressive strength and the error bar generated by the descriptive statistics function of Microsoft Office Excel 2003 are shown in Fig.4.3.

It is assumed that the compressive strength for the commercial product, BASF CSS 350 Al_2O_3 balls, is good enough for industrial use.

From Fig.4.3, it is clear that all the catalysts have equal or even stronger compressive strength than the alumina balls except BF-Mg-MgNiCo.

BF-1-MgNiCo and BF-1-0.25-MgNiCo-C were prepared with the same calcination steps and impregnation steps, but different metal content. The significant difference of compressive strength between these two samples indicates that the smaller metal content loaded would result

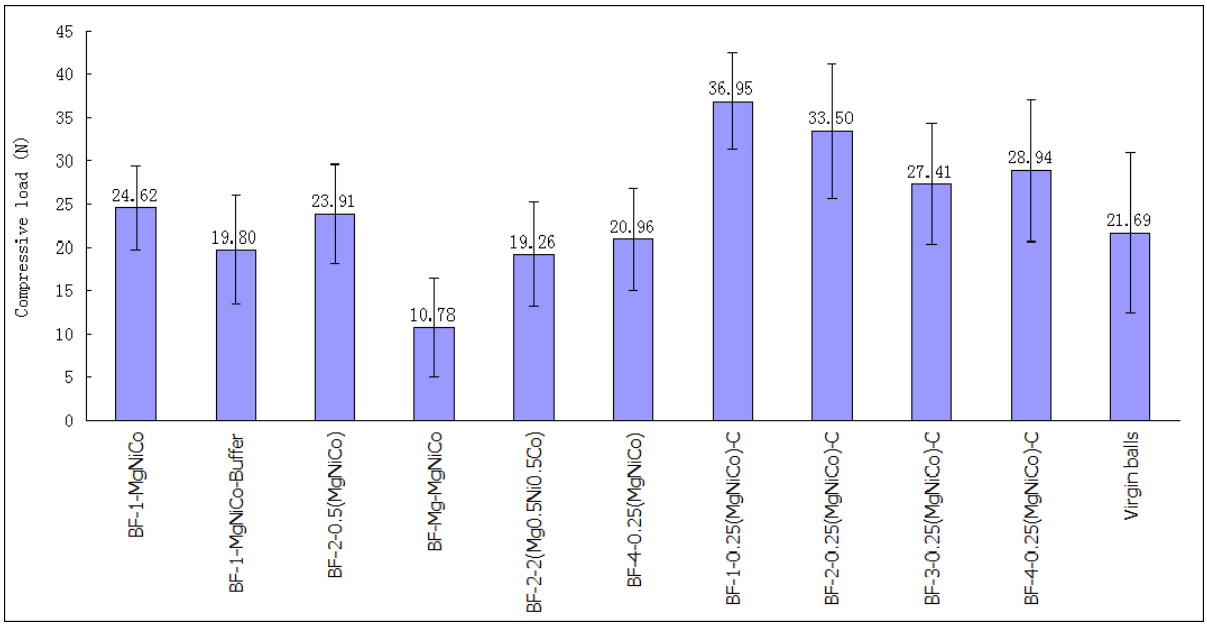

Figure 4.3 Compressive load (N) for the prepared catalyst samples. Instron 5566 electro, compress by 2 mm after sensing top of sample (0.5 N) (max load 1 KN). The sample standard deviation was calculated with 95% confidence level.

in the higher compressive strength.

BF-4-0.25(MgNiCo) and BF-4-0.25(MgNiCo)-C were made with the same metal content and impregnation step, the only difference is the number of calcination steps they were subjected to. The compressive strength of BF-4-0.25(MgNiCo) and BF-4-0.25(MgNiCo)-C are 20.96 N and 28.94 N, respectively. Especially, BF-4-0.25(MgNiCo)-C has even higher compressive strength than that of the virgin ball. This result indicates that multiple calcinations can help improve the mechanical strength of alumina support.

BF-1-MgNiCo, BF-2-0.5(MgNiCo) and BF-4-0.25(MgNiCo) have the similar metal content but were subjected the same times of calcination step, but different number of impregnation steps. The result shows that there is no significant difference among these three samples. That means impregnation steps alone do not have influence on catalyst compressive strength. It can be concluded that the mechanical strength is mainly impacted by calcination steps and metal content. Multiple calcination and lower metal loading can improve the compressive strength. On the other hand, impregnation steps did not have obvious effect on the compressive strength. According to the error bar, which calculated based on sample standard deviation (Error bars are a graphical representation of the variability of data, which gives a general idea of how accurate a measurement is, or how far from the reported value the true value might be), the true value of BASF CSS 350 alumina ball fell into the true value range of most catalyst, which means the excellent mechanical strength of alumina support did not change dramatically after metal loading

for most catalyst samples, which is an crucial criteria for a commercial catalyst.

4.1.4 *Effect of Impregnation steps and Calcination steps on Metal Oxides Reduction*

XAS (X-ray absorption spectroscopy) measurement of the prepared catalysts was conducted at the Canadian Light Source (CLS). For each catalyst, two XANES of Ni and Co K-edges were scanned, one for the sample before reduction (after calcination and cooling), the other one after reduction. XANES spectra also obtained for the standard samples of Co foil, CoO, Ni foil and NiO, which were used as the references. The reduction of the catalysts was conducted in a chemical engineering lab with H_2/N_2 mixture at 800 ˚C in a quartz tube reactor for 4 hours. Then the catalysts were cooled down to room temperature (~23 ˚C) in reductive gas. The reactor was sealed with N_2 filled within it. The reactor was then taken to CLS for scanning. The spectra were treated using Athena software. Those of Ni, Co foil and NiO and CoO standards were used as reference for curve fitting and comparison. The curve fitting results of Ni and Co reduction extents are given in Table 4.3. The XANES of Ni and Co K-edge, according to different groups, are shown in Figs. 4.4-4.15, respectively.

For all the catalysts, Co reduction extent is about 36%-72%, that of Ni is 79%-90%. This result is in agreement with our previous measurement for the loose powder catalyst made by impregnation method (Wang *et al*., 2012). Detailed analysis on the absorption spectra by groups is discussed below to investigate the effect of preparation steps on Ni and Co reduction.

Table 4.3 Active metal foil and metal oxide mole percentage of catalyst samples after reduction by linear combination fitting.

Catalyst Name	CoO (%)	Co (%)	NiO (%)	Ni (%)
BF-1-MgNiCo	40	60	17	83
BF-1-MgNiCo-Buffer	28	72	21	79
BF-2-Mg0.5Ni0.5Co	33	67	17	83
BF-2-Mg-MgNiCo	39	61	20	80
BF-4-0.25(MgNiCo)	61	39	11	89
BF-1-0.25(MgNiCo)-C	64	36	14	86
BF-2-0.25(MgNiCo)-C	60	40	20	80
BF-3-0.25(MgNiCo)-C	58	43	10	90
BF-4-0.25(MgNiCo)-C	56	44	12	88

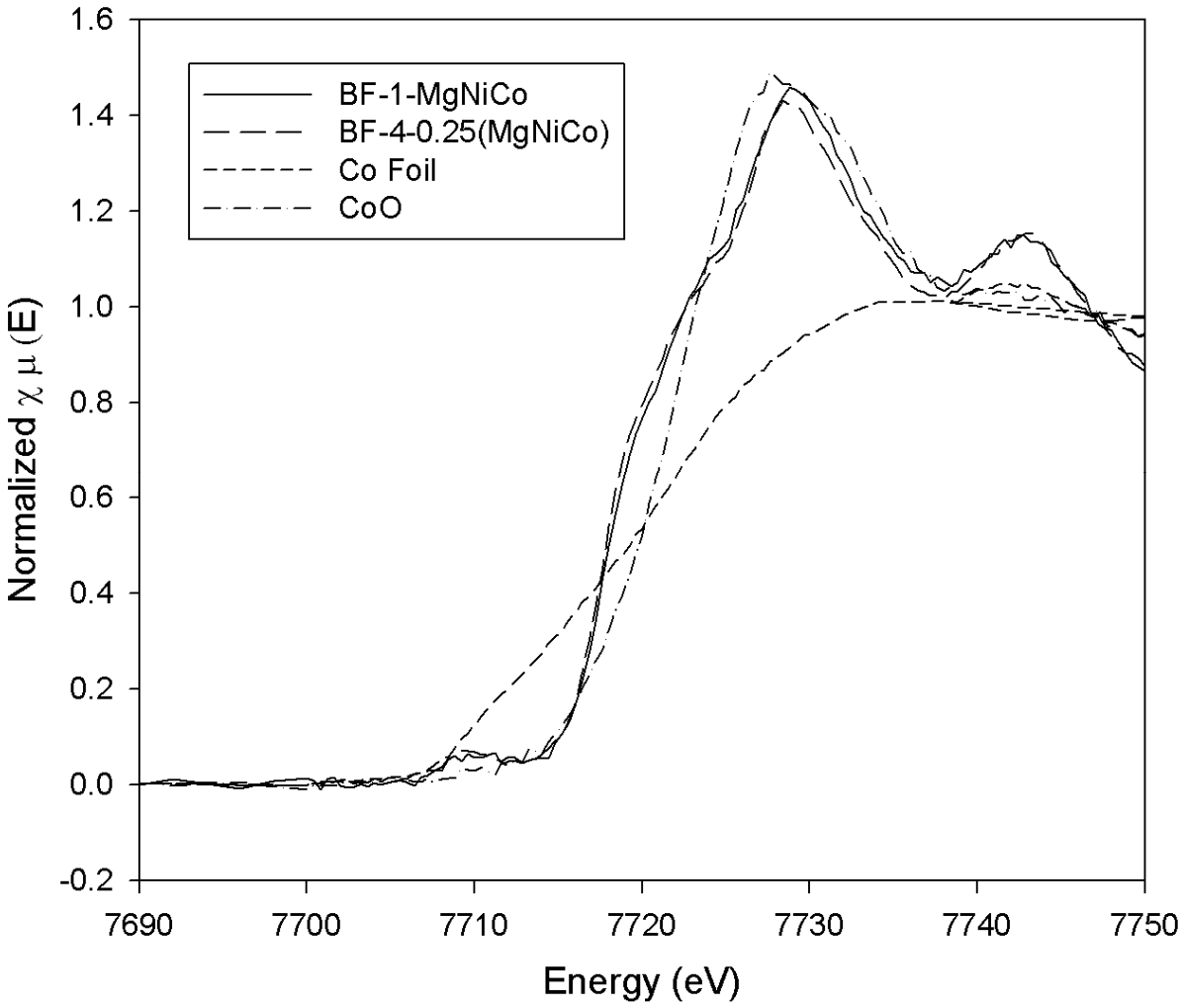

Figure 4.4 Co K-edge XANES spectra on BF-1-MgNiCo and BF-4-0.25(MgNiCo) before reduction

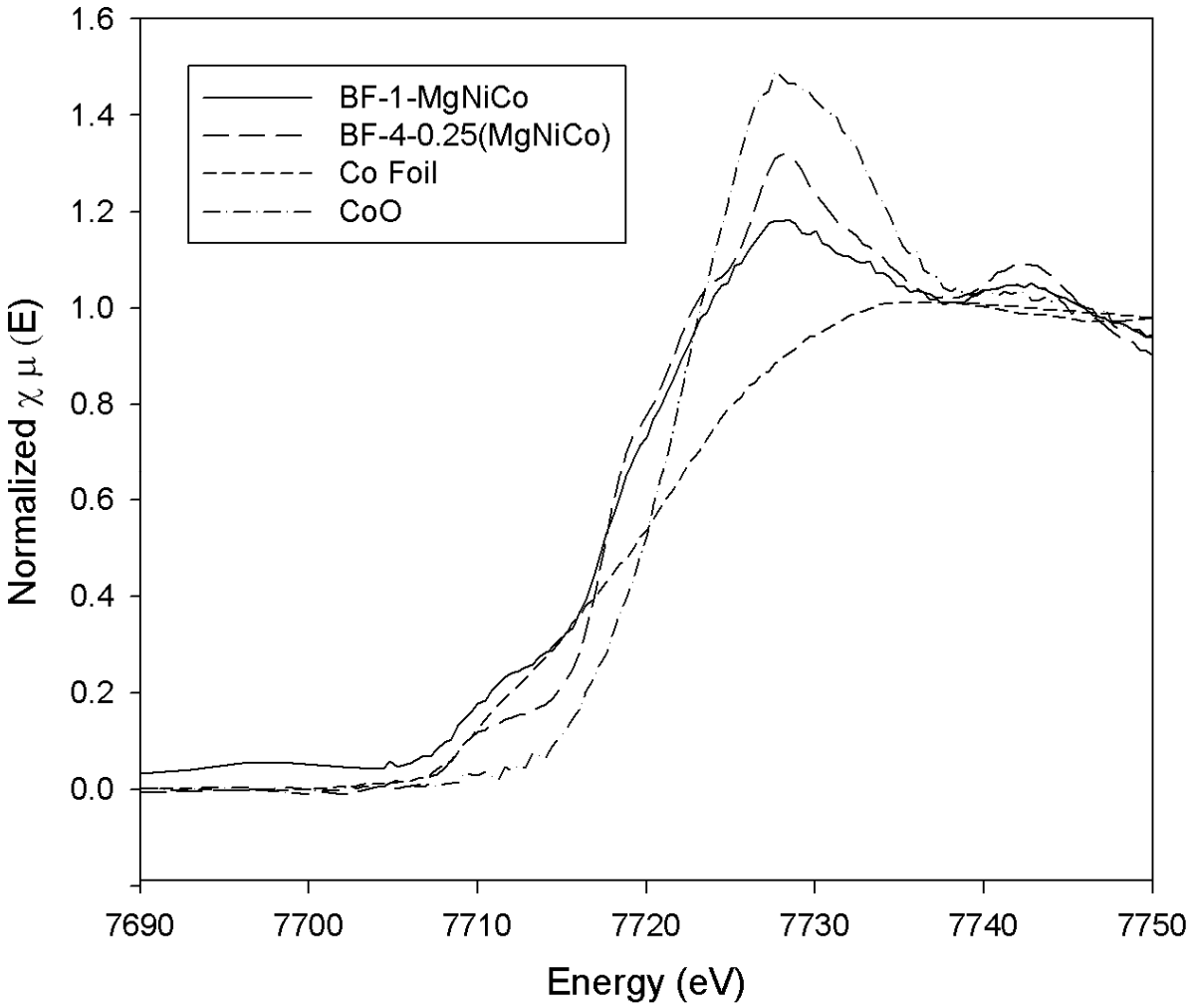

Figure 4.5 Co K-edge XANES spectra on BF-1-MgNiCo and BF-4-0.25(MgNiCo) after reduction

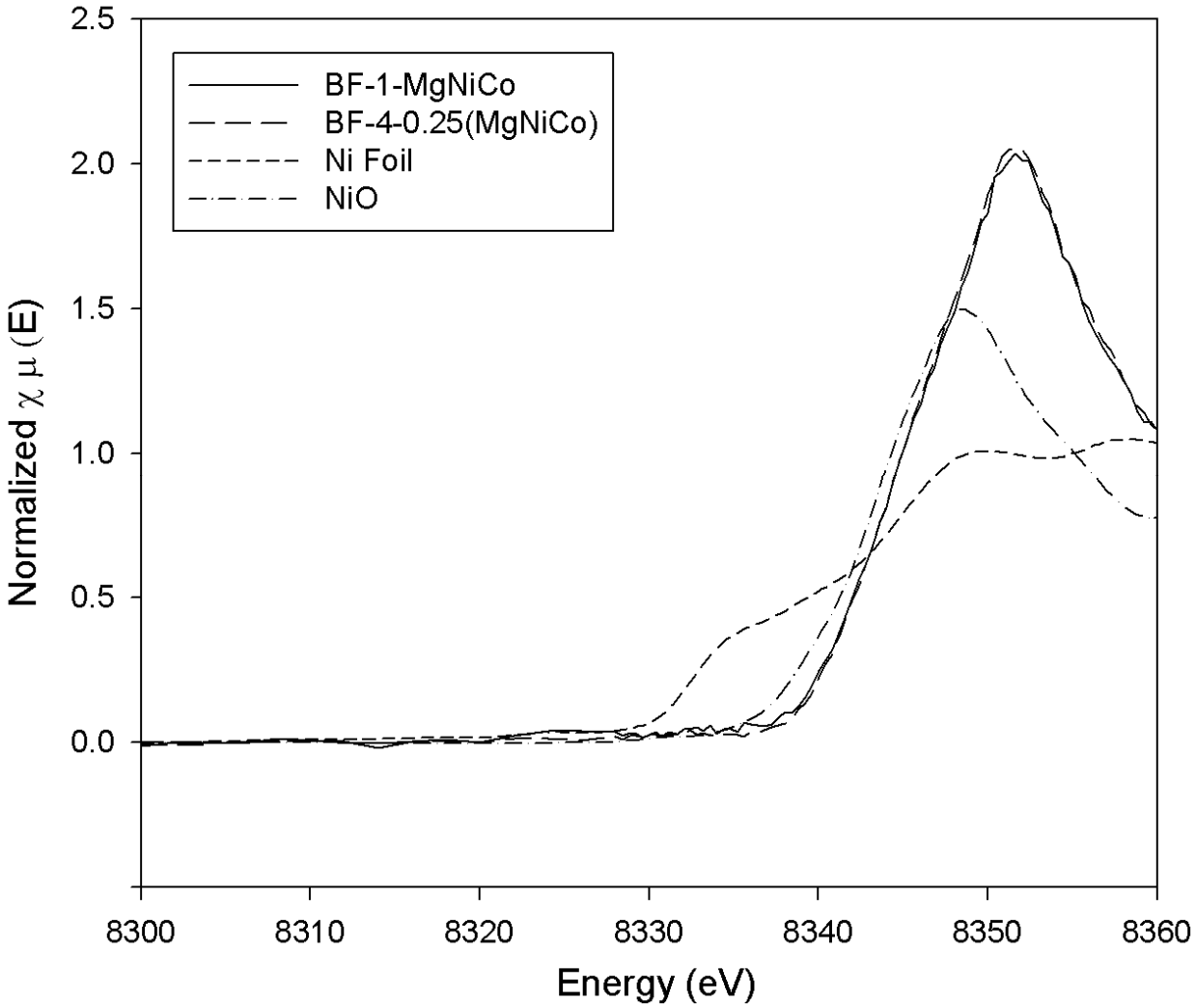

Figure 4.6 Ni K-edge XANES spectra for BF-1-MgNiCo and BF-4-0.25(MgNiCo) before reduction

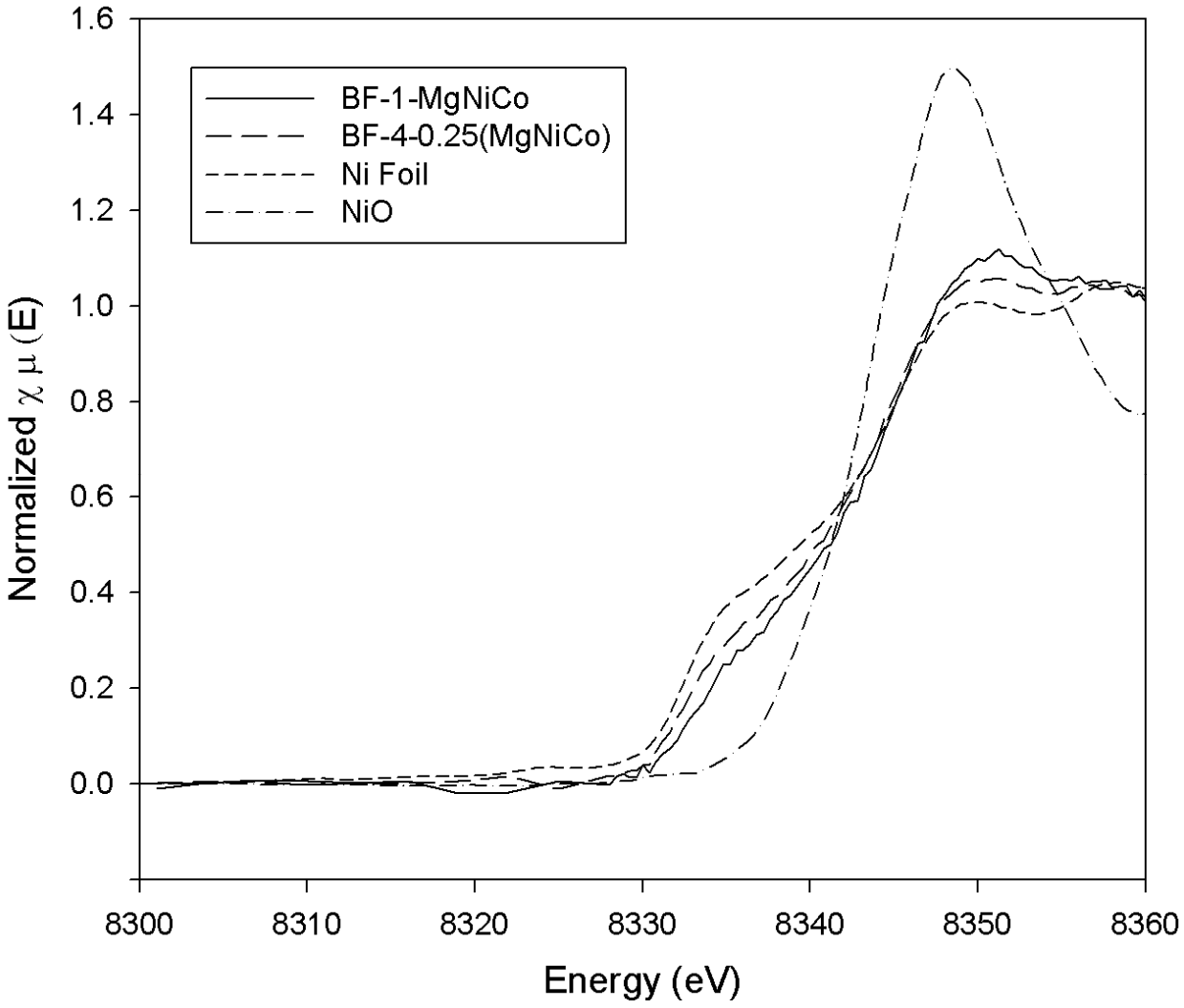

Figure 4.7 Ni K-edge XANES spectra on BF-1-MgNiCo and BF-4-0.25(MgNiCo) after reduction

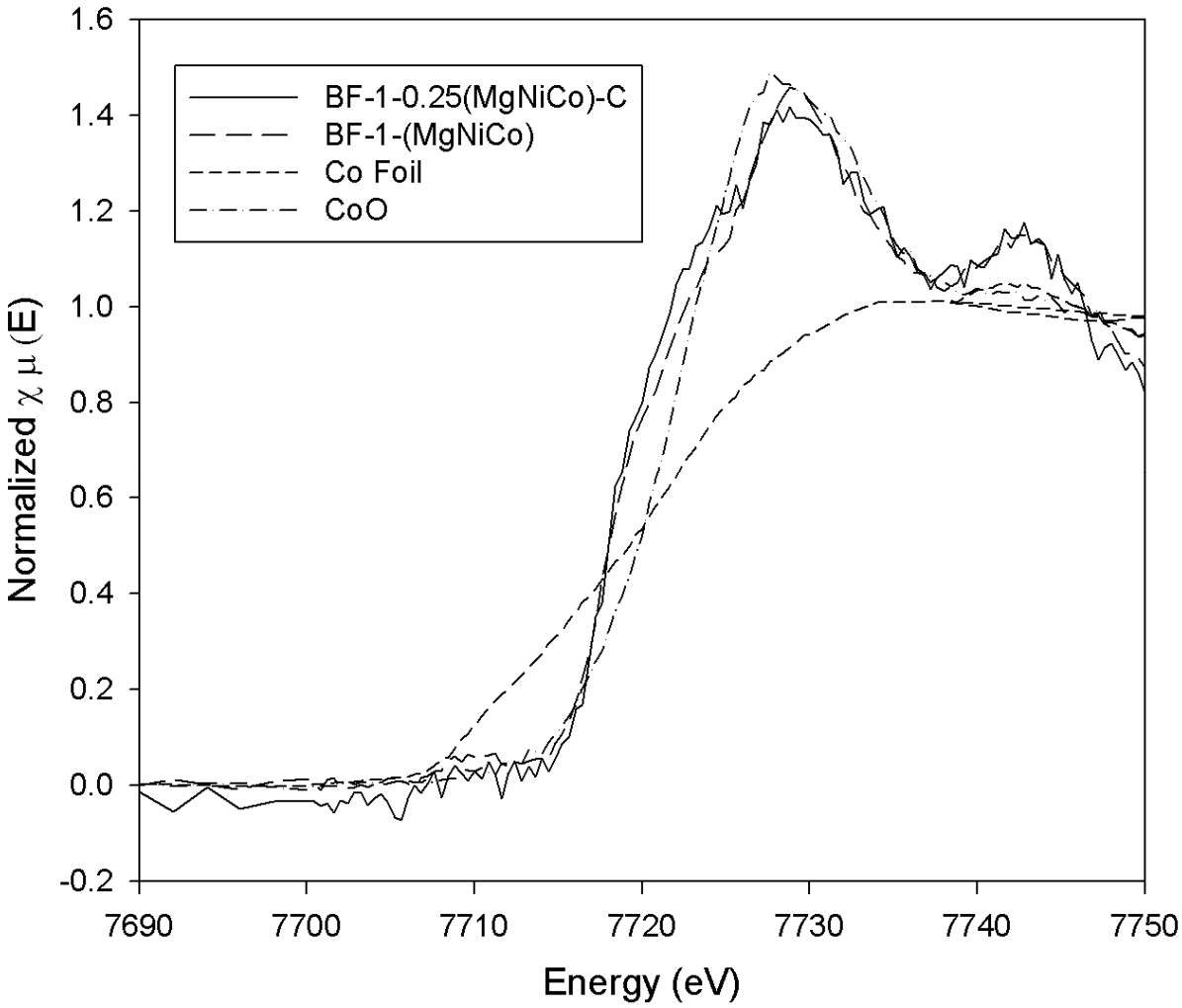

Figure 4.8 Co K-edge XANES spectra on BF-1-MgNiCo and BF-1-0.25(MgNiCo)-C before reduction

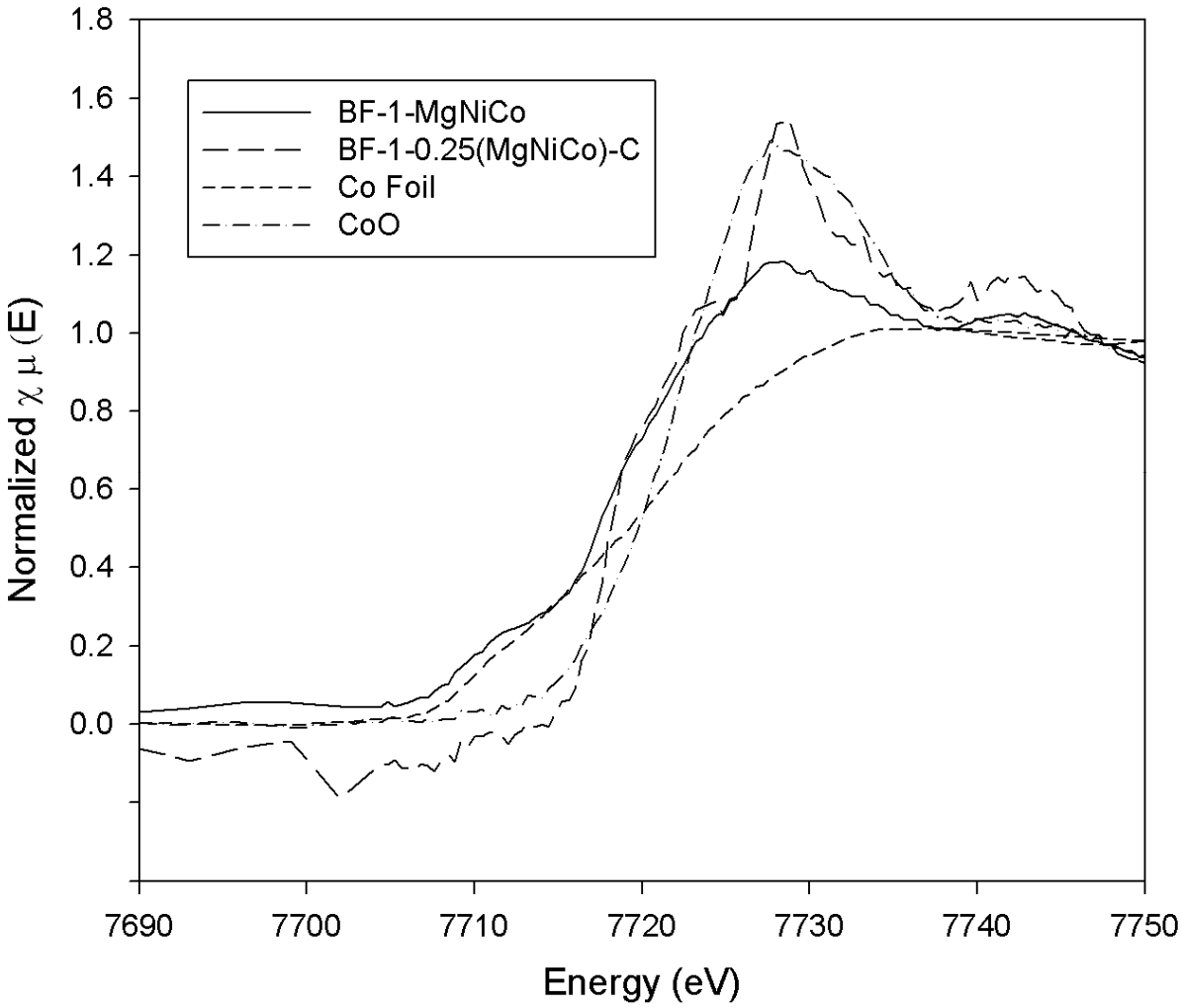

Figure 4.9 Co K-edge XANES spectra on BF-1-MgNiCo and BF-1-0.25(MgNiCo)-C after reduction

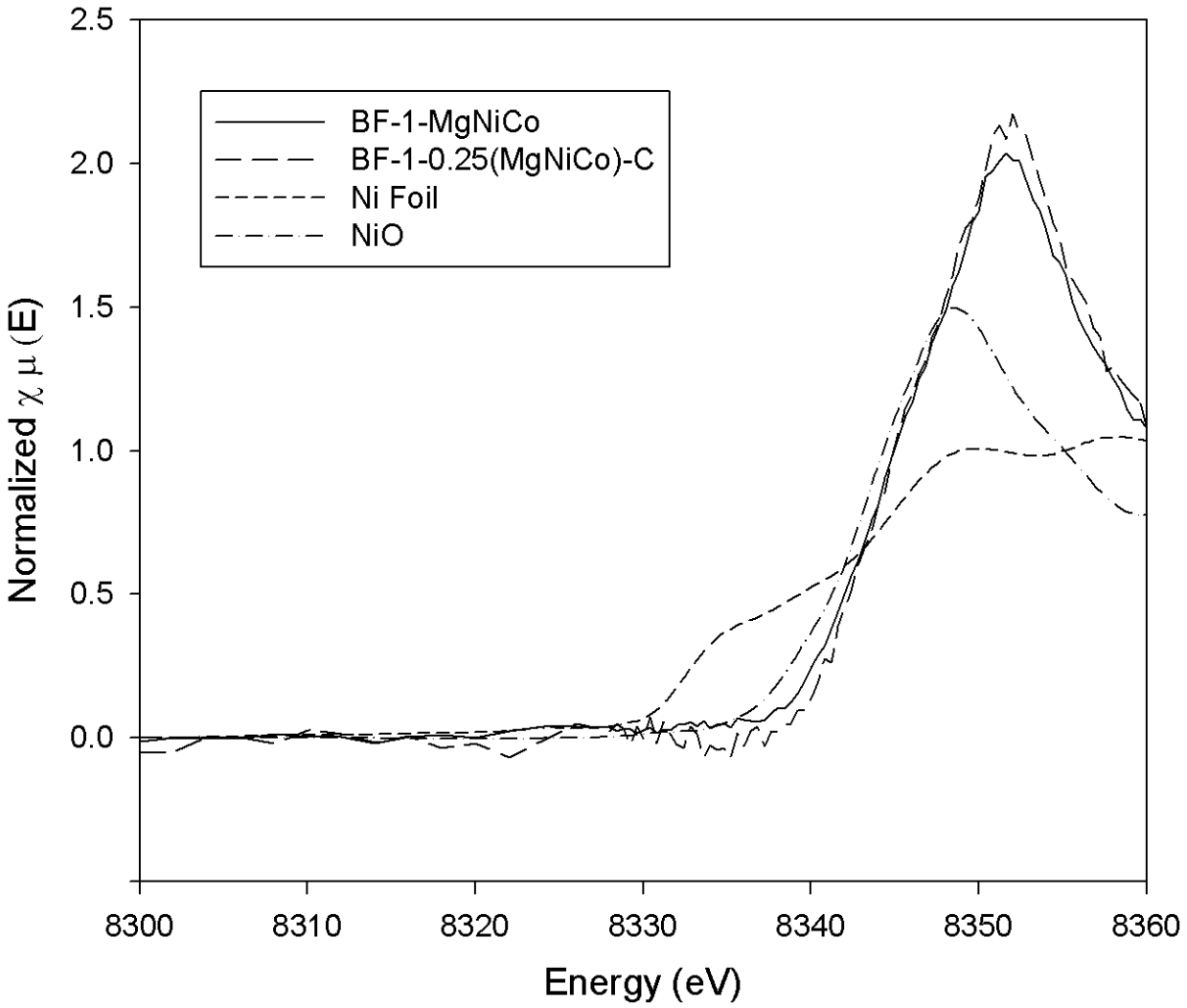

Figure 4.10 Ni K-edge XANES spectra on BF-1-MgNiCo and BF-1-0.25(MgNiCo)-C before reduction

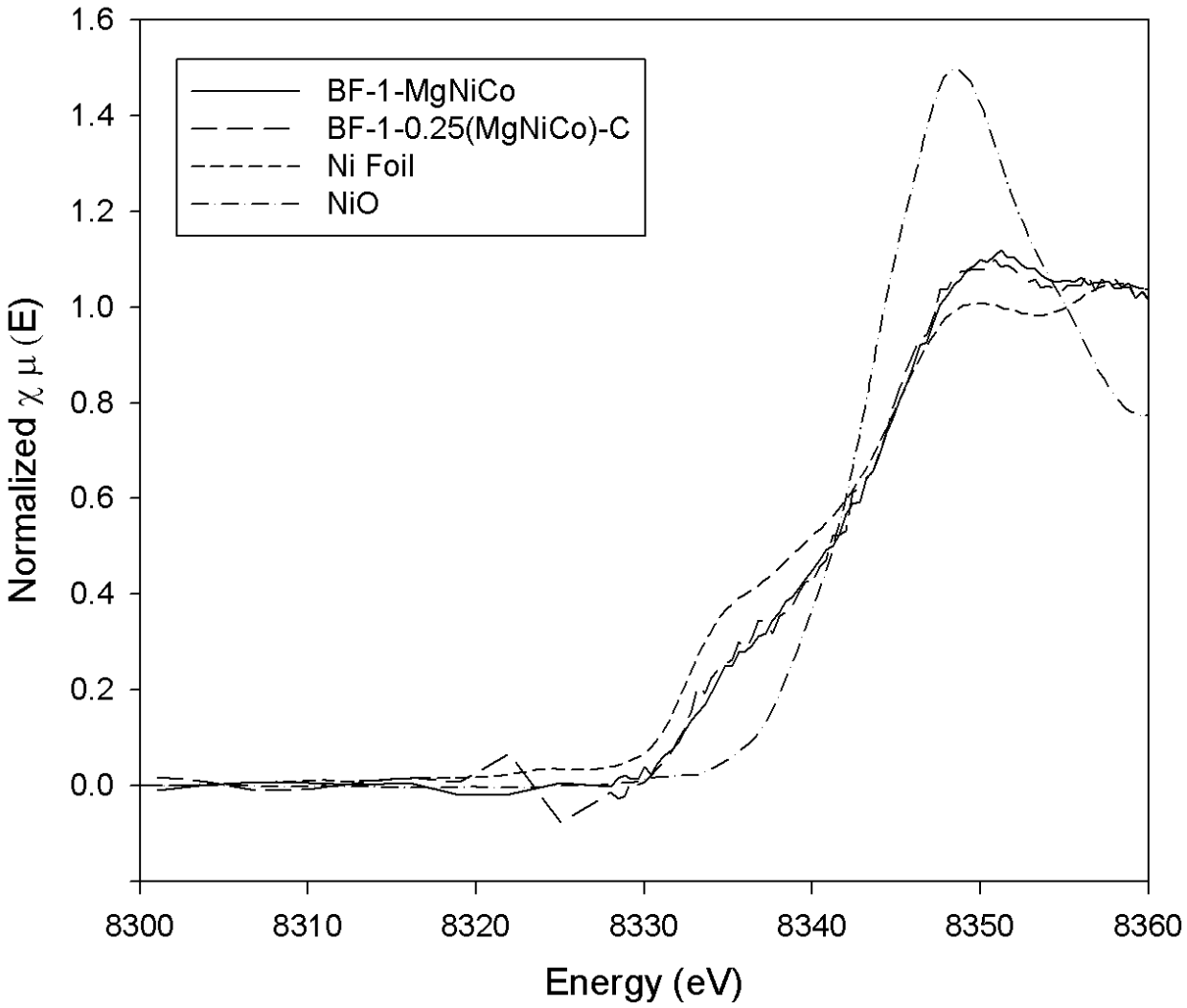

Figure 4.11 Ni K-edge XANES spectra on BF-1-MgNiCo and BF-1-0.25(MgNiCo)-C after reduction

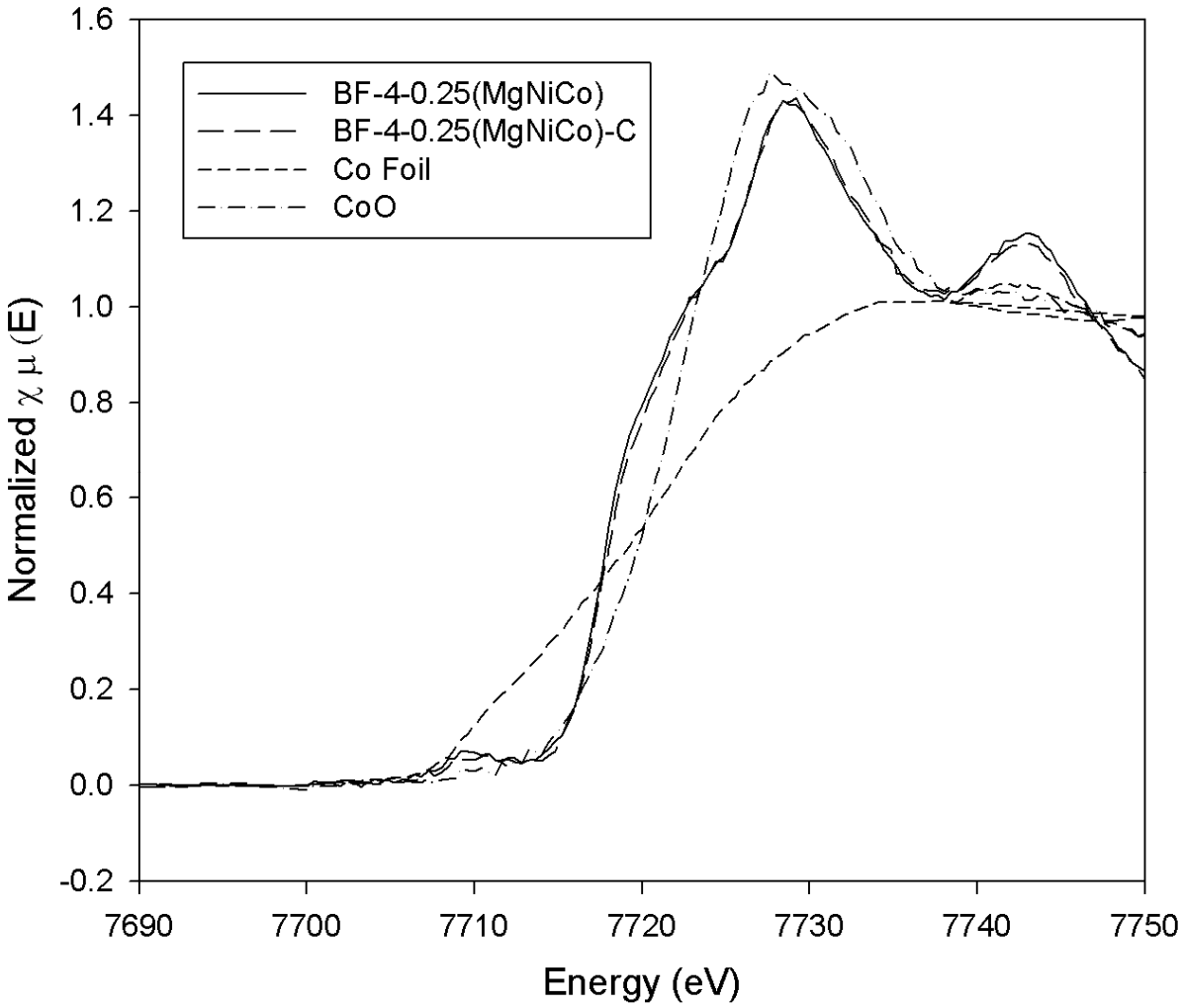

Figure 4.12 Co K-edge XANES spectra on BF-4-0.25(MgNiCo) and BF-4-0.25(MgNiCo)-C before reduction.

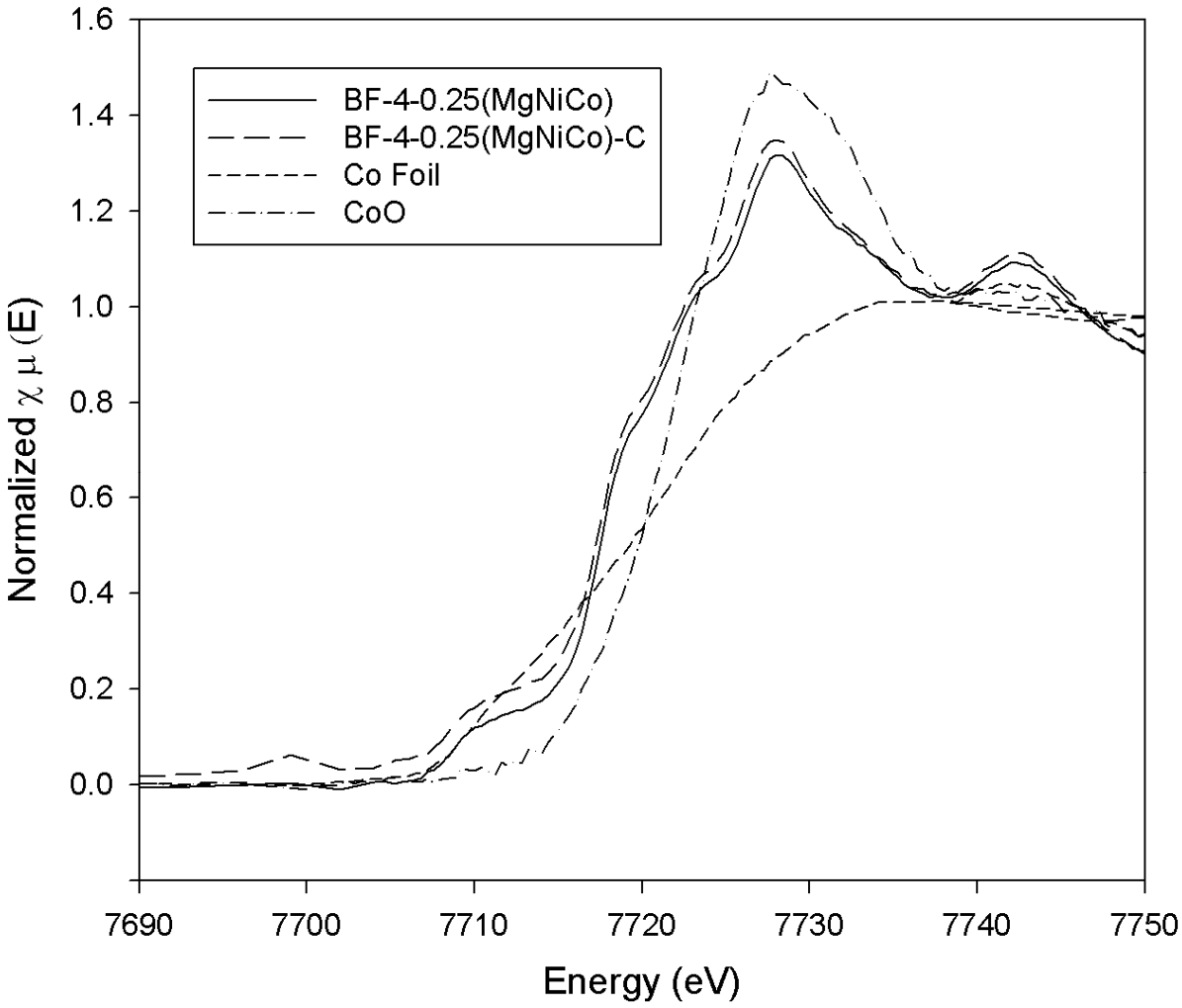

Figure 4.13 Co K-edge XANES spectra on BF-4-0.25(MgNiCo) and BF-4-0.25(MgNiCo)-C after reduction.

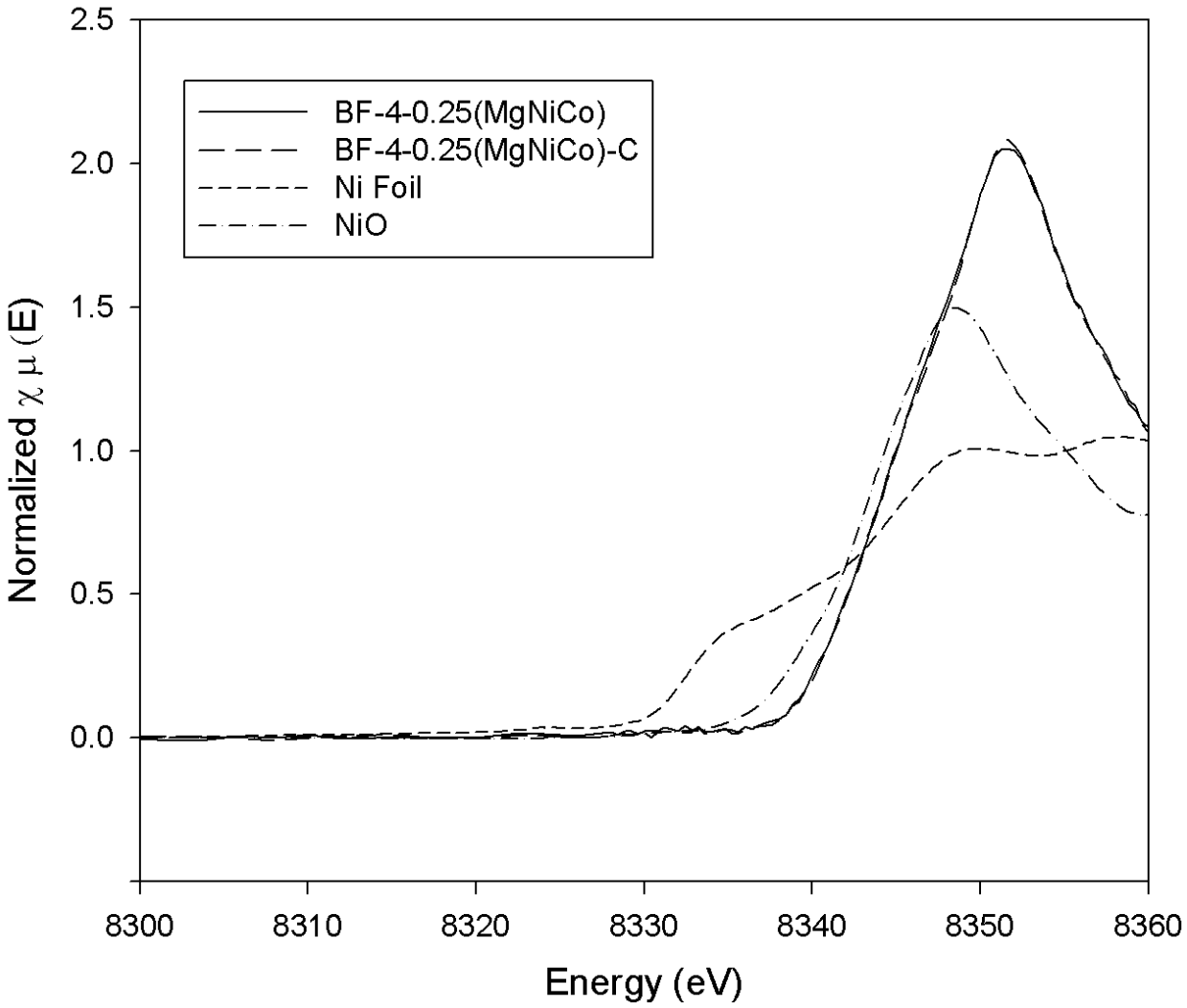

Figure 4.14 Ni K-edge XANES spectra on BF-4-0.25(MgNiCo) and BF-4-0.25(MgNiCo)-C before reduction.

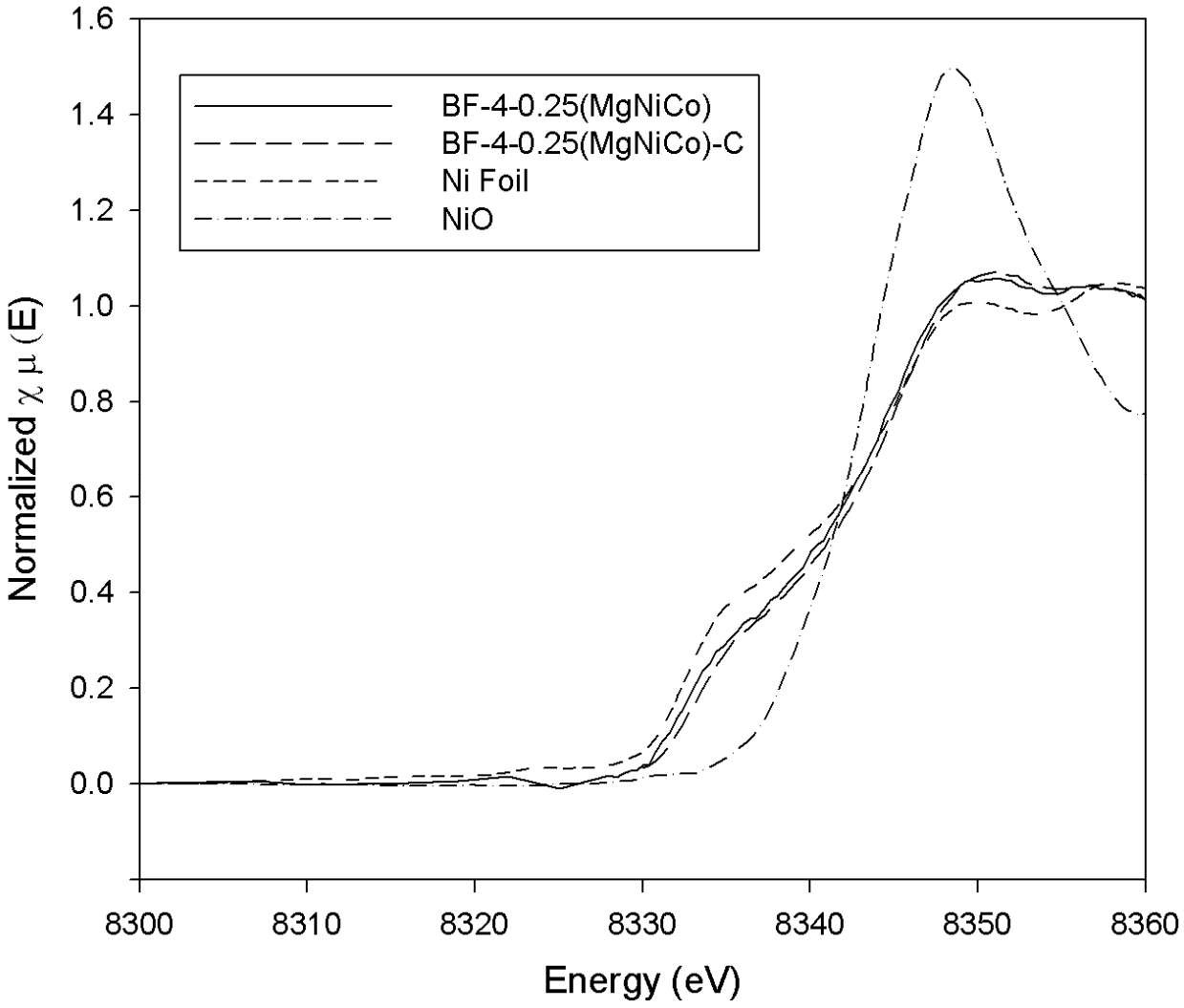

Figure 4.15 Ni K-edge XANES spectra on BF-4-0.25(MgNiCo) and BF-4-0.25(MgNiCo)-C after reduction.

Generally, for all the pre-reduction catalysts, Co K-edge XANES is either overlapped with or close to that of the CoO standard reference, meaning most of Co phase in catalysts is Co^{2+}. However, the Ni K-edge XANES has stronger white line shifted to higher energy direction compared with NiO standard, indicating that higher oxidized state of Ni (Ni^{3+}) exists in these unreduced catalysts. But in curve fitting, NiO was still used because the transition from Ni^{3+} to Ni^{2+} in reduction occurs at 600 ^{o}C once it contacted with H_2. After reduction at 800 ˚C for 4 h, presumably, there is no more Ni^{3+} in the catalysts.

BF-1-MgNiCo and BF-4-0.25(MgNiCo) are two catalysts that have the same level of Mg, Ni, and Co contents loaded with various impregnation times. Figs. 4.4 to 4.7 show the XANES of Co and Ni for this group of catalysts, respectively, comparing the Co and Ni change during catalyst reduction and investigating the effect of impregnation times on this change. Figs. 4.4 and 4.5 give the results of Co XANES before and after reduction respectively. It is clear that before reduction the Co phase existing in both catalyst samples is almost CoO. But after reduction, the Co phase is a combination of Co metal and CoO. BF-1-MgNiCo showed a higher CoO reduction extent. Figs. 4.6 and 4.7 show the Ni K-edge XANES spectra for these two samples before and after reduction. Before reduction, both samples have a quite similar result which means the Ni in these samples was in metal oxide state. After reduction, the Ni spectrum became more like to that of the Ni, meaning more NiO had been reduced.

Data in Table 4.3 shows that for BF-1-MgNiCo, which Mg, Ni, Co were loaded by one time

impregnation, the Co reduction extent achieved 60 %. However, when these elements were loaded by four times of impregnation, BF-4-0.25(MgNiCo) only achieved 39 % Co reduction. On the other hand, for Ni, both catalysts achieved 83 to 89 % reduction. The multi-impregnation seemed to have slight effect on the Ni reduction.

The Co K-edge spectra and Ni K-edge spectra of BF-1-MgNiCo and BF-1-0.25(MgNiCo)-C are shown in Figs. 4.8 to 4.11. This group of catalysts has the same impregnation steps and calcination steps but different metal content. How the metal content influenced the Co and Ni reduction can be determined by comparing these two catalysts. Fig. 4.8 shows that the major Co phase in both fresh samples is CoO, which is very similar. But the spectra after reduction (Fig. 4.9) shows a dramatic difference. The metal oxides in BF-1-0.25(MgNiCo)-C, which has smaller metal (Mg, Ni, Co) loading, were poorly reduced while the reduction extent was higher in BF-1-MgNiCo. The result of fitting given in Table 4.3 quantitatively shows that the CoO reduction of BF-1-MgNiCo is 60% and that of BF-1-0.25(MgNiCo)-C is 36%. It means that higher Co loading increases CoO reduction. Fig. 4.10 and Fig. 4.11 shows Ni K-edge XANES spectra on BF-1-MgNiCo and BF-1-0.25(MgNiCo)-C before and after reduction. Although before reduction there is a minor difference of the Ni K-edge XANES spectra, after reduction the spectra are almost overlapped, both catalysts achieved 83 to 86 % reduction, which means no dramatic difference was observed of NiO reduction between catalysts with different metal loading.

To investigate the effect of calcination step on metal oxides reduction, the Co and Ni XANES spectra BF-4-0.25(MgNiCo) and BF-4-0.25(MgNiCo)-C were compared. Figs. 4.12 and 4.13 show the Co K-edge XANES spectra of BF-4-0.25(MgNiCo) and BF-4-0.25(MgNiCo)-C samples before and after reduction, respectively. The results indicate that the Co in this two catalyst samples are close to CoO phase before reduction, which is in consistence with the other group discussed before. Although Fig. 4.13 shows CoO in BF-4-0.25(MgNiCo)-C, which was subjected for 4 times of calcination step, has slightly stronger white line than BF-4-0.25(MgNiCo), which was calcined once, the fitting result shows Co reduction extent in BF-4-0.25(MgNiCo) is 39% while that in BF-4-0.25(MgNiCo)-C is 44%. Considering the error which may exist in fitting process, these two results are not in conflict. The multiple calcination does not have significant influence Co reduction. Fig. 4.14 and Fig. 4.15 give the information about Ni K-edge XANES spectra on BF-4-0.25(MgNiCo) and BF-4-0.25(MgNiCo)-C before and after reduction, respectively. The spectra for the samples are overlapped in both figures and the simulation fitting result of the NiO reduction extent of both catalysts is 89%-90%. This means that calcination steps have no dramatic effect on Ni reduction either.

In conclusion, CoO is harder to be reduced than NiO. This is partially due to the nature of CoO. Cobalt is a weak reducing metal. Like Al_2O_3 to aluminum metal, the CoO film can also be used as a protecting layer to the metal. The other reason is that when mixing in spinel structures with oxides such as Al_2O_3 and/or MgO, Co is inclined to stay in the crystal structure and make the

structure stable rather than coming out during reduction (Wang et al., 2012). The multistep impregnation results in more Co staying in the oxide structure. However, Ni behaves differently in reduction.

The Ni reduction extent of the prepared catalysts is from 79-90%. This result shows an agreement with that of loose powder catalyst developed in our previous research, which the Ni reduction of loose powder catalyst maintains very close in a range of 79–84%, while the Co reduction is between 37 and 51% (Wang et al., 2012). The different reducibility among the catalyst samples may be contributed by the crystal structure and the metal-support interaction. Wang *et al*. (2012) reported that the difference in metal reducibility can be caused by the variation of the interaction of metal Ni and Co with the magnesium and aluminum oxide matrix and the reduction mechanism.

4.2 Catalyst Performance Evaluation

Catalyst evaluation was carried out in a quartz tube reactor with an inner diameter of 6 mm. Before the DRM reaction, 0.10 g catalyst was reduced with a mixture of H_2/N_2 at the ratio 1:4 at 800 ^oC for 4 hours n the same reactor. The furnace temperature then was reduced to 750 ^oC for the reaction. The feed gases, with the ratio of CH_4:CO_2:N_2 in 1:1:1, were introduced at a flow rate 10 L/h.

4.2.1 *Control Experiment*

0.10 g powder of 250 – 355 micrometer, obtained by grinding the virgin BASF-350 alumina ball, was used as catalyst in the control experiment. Fig. 4.16 shows CH_4 conversion during the 16h test, which is steadily between 8.3 % and 8.8 %. Due to the possible 8.1 % error in GC measurement (calculated based on the reference gas, see details in appendix A), this low conversion cannot claim that the BASF-CSS-350 alumina balls have noticeable activity for DRM process.

4.2.2 *Repeat Experiment*

The activity and stability experiment of BF-4-0.25(MgNiCo)-C catalyst was repeated two times under the same experiment condition for 160 h (0.10 g catalyst, 750 ^{o}C, 1 atm, 10 L/h gas flow rate, and $CH_4/CO_2/N_2$ = 1/1/1). Fig. 4.17 shows the CH4 conversion for the repeat tests. In the first test, CH_4 conversion of BF-4-0.25(MgNiCo)-C started at 66.7% and reached at 52.9% after 160 h test. The initial CH4 conversion of the second test for the same catalyst sample was 64.3% and dropped to 58.4% after 160 h reaction. H_2/CO ratio for the first test of BF-4-0.25(MgNiCo)-C started at 0.84 then dropped to 0.76 and for the second test, it was from 0.82 to 0.81. Considering there is 8.1 % error on GC, the catalyst performance test experiment can be reasonably repeated.

4.2.3 *Catalyst Selection*

Catalyst selection was conducted for the prepared samples. The activity and stability within a 5 h TOS was investigated over 0.10 g of catalyst at 750 °C, 1 atm, F = 10 L/h, and $CH_4/CO_2/N_2$ = 1/1/1. The catalyst activity in terms of CH_4 conversion is shown in Fig. 4.19. It is clear that the CH_4 conversion of BF-1-MgNiCo, BF-2-0.5(MgNiCo) BF-4-0.25(MgNiCo) and BF-4-0.25(MgNiCo)-C are much higher than that of the other samples. Among them, BF-4-0.25(MgNiCo)-C shows the highest activity, for which CH_4 conversion was steadily at 66.3 % during the 5 h test. BF-4-0.25(MgNiCo) catalyst had a relatively high initial activity (59.9 % CH_4 conversion) and remained at this level throughout the 5 h of time-on stream. BF-2-0.5(MgNiCo) and BF-1-MgNiCo catalysts also have high initial activities, with CH_4 conversion of 57.0% and 54.4%, respectively; The initial activity follows the order BF-4-0.25(MgNiCo)-C>BF-4-0.25(MgNiCo)>BF-2-0.5(MgNiCo)>BF-1-MgNiCo>BF-1-Mg NiCo-Buffer>BF-2-Mg-MgNiCo. The average ratio of H_2 to CO over BF-4-0.25(MgNiCo)-C, BF-4-0.25(MgNiCo), BF-2-0.5 (MgNiCo) and BF-1-MgNiCo is ranged from 0.77 to 0.84, which may indicate the occurrence of RWSR with less significance. The selectivity results in terms of H_2/CO ratio are shown in Fig. 4.20. The H_2/CO ratio for BF-1-MgNiCo-Buffer was 0.62. For BF-2-Mg-MgNiCo it was 0.62 at the beginning, then dropped to 0.22 suddenly, which means at this point RWSR became more severe for this catalyst.

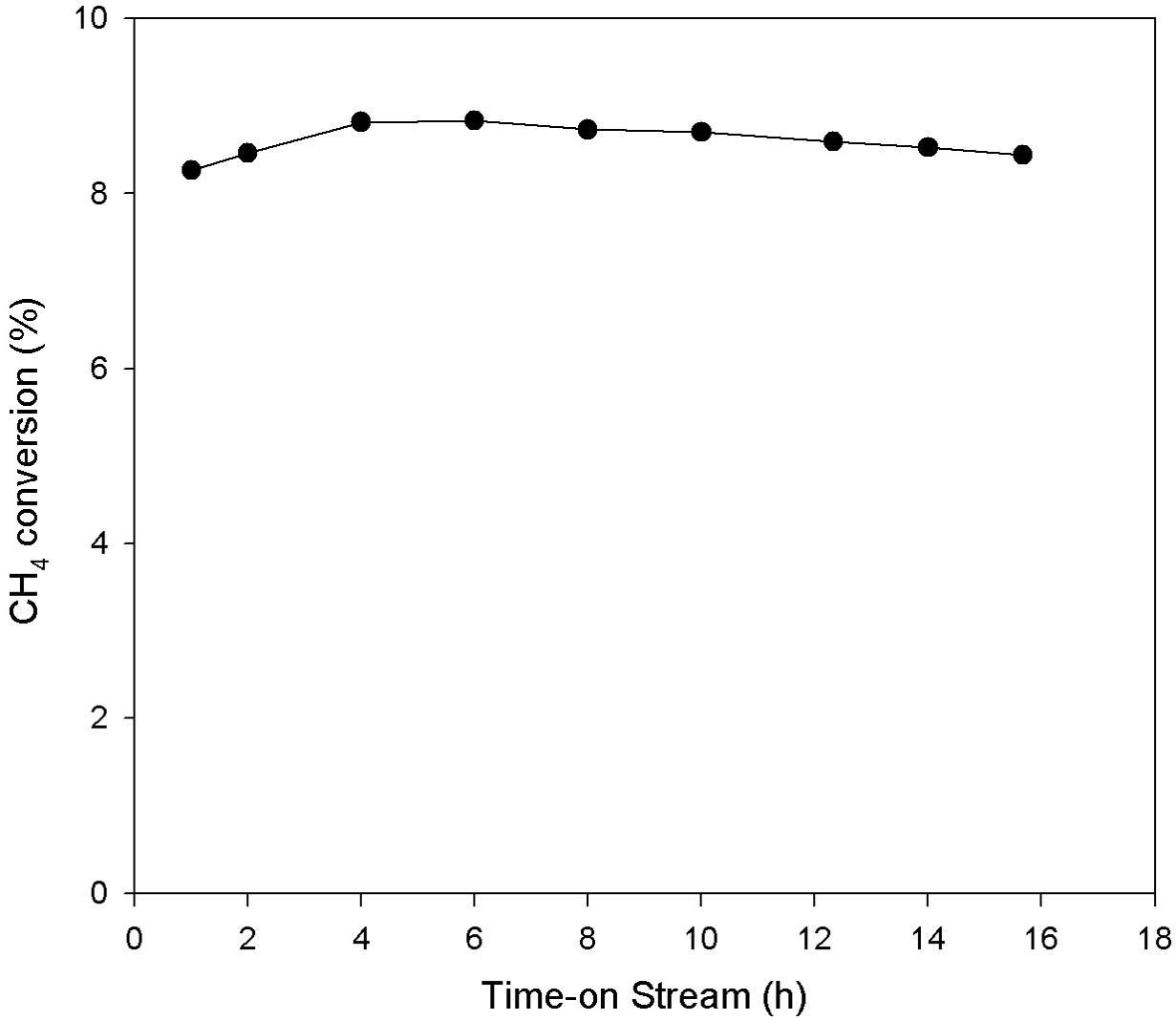

Figure 4.16 CH_4 conversion of BASF-CSS-350 alumina ball. The reaction condition: 0.10 g catalyst, 750 ◦C, 1 atm, F = 10 L/h, $CH_4/CO_2/N_2$ = 1/1/1.

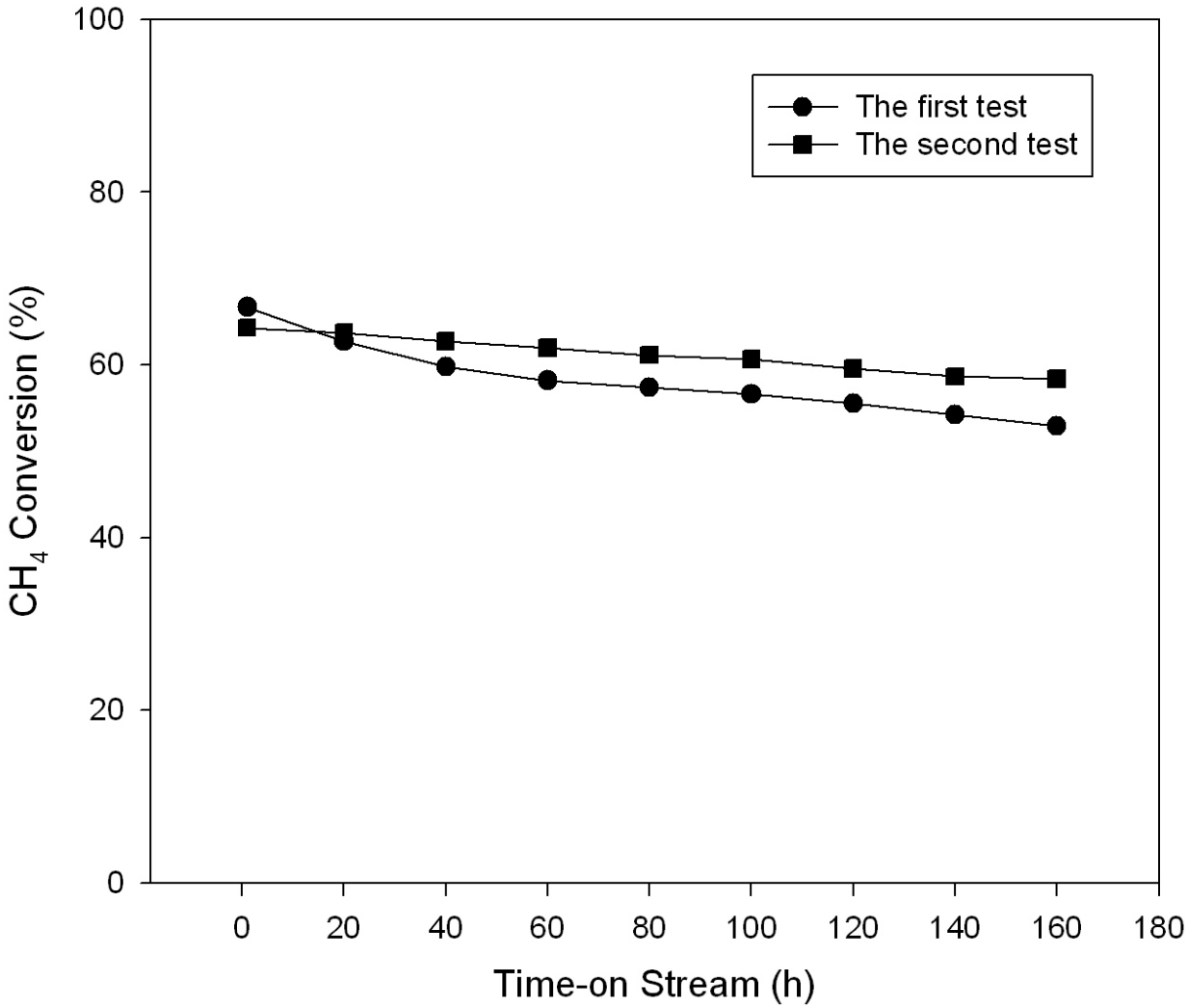

Figure 4.17 Repeat experiment: CH_4 conversion of BF-4-0.25(MgNiCo)-C. The reaction condition: 0.10 g catalyst, 750 ◦C, 1 atm, F = 10 L/h, $CH_4/CO_2/N_2$ =1/1/1.

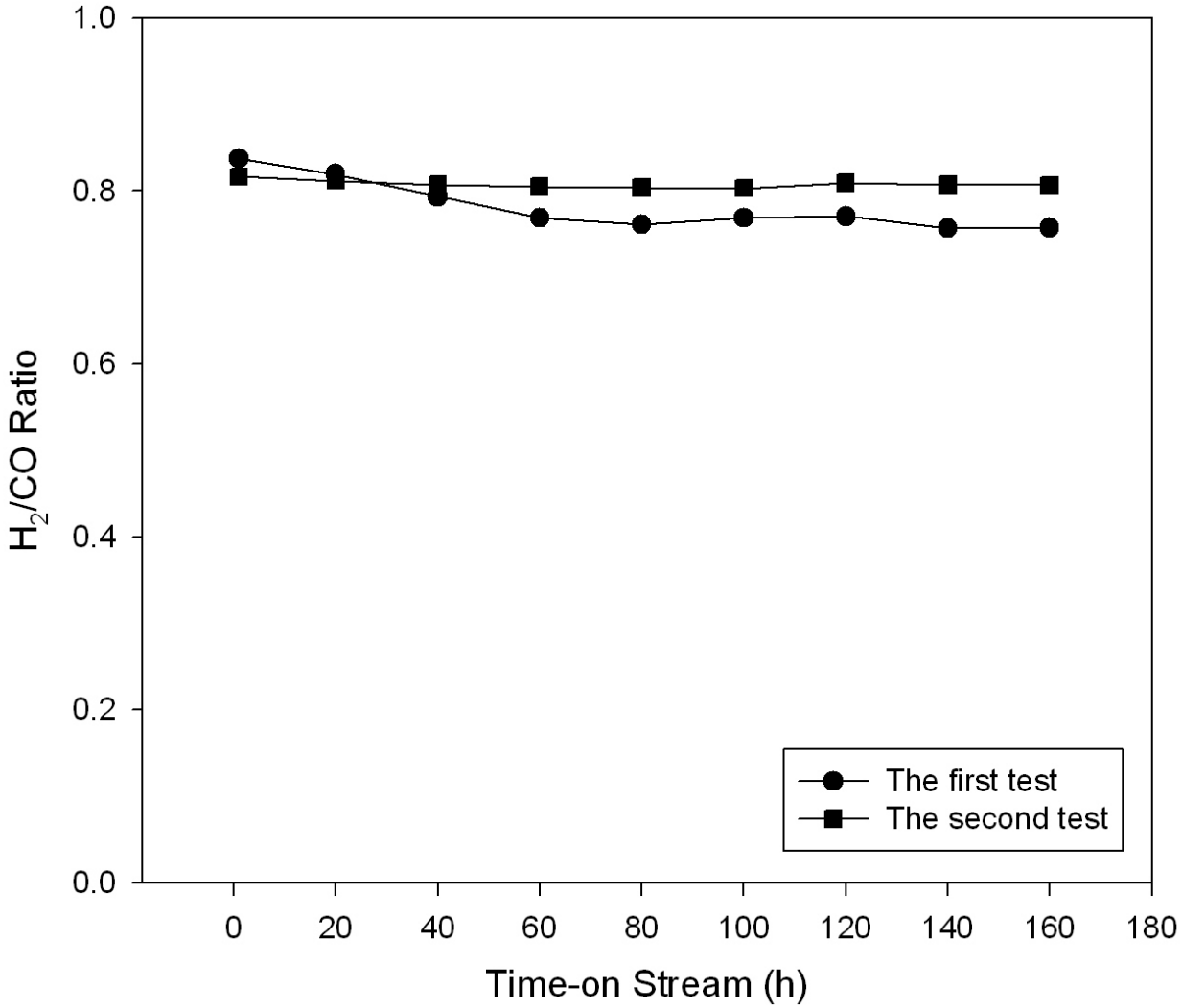

Figure 4.18 Repeat experiment: H_2/CO ratio of BF-4-0.25(MgNiCo)-C. The reaction condition: 0.10 g catalyst, 750 ◦C, 1 atm, F = 10 L/h, $CH_4/CO_2/N_2$ = 1/1/1.

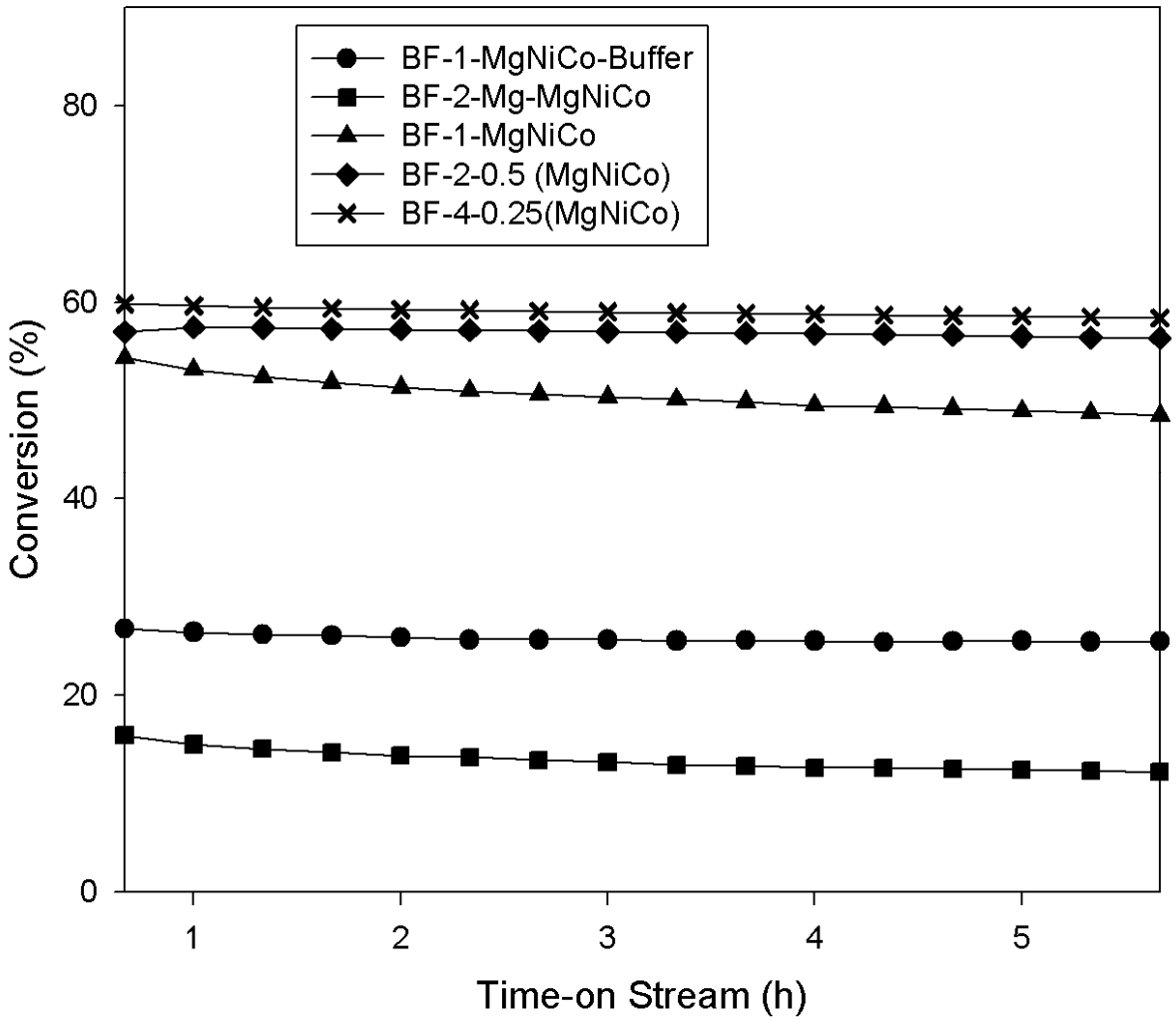

Figure 4.19 Catalyst selection: CH_4 conversion for different catalyst. The reaction condition: 0.10 g catalyst, 750 °C, 1 atm, F = 10 L/h, $CH_4/CO_2/N_2$ = 1/1/1.

The low conversion and H_2/CO ratio of BF-1-MgNiCo-Buffer may be due to the addition of buffer solution (0.26% sodium carbonate and 0.2% sodium bicarbonate) for pH adjustment purpose. Shi *et al*. (1994) reported that the pH of solution has significant influence on both rate and dispersion of the impregnation procedure. Impregnation rate drops with the increase of pH, so the active component is concentrated close to the external pellet surface to form egg-shell catalyst. On the other hand, impregnation rate increases with the decrease of pH, so the egg-york, egg-white, or uniform format of the metal particles will be formed. The pH value of the nitrate salt solutions for making of BF-1-MgNiCo-Buffer is 8.5, but the pH value of the nitrate salt solution for making other catalysts are all around 4.0. This may lead to the active metal concentrated on the surface of the alumina balls in the case of BF-1-MgNiCo-Buffer, which is confirmed by cutting apart the sample. So that may be the reason why it has less effective surface area which causes the relatively low CH_4 conversion and H_2/CO ratio. The samples with better performance, BF-1-MgNiCo, BF-2-0.5(MgNiCo), BF-4-0.25(MgNiCo) and BF-4-0.25(MgNiCo)-C were selected for long-term activity test.

4.2.4 *Long-term Activity Test*

4.2.4.1 Effect of impregnation steps on catalyst reactivity

Longer activity tests were conducted for catalysts BF-1-MgNiCo, BF-2-0.5(MgNiCo) and BF-4-0.25(MgNiCo), respectively to determine the effect of impregnation step on catalyst

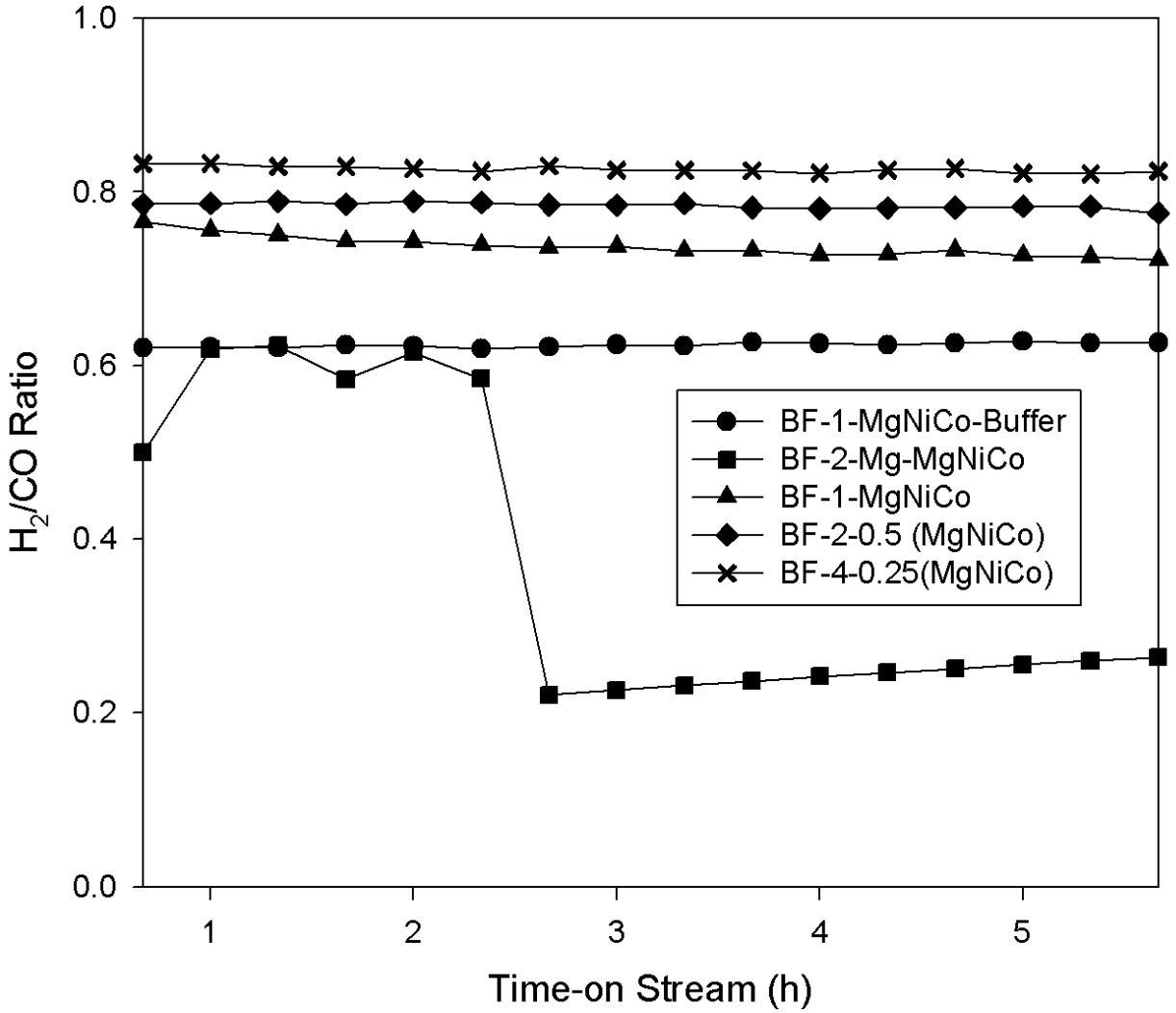

Figure 4.20 Catalyst selection: H_2/CO ratio for different catalyst. The reaction condition: 0.10 g catalyst, 750° C, 1 atm, F = 10 L/h, $CH_4/CO_2/N_2$ = 1/1/1.

activity. Fig. 4.21 shows the results. CH_4 conversion of BF-1-MgNiCo dropped from 53.2 % to 14.0 % in 40 h time-on stream (TOS) while for BF-2-0.5(MgNiCo) it began at 57.5% and decreased to 31.5%. On the other hand, for BF-4-0.25(MgNiCo), CH_4 conversion started from 59.7% and decreased to 41.3% after 200 hours TOS. Based on the results, BF-4-0.25(MgNiCo) has the best activity and stability among the three catalysts. Fig. 4.22 indicates that the H_2/CO ratio of BF-1-MgNiCo, BF-2-0.5(MgNiCo), BF-4-0.25(MgNiCo) started from 0.77, 0.79 and 0.83 and dropped to 0.74 in 40 h TOS, 0.63 in 93 h TOS, and 0.77 in 200 h TOS, respectively. BF-4-0.25(MgNiCo) facilitated higher and more stable H_2/CO ratio, although RWSR may exist but occurrence was less significant.

The results show that multiple impregnation steps can help to enhance the performance of catalyst activity. Zhu *et al*. (2006) reported that the double-step impregnation could enhance the dispersion capacity of copper oxide on the surface of anatase to 0.98 mmol CuO /100m^2 TiO_2, compared with 0.52 mmol CuO /100m^2 TiO obtained in one-step impregnation. They predicted that the CuO/TiO_2 catalysts with double and multiple impregnations would show better activity than those with one-step impregnation. The effect of impregnation to metal dispersion need further research to confirm.

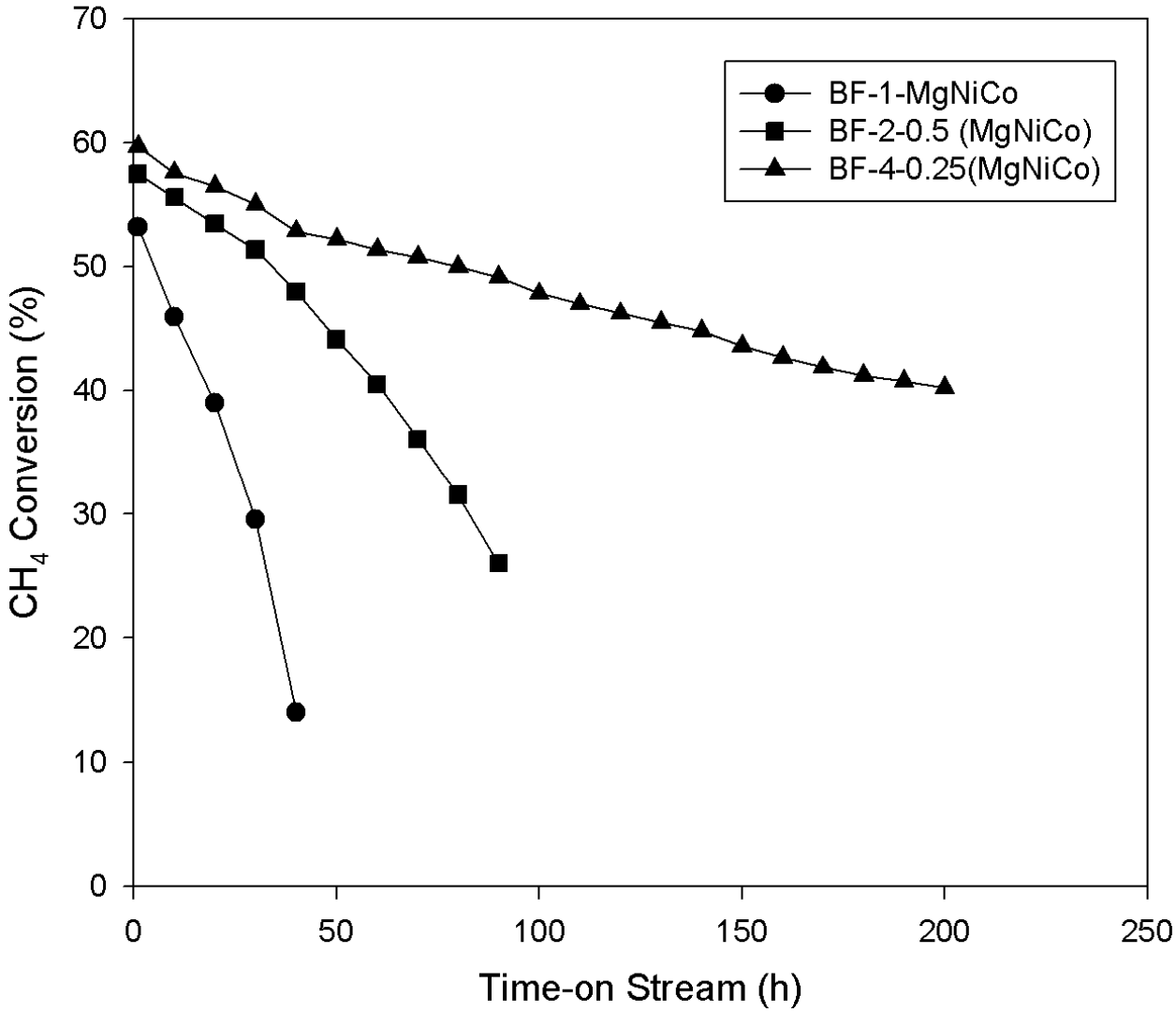

Figure 4.21 Effect of impregnation steps on catalyst reactivity: CH_4 conversion of BF-1-MgNiCo, BF-2-0.5(MgNiCo) and BF-4-0.25(MgNiCo). The reaction condition: 0.10 g catalyst, 750 °C, 1 atm, F = 10 L/h, $CH_4/CO_2/N_2$ = 1/1/1.

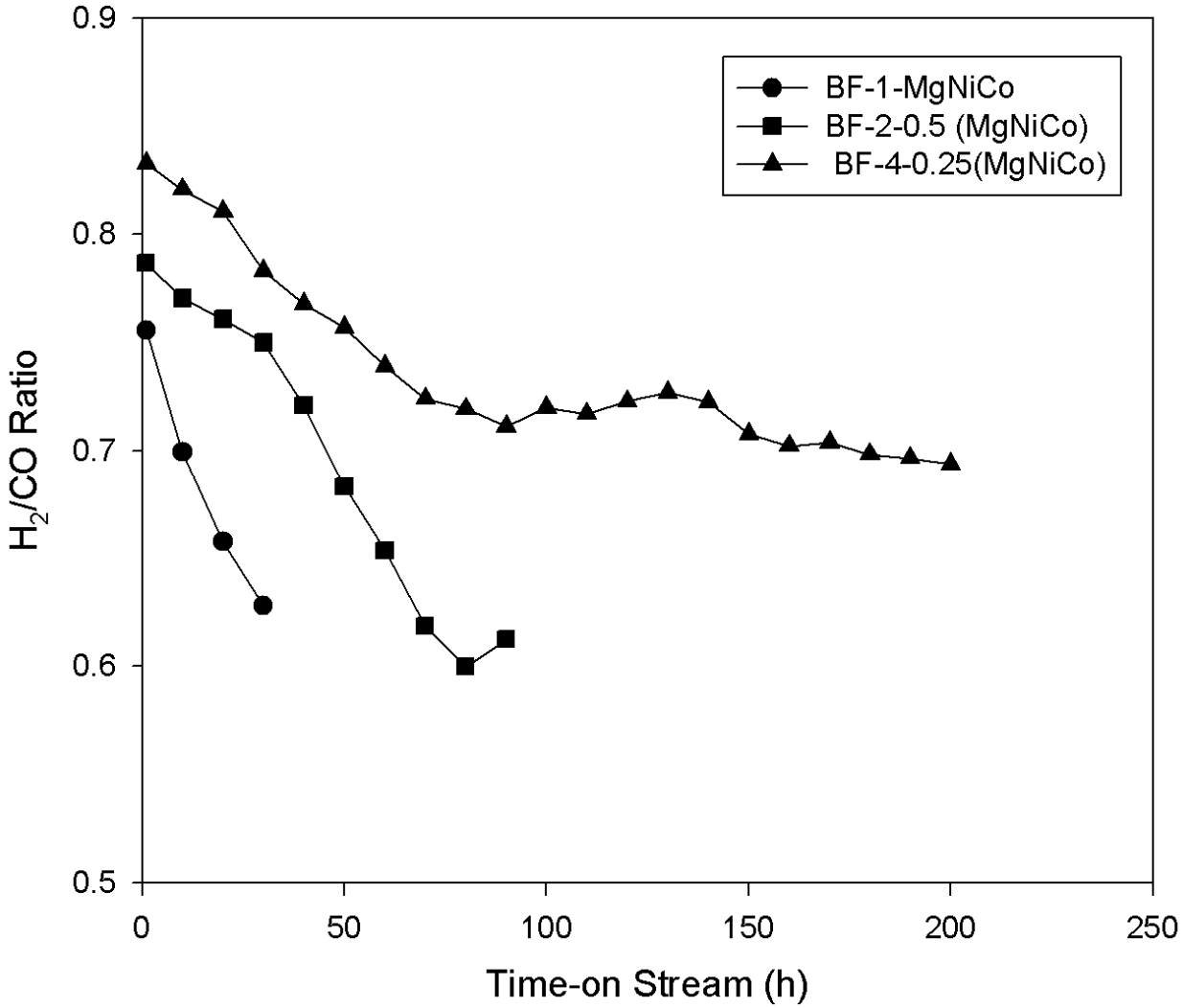

Figure 4.22 Effect of impregnation steps on catalyst reactivity: H_2/CO ratio of BF-1-MgNiCo, BF-2-0.5(MgNiCo) and BF-4-0.25(MgNiCo). The reaction condition: 0.10 g catalyst, 750 °C, 1 atm, F = 10 L/h, $CH_4/CO_2/N_2$ = 1/1/1.

4.2.4.2 Effect of calcination steps on catalyst reactivity

BF-4-0.25(MgNiCo) and BF-4-0.25(MgNiCo)-C have the same target metal loading, the only difference with the two catalysts is the number of calcination steps. Thus, the experiment was conducted with these two catalysts to understand the effect of calcination steps on catalyst activity.

Fig. 4.23 shows CH_4 conversion of the two catalysts, indicatong that during 200 h TOS, CH_4 conversion of BF-4-0.25(MgNiCo) dropped from 59.7% to 41.1% while that of BF-4-0.25(MgNiCo)-C did from 66.7% to 52.8% in 180 h. Fig. 4.24 shows H_2/CO ratio of BF-4-0.25(MgNiCo) and BF-4-0.25(MgNiCo)-C. H_2/CO ratio of BF-4-0.25(MgNiCo) began at 0.83, then drops to 0.70 after 184 h reaction. BF-4-0.25(MgNiCo)-C started at 0.84, then after 50 h reaction, maintained around 0.77.

BF-4-0.25(MgNiCo)-C has better performance and higher stability during the reaction than BF-4-0.25(MgNiCo). This phenomenon (multiple impregnation and calcination can improve the catalytic performance) was also observed by Potdar *et al* (2002). They reported a catalyst of 15 % Ni loaded on $CeZrO_2$ support for CO_2 reforming of CH_4. For one-step calcination, the CH_4 conversion slowly dropped from 95% to 90% during 35 h test. For the same catalyst re-calcined at the same condition, the CH_4 conversion was stabilized around 98 % up to 100 h without significant deactivation. Multiple calcinations is believed to be able to improve metal

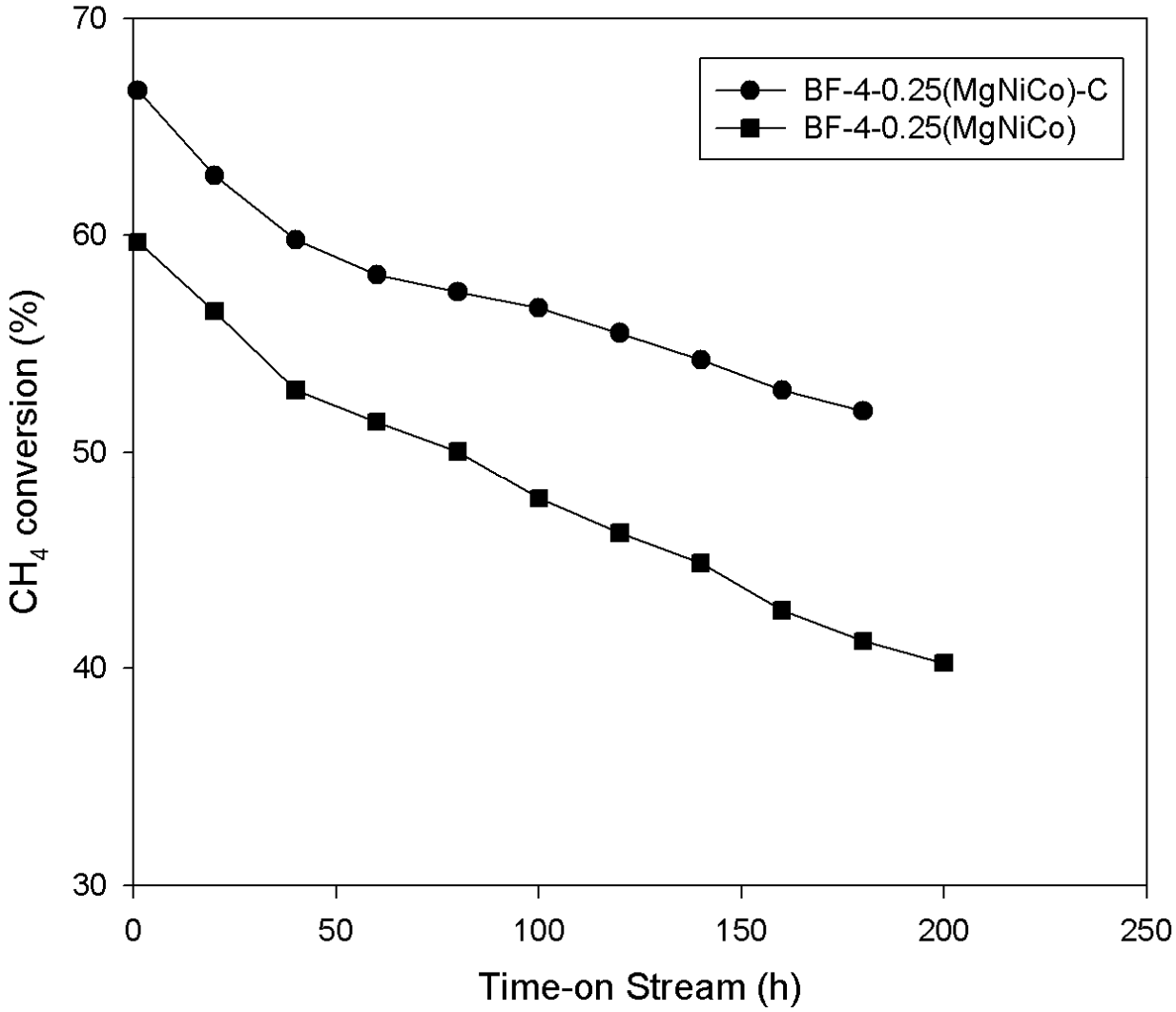

Figure 4.23 Effect of calcination steps on catalyst reactivity: CH_4 conversion of BF-4-0.25(MgNiCo) and BF-4-0.25(MgNiCo)-C. The reaction condition: 0.10 g catalyst, 750°C, 1 atm, F=10 L/h, $CH_4/CO_2/N_2$=1/1/1.

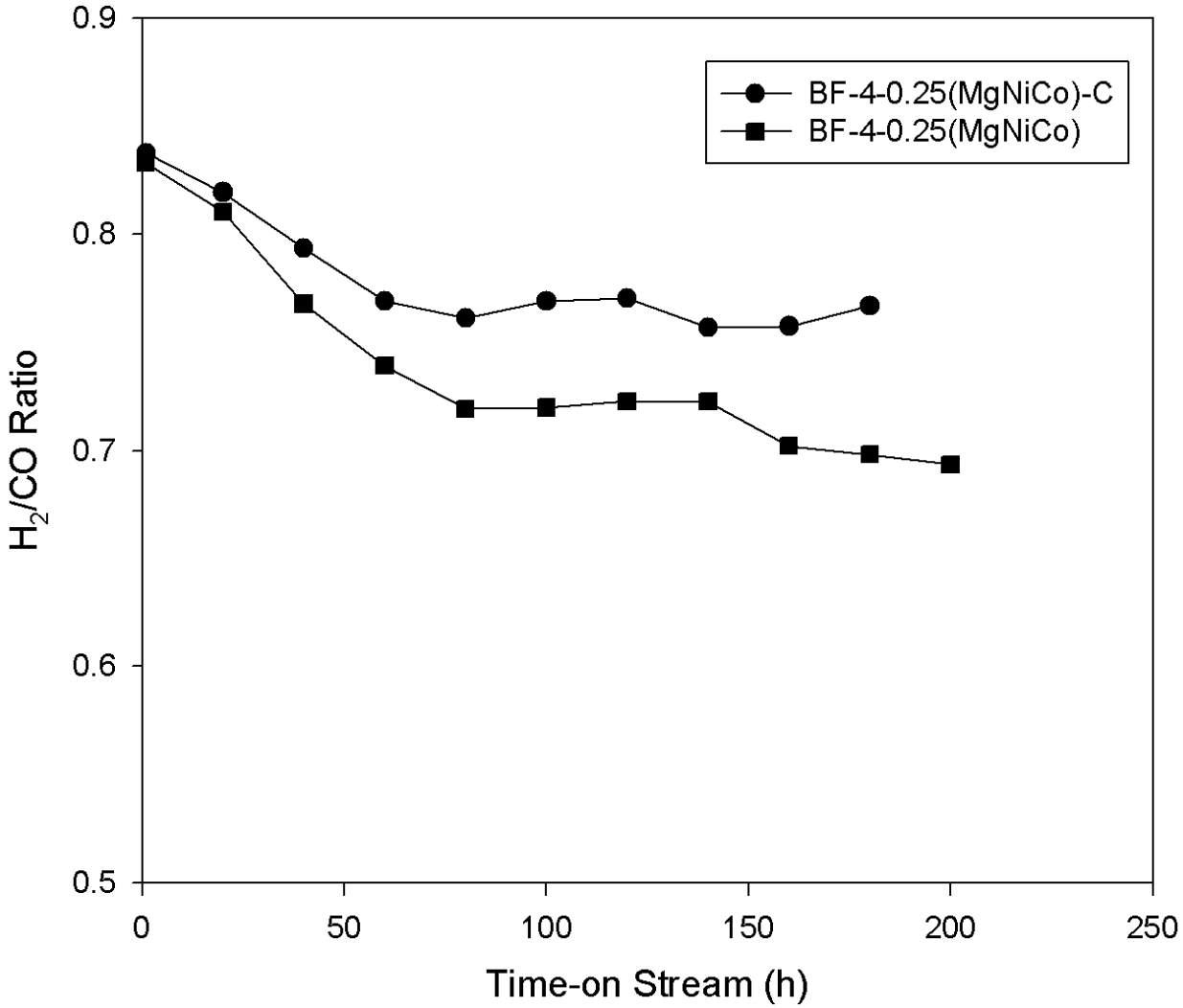

Figure 4.24 Effect of calcination steps on catalyst reactivity: H_2/CO ratio of BF-4-0.25(MgNiCo) & BF-4-0.25(MgNiCo)-C. Reaction condition: 0.10 g catalyst, 750 °C, 1 atm, F=10 L/h, $CH_4/CO_2/N_2$=1/1/1.

distribution on the alumina balls, as well as to provide stronger Ni-support interaction. As a result, the Ni sintering and carbon formation can be prevented. It is recommended that catalyst BF-4-0.25(MgNiCo)-C shoed the best performance among the 10 catalysts prepared in terms of activity, stability and H_2 to CO ratio.

4.2.5 *Comparison of the performance of BF-4-0.25(MgNiCo)-C with loose powder catalysts*

The catalytic activity and stability of the best shaped catalyst made with the BASF CSS 350 alumina balls, BF-4-0.25(MgNiCo)-C, are compared with those of the loose powder catalyst that this group has reported as one of the best catalysts for CO_2 reforming of CH_4 (Zhang *et al*., 2008). The comparison was also made between BF-4-0.25(MgNiCo)-C and the other teo catalysts in publication which are all Ni supported on Al. Because the experiments were conducted in different evaluation condition, the CH_4 conversion was transferred to CH_4 reaction rate for comparison. The following equation was used for calculation:

$$-r_{CH_4} = \frac{F_{CH_4,O} - \Delta F_{CH_4,I}}{22.4 \times 60 \times W_{Cat}} \tag{4.1}$$

where, $F_{CH_4,O}$ stands for the outlet flow rate of CH_4 (mL/min), $F_{CH_4,I}$ stands for the inlet flow rate of CH_4 (mL/min), and $-r_{CH_4}$ means reaction rate of CH_4 (mmol/g-cat/s). W_{Cat} is the weight of catalyst (g-cat).

Fig. 4.25 shows the CH_4 disappearance rate versus TOS for BF-4-0.25(MgNiCo)-C, Ni-Co loose powder catalyst (Zhang *et al*., 2008), MgO-promoted Ni-Al_2O_3 (Koo *et al*., 2008), and

Ni/MgO-Al_2O_3 catalyst (Wang et al., 2000). The CH_4 reaction rate of catalyst started at 0.28 mmol/gcat-s, then dropped slowly to 0.22 mmol/gcat-s after 180 h TOS. According to Zhang *et al*. (2008), the Ni-Co bimetallic loose powder catalyst which was developed in our previous research showed a stable CH_4 reaction rate at 0.68 mmol/gcat/s during 250 h TOS. The loose powder format shows a much better activity. This may due to the better metal dispersion and smaller metal particles obtained in making loose powder Ni-Co bimetallic catalyst. BF-4-0.25(MgNiCo)-C shows a high reaction rate around 0.27 mmol/gcat-s compared with the other two loose powder catalyst samples MgO-promoted Ni-Al_2O_3 (0.09 mmol/gcat-s) and Ni/MgO-Al_2O_3 (around 0.24 mmol/gcat-s).

In conclusion, BF-4-0.25(MgNiCo)-C spherical catalyst shows lower reaction rate compared to the loose powder format but shows compatible or higher activity to other two reported catalysts in similar compositions. Most importantly, it is a shaped catalyst ready for industrial use.

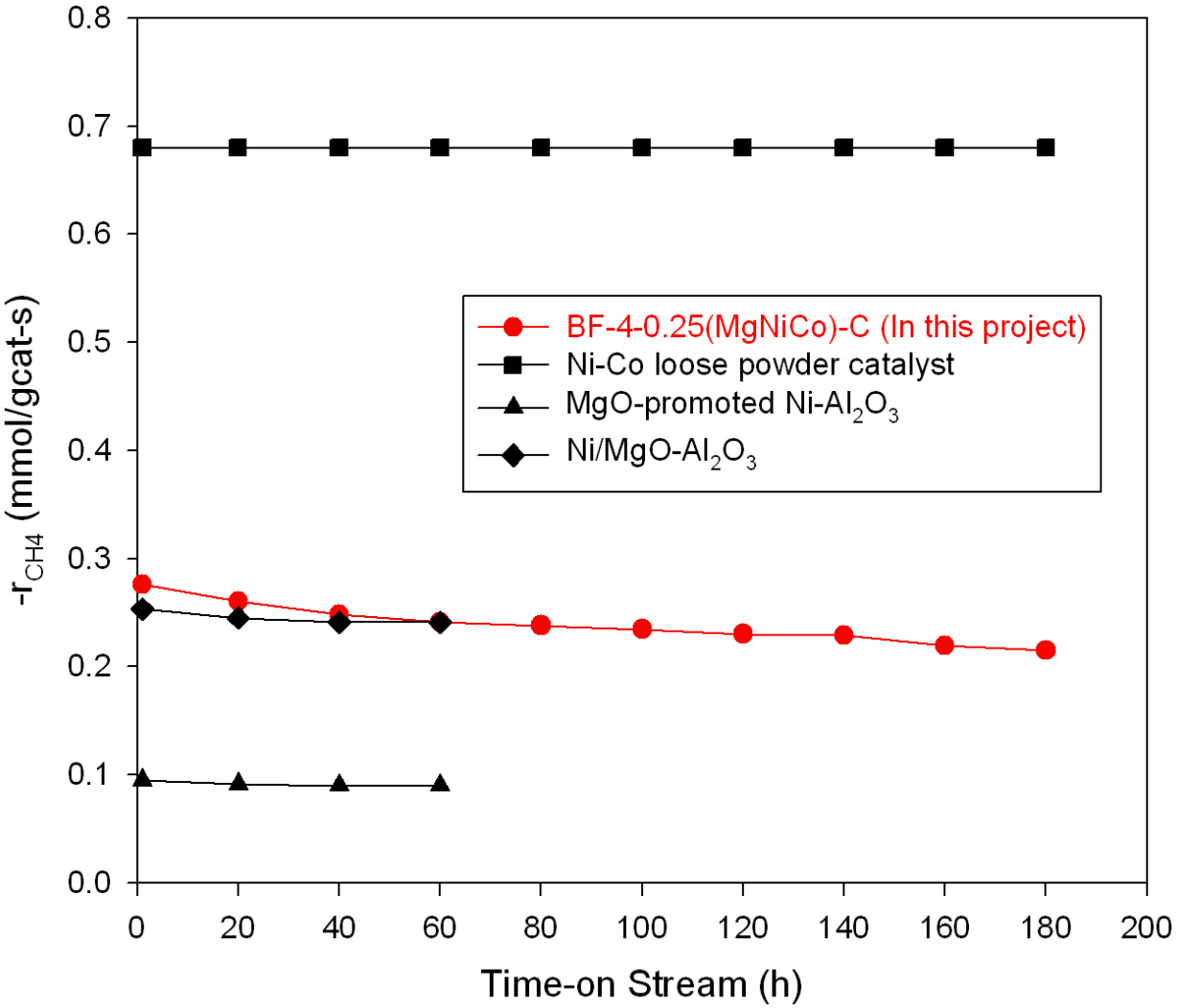

Figure 4.25 Comparison between the performance of shaped catalyst developped in this research and the published ones. CH_4 reaction rate as a function of time-on-stream of BF-4-0.25(MgNiCo)-C, Ni-Co loose powder catalyst (Zhang *et al*., 2008), MgO-promoted Ni-Al_2O_3 (Koo *et al*., 2008), and Ni/MgO-Al_2O_3 (Wang *et al*., 2000).

4.3 Discussion

The major purpose of this project is to find a proper procedure to form a shaped catalyst for CO_2 reforming of CH_4 reaction based on the formula of synthesizing the loose powder catalyst that Dr. Hui Wang and his former students have achieved. The shaped catalyst should have acceptable mechanical strength and catalytic performance. From the results mentioned above, BF-4-0.25(MgNiCo)-C, which was made by multiple impregnation-calcination cycles, shows the best activity and stability among all the samples under investigation. The similar phenomenon was also observed by Postdar *et al*. who found that Ni/Ce-ZrO_2 had 95% initial activity and kept dropping in 35 h activity test, but after recalcined, it showed a 3% increase of initial activity and had steady performance during 100 h test without obvious deactivation. Zhu *et al*. (2006) reported that the double-step impregnation could enhance the dispersion capacity of copper oxide on the surface of anatase TiO_2 than single-step impregnation. They predicted that the CuO/TiO_2 catalysts with double and multiple impregnations would show better activity than those with single-step impregnation. Several characterization tests were conducted attempting to understand the phenomenon. Metal content (Mg, Ni, Co) measured by ICP-MS test shows the metal content of BF-4-0.25(MgNiCo)-C is slightly higher than others among all the prepared catalyst samples in group 1. It means that multiple impregnation-calcination cycles can enhance the metal solution loading on the support. BET test has shown that BF-4-0.25(MgNiCo)-C has lower surface area and smaller pore volume than other catalysts (Table 4). The activity of the catalysts in terms of CH_4 reaction rate follows the order: BF-4-0.25(MgNiCo)-C > BF-4-0.25(MgNiCo) >

BF-2-0.5(MgNiCo) > BF-1-MgNiCo, which is the opposite order of their specific surface area. But it is well established that high BET surface area can provide large accessing area for the reactants to interact with the catalyst, thus resulting in high reaction activity. Surface area is not the dominant factor of catalytic performance for this group of the catalysts. Active sites on the catalysts are another factor. The active metallic Ni and Co are formed during reduction with hydrogen gas (Zhang *et al*., 2007). Therefore, catalyst activity may depend more on the metal dispersion, and other factors such as metal crystalline structure and metal support environment. The possible explanation for the better performance of BF-4-0.25(MgNiCo)-C is that multiple impregnation-calcination cycles have influence on metal dispersion and crystal structure. Zhu *et al*. (2006) pointed out that multiple impregnation steps along with multiple calcination steps have great influence on the dispersion and crystal structure of the catalyst. To confirm this, more characterization tests, TPR, XRD, TEM, need to be done in the future.

The compressive strength test shows that BF-4-0.25(MgNiCo)-C has excellent compressive strength, which is an important factor to a commercial catalyst. The compressive strength of BF-4-0.25(MgNiCo)-C is even higher than CSS-350 alumina support. It means that the mechanical strength of this catalyst is suitable for commercial utilization in industry.

CHAPTER 5 CONCLUSIONS AND RECOMMENDATIONS

The following conclusions can be drawn from this research:

1. BF-4-0.25(MgNiCo)-C made using the preparation procedure proposed by this research has achieved good activity and stability, where the initial conversion was 66.7% and dropped slowly to 52.8% after 200 h reaction, and has even higher mechanical strength compared with the BASF CSS350 alumina ball support. This catalyst will be an excellent candidate for DRM process to be commercialized subject to the further modification and optimization.

2. The two important procedures in the supported catalyst preparation process, impregnation step and calcination step, influence the surface area, pore volume and pore diameter of the prepared catalyst samples. For the desired metal loading amount, multiple impregnation-calcination cycles can improve the performance of the catalyst.

3. Results of XANES show that NiO is easier to reduce than CoO in this catalyst system. The reduction extents for Ni and Co are in the same magnitude as in other catalyst system synthesized by impregnation. However, the multiple impregnation seems to have improved the Ni reduction but inhibited Co reduction.

Based on this research, further investigations should focus on the following respects:

1. To investigate the metal dispersion with characterization method, such as TEM, XPS, and XRD, so that the catalytic activity difference among the prepared samples can be further explained.

2. To improve the catalytic performance of this spherical Ni-Co/MgAlO bimetallic catalyst by optimizing the preparation condition i.e., drying rates, drying temperature and metal impregnation sequence.

3. To conduct catalyst evaluation experiment in a larger reactor with the ball catalysts in order to explore how mass transfer and heat transfer influence the performance of the actual catalyst.

References

Ashcroft, A.T., Cheetham, A.T., Green, M.L.H., Vernon, P.D.F., "Partial oxidation of methane to synthesis gas using carbon dioxide", Nature, **352**, (1991), 225.

Avila, P., Blanco, J., Bahamonde, A., Palacios, J.M., and Barthelemy, C., "Influence of the binder on the properties of catalysts based on titanium-vanadium oxides", Journal of Materials Science, **28**, (1993), 4113

BASF, http://www.basf.com/group/corporate/en/brand/CATALYST_SUBSTRATE_SPHERES, October 7, 2012

Boersma, M.A.M., W.H.M. Thielen, and H.S. Van den Baan, "Experimental and theoretical study of the simultaneous development of the velocity and concentration profiles in the entrance region of a monolithic converter", *Proc. 5th Int. Symp. Chem. React. Eng., Houston,* **72,** (1978) 82.

Boersma, M.A.M., J.A.M. Spierts, W. J. G. Van Lith, and H. S. Van der Baan, "The oxidation of ethene in an empty and packed tubular wall reactor operating in the reaction- and diffusion-controlled regimes", *Chem. Eng. J. (Lausanne)*, **20,** (1980) 177.

Boix, A.V., Miró, E.E., Lombardo, E.A., Mariscal, R., Fierro, J.L.G., "Binder effect upon the catalytic behavior of PtCoZSM5 wash-coated on cordierite monoliths", *Applied Catalysis A: Genera*l, **276,** (2004), 197

Bradford, M.C.J., Vannice, M.A., "CO_2 Reforming of CH_4", *Catalysis Reviews: Science and Engineering*, **41**, (1999), 1

Choudhary, V.R., Devadas, P., Kinage, A.K., Guisnet, M., "Influence of binder on the acidity and performance of H-Gallosilicate (MFI) zeolite in propane aromatization", *Applied Catalysis A: Genera*l, **162**, (1997), 223

Chubb, T.A., "Characteristics of CO_2 CH_4 reforming-methanation cycle relevant to the solchem thermochemical power system", *Solar Energy*, **24**, (1980), 341

Dorado, F., Romero, R., Cañizares, P., "Influence of Clay Binders on the Performance of Pd/HZSM-5 Catalysts for the Hydroisomerization of *n*-Butane", *Industrial & Engineering Chemistry Research*, **40**, (2001), 3428

Dyrssen, D., Turner, D.R., *Carbon dioxide chemistry: Environmental issues*, Edited by Paul, J.,

Pradier, C.M., (1994)

Erdohelyi, A., Cserenyi, J., Solymosi, F., "Activation of CH_4 and Its Reaction with CO_2 over Supported Rh Catalysts", J. Catal. **141**, (1993), 287.

Ertl, G., Knözinger, H., Schüth, F., Weitkamp, J., *Handbook of Heterogeneous Catalysis*, (2008)

Feenan. J.J., Anderson, R.B., Swan, H.W., Hofer, L.J.E., "Chromium Catalysts for Oxidizing Automotive Exhaust", *Journal of the Air Pollution Control Association*, **14**, (1964), 113

Fischer.F, Tropsch.H, Brennst. Chem. **9**, (1928) 39.

Fish, J.D., Hawn, D.C., "Closed Loop Thermochemical Energy Transport Based on CO_2 Reforming of Methane: Balancing the Reaction Systems", *Journal of Solar Energy Engineering*, **109**, (1987), 215

Flytzani-Stephanopoulos, M. and G. E. Voecks, "Conversion of hydrocarbons for fuel cell applications ", Final Report to DOE, DOE/ET-11326, Jet Propulsion Laboratory Publ. 82-37, Pasadena, CA, 1980.

Gadalla, A.M., Bower, B., "The role of catalyst support on the activity of nickel for reforming methane with CO_2", *Chemical Engineering Science*, **43**, (1988), 3049

Hileman, B., "Paper describing synergy of estrogenic chemicals retracted", *Chemical & Engineering News*, **75**, (1997), 9

Hu, Y.H., Ruckemstein, E., "Catalytic conversion of methane to synthesis gas by partial oxidation and CO_2 reforming", *Advances in Catalysis*, **48**, (2004), 297

IPCC (2001b), Climate Change 2001: The Scientific Basis, Contribution of Working Group 1 to the Third Assessment Report of the Intergovernmental Panelon Climate Change, Cambridge University Press, U.K. 944 pp.

Jarvi, G.A., K.B. Mayo, and C.H. Bartholomew, "Monolithic-supported nickel catalysts. I. Methanation activity relative to pellet catalysts", *Chem. Eng. Commun*., **4**, (1980) 325.

Jasra, R.V., Tyagi, B., Badheka, Y.M., Choudary, V.N., Bhat, T.S.G., "Effect of Clay Binder on Sorption and Catalytic Properties of Zeolite Pellets", *Industrial & Engineering Chemistry Research*, **42**, (2003), 3263

Koo, K.Y., H.S. Roh, Y.T. Seo, D.J. Seo, W.L. Yoon, S.B. Park, "Coke study on MgO-promoted

Ni/Al2O3 catalyst in combined H_2O and CO_2 reforming of methane for gas to liquid (GTL) process", *Applied Catalysis A: Genera*l, **183**, (2008), 190.

Li, Y.D., Chang, L., Li, Z., "Measurement methods and reliability analyses for mechanical strength of solid oxide catalysts". *J Tianjin Univ.,* **3,** (1989), 9.

Li, Y.D., Li, X.M., Chang, L., Wu, D.H., Fang, Z.P., Shi, Y.H., "Understandings on the scattering properties of the mechanical strength data of solid catalysts: a statistical analysis of iron-based high-temperature shift catalysts". *Catal Today.,* **51,** (1999), 84.

Li, Y.D., Wu, D.F., Zhang, J.P., Chang, L., Wu, D.H., Fang, Z.P., Shi, Y.H.. "Measurement and statistics of single pellet mechanical strength of differently shaped catalysts". *Powder Technol.,* **113, (**2000), 184.

Marjolein L. Toebes, Jos A. Van Dillen, Krijn P. De Jong., "Synthesis of supported palladium catalysts", Mol. Catal., **75**, (2001) 98.

McCrary, J.H., McCrary, G.E., Chubb, T.A., Nemecek, J.J., Simmons, D.E., "An experimental study of the CO_2 CH_4 reforming-methanation cycle as a mechanism for converting and transporting solar energy", *Solar Energy*, **19**, (1982), 141

Nguyen, S.V., Szabo, V., Trong On, D., Kaliaguine, S., "Mesoporous silica supported $LaCoO_3$ perovskites as catalysts for methane oxidation", *Microporous and Mesoporous Materials*, **54**, (2002), 51

Ostrupnielsen, J.R., Hansen, J.H.B., "CO_2-Reforming of Methane over Transition Metals", J. Catal., **144**, (1993), 38.

Portugal, U.L., Santos, A., Damyanova, S., Marques, C., Bueno, J.M.C., "CO_2 reforming of CH_4 over Rh-containing catalysts", J. Mol. Catal., **184**, (2002), 311.

Potdar, H.S., Roh, H.S., Jun, K.W., Ji, M., Liu, Z.W., "Carbon dioxide reforming of methane over co-precipitate Ni-Ce-ZrO_2 catalysts", Cata. Lett., 95 (2002) 100.

Richardson, T.J., Garrait, M., Hung, J-K., "Carbon dioxide reforming with Rh and Pt–Re catalysts dispersed on ceramic foam supports", Appl. Catal. A, **255**, (2003), 69.

Richerson, D.W., *Modern Ceramic Engineering: Properties, Processing, and Use in Design*, New York, (1922)

Rostrup-Nielsen, J.R., "Industrial relevance of coking", Catal. Today, **37**, (1997), 225.

Ross, J.R.H., “Natural gas reforming and CO_2 mitigation”, *Catalysis Today*, **100**, (2005), 151

Ross, J.R.J., Van Keulen, A.N.J., Hegarty, M.E.S., Seshan, K., “The catalytic conversion of natural gas to useful products”, *Catalysis Today*, **30**, (1996), 193

Rostrup-Nielsen, J.R., “Industrial relevance of coking”, *Catal. Today*, **37**, (1997), 225.

Slagtern, A. , Olsbye, U., Blom, R., Dahl,I . M., “The influence of rare earth oxides on Ni/Al_2O_3 catalysts during CO_2 reforming of CH_4”, Stud. Surf. Sci. Catal. **107,** (1997), 497.

Sun, H., “Preparation and Evaluation of Sol-Gel Made Nickel Catalysts for Carbon Dioxide Reforming of Methane”, M.Sc Thesis, Department of Chemical Engineering, University of Saskatchewan, Saskatoon, SK, Canada (2005)

United Nations Environmental Program (UNEP) and UN framework convention on climate change (2001): Climate change information kit.

Vannice, M.A., “The Catalytic Synthesis of Hydrocarbons from Carbon Monoxide and Hydrogen”, *Catalysis Reviews: Science and Engineering*, **14**, (1976), 153

H. Wang, et al., "XANES and EXAFS studies on metal nanoparticle growth and bimetallic interaction of Ni-based catalysts for CO_2 reforming of CH_4", *Catal. Today* (2012), http://dx.doi.org/10.1016/j.cattod.2012.09.015

Wang, S.B., Lu, C.Q., "Effects of promoters on catalytic activity and carbon deposition of Ni/ ɣ -Al_2O_3 catalysts in CO_2 reforming of CH_4", J Chem Technol Biotechnol, **589**, (2000), 595

Yaakob, Z., Satheesh Kumar, M.N., Ibrahim, M.A., Daud, W.R.W., Kadhum, A.A.H., “Multi-composition Cu-Zn-Al catalyst supported on ZSM-5 for hydrogen production”, *European Journal of Scientific Research*, **28**, (2009), 141

Zakeri, M., Samimi, A., Khorram, M., Atashi, H., Mirzaei, A., “Effect of forming on selectivity and attrition of co-precipitated Co–Mn Fischer–Tropsch catalysts”, *Power Technology*, **200**, (2010), 164

Zhang, J.G., Wang, H., Dalai, A.K., “Development of stable bimetallic catalysts for carbon dioxide reforming of methane”, *Journal of Catalysis*, **249**, (2007), 300.

Zhu, H., Wu, Y., Zhao, X., Wan, H., Yang, L., Hong, J., Yu, Q., Dong, L., Chen, Y., Jian, C., Wei, J., Xu, P., “Influence of impregnation times on the dispersion of CuO on anatase”, *Journal of*

Molecular Catalysis A: Chemical, **243**, (2006), 24.

Zhu, X., Lü, Z., Wei, B., Huang, X., Zhang, Y., Su, W., "A symmetrical solid oxide fuel cell prepared by dry-pressing and impregnating methods", *Journal of Power Sources*, **196**, (2011), 729

APPENDICES

Appendix A Details of Catalyst Preparation

The detailed procedure of catalyst preparation is given as follows.

A.1 BF-1-MgNiCo and BF-1-MgNiCo-Buffer

7.08 g $Mg(NO_3)_2$•$6H_2O$, 1.50 g $Ni(NO_3)_2$•$6H_2O$ and 1.50 g $Co(NO_3)_2$•$6H_2O$ were weighted, then added 4.3 ml water to make the saturated solution. After stirring, the total solution volume is 7.5 ml.

Separate the alumina balls as two groups, each of them contains 2.5g alumina balls. Titrate metal salt solution in the alumina balls evenly.

After titration, added 0.5 ml PH 10 buffer solution (0.26% sodium carbonate and 0.2% sodium bicarbonate) to one sample, named **BF-1-MgNiCo-Buffer.** And the other sample named **BF-1-MgNiCo**. Dry both samples in the air for 4 hours, followed by drying in oven at 120 ^{o}Covernight. Then calcined for 6 hours at 800 ^{o}C.

A.2 BF-2-Mg-MgNiCo

To improve the activity of this catalyst, double the loading amount of Mg to make the ratio of component closer to our powder catalyst.

2.5 g alumina balls were used in this test. For the first impregnation, add $Mg(NO_3)_2 \cdot 6H_2O$ only, 7.07 g $Mg(NO_3)_2 \cdot 6H_2O$ were added, then added 4.0 ml water to make the saturated solution. After stirring, the total solution volume is 6.7 ml. Titrate 1.4 ml to the ball, dried in the air for 4 hours then dried in oven at 120 ^{o}C overnight.

For the second impregnation, 7.08 g $Mg(NO_3)_2 \cdot 6H_2O$, 1.50 g $Ni(NO_3)_2 \cdot 6H_2O$ and 1.50 g $Co(NO_3)_2 \cdot 6H_2O$ were added, then added 5.0 ml water to make the saturated solution. After stirring, the total solution volume is 8.6 ml. Take the balls from the oven, titrate 1.4 ml metal solution to the balls evenly (after titration, some crystal appeared on the surface) , dried in the air for 4 hours then dried in oven at 120 ^oC over night. Calcine for 6 hours at 800 ^oC.

A.3 BF-2-(Mg0.5Ni0.5Co)

2.5 g alumina balls were used in this test, 7.04 g $Mg(NO_3)_2 \cdot 6H_2O$, 0.76 g $Ni(NO_3)_2 \cdot 6H_2O$and 0.76 g $Co(NO_3)_2 \cdot 6H_2O$ were added, then added 4.8 ml water to make the saturated solution. After stirring, the total solution volume is 7.5 ml. Titrate 1.5 ml metal solution to the balls evenly. Dry in the air for 4 hours then in oven at 120 ^oC over night.

For the second impregnation, use the same metal solution, titrate 1 ml evenly to the balls. Dry in the air for 4 hours then dry in oven at 120 ^oC overnight. Calcine for 6 hours at 800 ^oC.

A.4 BF-2-0.5(MgNiCo)

1.25 g alumina balls were used in this test, 3.52 g $Mg(NO_3)_2 \cdot 6H_2O$, 0.76 g Ni(NO3)2·$6H_2O$ and 0.75 g Co(NO3)2·$6H_2O$ were added, then added 4.3 ml water to make the saturated solution. After stirring, the total solution volume is 7.5 ml.

For the first titration, 0.8 ml metal solution was dripped to the balls evenly. Dry in the air for 4 hours then dry in oven at 120 ^oC overnight.

After that repeat the same procedure for the second titration. Calcine for 6 hours at 800 ^oC.

A.5 BF-4-0.25(MgNiCo)

1.26 g alumina balls were used in this test, 1.76 g $Mg(NO_3)_2 \cdot 6H_2O$, 0.38 g $Ni(NO_3)2 \cdot 6H_2O$ and 0.35 g $Co(NO_3)_2 \bullet 6H_2O$ were added, then added water to make the saturated solution. After stirring, the total solution volume is 7.5 ml.

First impregnation: Add 0.8 ml metal solution to alumina balls evenly, dried in the air for 4 hours, then dried at 120C over night.

Second impregnation: Add 0.8 ml metal solution to alumina balls evenly, dried in the air for 4 hours, then dried at 120C over night.

Third impregnation: Add 0.8 ml metal solution to alumina balls evenly, dried in the air for 4 hours, then dried at 120C over night.

Fourth impregnation: Add 0.8 ml metal solution to alumina balls evenly, dried in the air for 4 hours, then dried at 120C over night.

After all impregnation, calcine for 6 hours at 800 ^oC.

A.6 BF-1-0.25(MgNiCo)-C, BF-2-0.25(MgNiCo)-C, BF-3-0.25(MgNiCo)-C and BF-4-0.25(MgNiCo)-C

Weight 10g BASF-350 alumina balls. 1.76 g $Mg(NO_3)_2 \bullet 6H_2O$, 0.38 g $Ni(NO_3)_2 \bullet 6H_2O$ and 0.35 g $Co(NO_3)_2 \bullet 6H_2O$ were added, then added water to make the saturated solution. After stirring, the total solution volume is 7.5 ml.

First impregnation: Add 0.8 ml metal solution to alumina balls evenly, dried in the air for 4 hours, then dried at 120 ^oC over night. Calcine for 6 hours at 800 ^oC. Weight 2.5g catalyst, named **BF-1-0.25(MgNiCo)-C.**

Second impregnation: Add 0.8 ml metal solution to alumina balls evenly, dried in the air for 4 hours, then dried at 120 ^{o}C over night. Calcine for 6 hours at 800 ^{o}C. Weight 2.5g catalyst, named **BF-2-0.25(MgNiCo)-C.**

Third impregnation: Add 0.8 ml metal solution to alumina balls evenly, dried in the air for 4 hours, then dried at 120 ^{o}C over night. Calcine for 6 hours at 800 ^{o}C. Take 2.5g catalyst, named **BF-3-0.25(MgNiCo)-C**.

Fourth impregnation: Add 0.8 ml metal solution to alumina balls evenly, dried in the air for 4 hours, then dried at 120 ^{o}Cover night. Calcine for 6 hours at 800 ^{o}C. Named **BF-4-0.25(MgNiCo)-C**.

Appendix B Instrument Calibration

B.1 MFC (Mass Flow Controller) Calibration Data and Curve

The calibration of mass flow controllers was performed by using DryCal DC1/DC2 Flow meter (BIOS International Corporation) and nitrogen gas. The flow meter was connected after the MFC. At a given (set) "read" flow rate shown in the MFC control panel, the actual flow rate (mL/min) of nitrogen at standard temperature and pressure (STP) was measured by the flow meter. The procedure was repeated 10 times and the average was taken as the actual flow rate for this read.

There are four channels in the MFC. For the channels used to control the other gases than N_2, the flow rate was converted from N_2 to CO_2, CH_4 and H_2, respectively, with the equation:

$$F_X = F_{N_2} \cdot (C_{N_2} / C_X) \tag{B.1}$$

where, F_X is the flow rate of CO_2, CH_4 or H_2 gas, F_{N_2} is the flow rate of N_2, C_{N_2} stands for the heat capacity of N_2 at 21°C and C_X stands for the heat capacity of CO_2, CH_4 or H_2 at 21°C.

Gas	Heat capacity
N_2	0.2885
H_2	0.2847
CO_2	0.3749
CH_4	0.3547

In the following calibration data and curves, except for N2, the actual flow rate is for the specific gas after the calculation.

B.1.1 MFC Calibration Data and Curve for N_2 channel (Channel 1 in MFC control box)

Table B-1 N_2 MFC Calibration Data

Read (mL/min)	Actual at STP (mL/min)
19.6	34.0
29.6	45.6
39.7	55.5
49.7	66.4
59.7	77.1
69.7	87.9
79.7	98.7
89.7	109.4
99.7	120.3
109.7	131.0
119.7	141.7
129.5	152.2
139.5	162.9
149.5	172.6
159.5	184.2
169.5	195.1
179.5	205.7
189.5	216.6
199.5	227.4
209.5	237.8
219.5	248.7
229.5	259.5
239.5	270.5
249.6	281.7
259.6	292.5
269.6	303.4
279.6	314.5
289.6	325.7

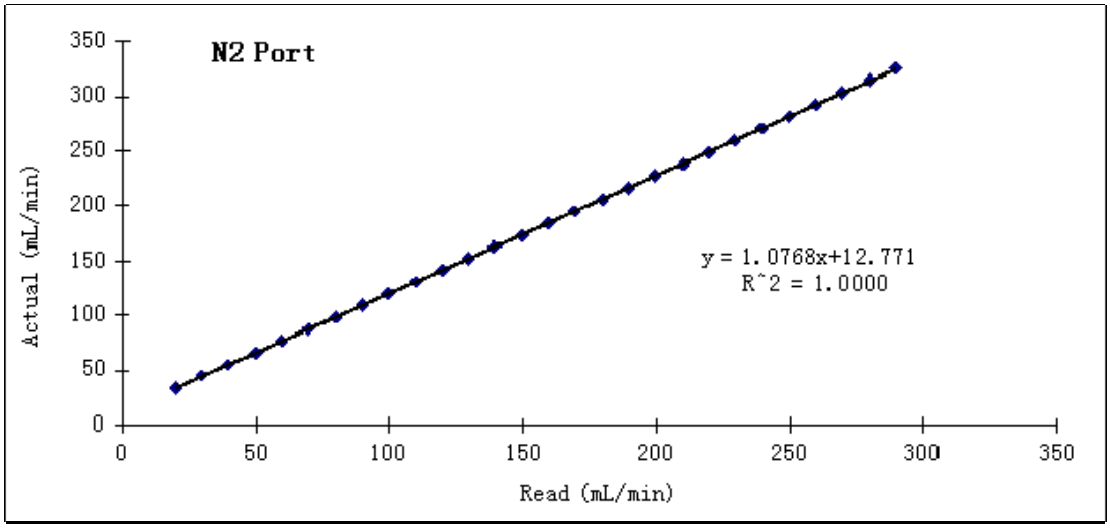

Fig. B-1 N_2 MFC Calibration Curve

B.1.2 CO_2 MFC Calibration Data and Curve (Channel 2)

Table B-2 CO_2 MFC Calibration Data

Read (mL/min)	Actual at STP (mL/min)
19.8	25.0
29.8	36.0
39.8	47.0
49.8	58.0
59.8	69.0
69.7	79.7
79.7	90.7
89.7	101.6
99.7	112.5
109.7	123.5
119.7	134.3
129.8	145.1
139.8	156.0
149.8	166.8
159.8	177.5
169.8	188.5
179.8	199.3
189.7	210.2
199.7	220.9
209.7	231.3
219.7	242.6
229.7	253.3
239.7	264.4
249.8	275.3
259.8	286.9
269.7	296.7
279.8	308.6
289.8	318.9

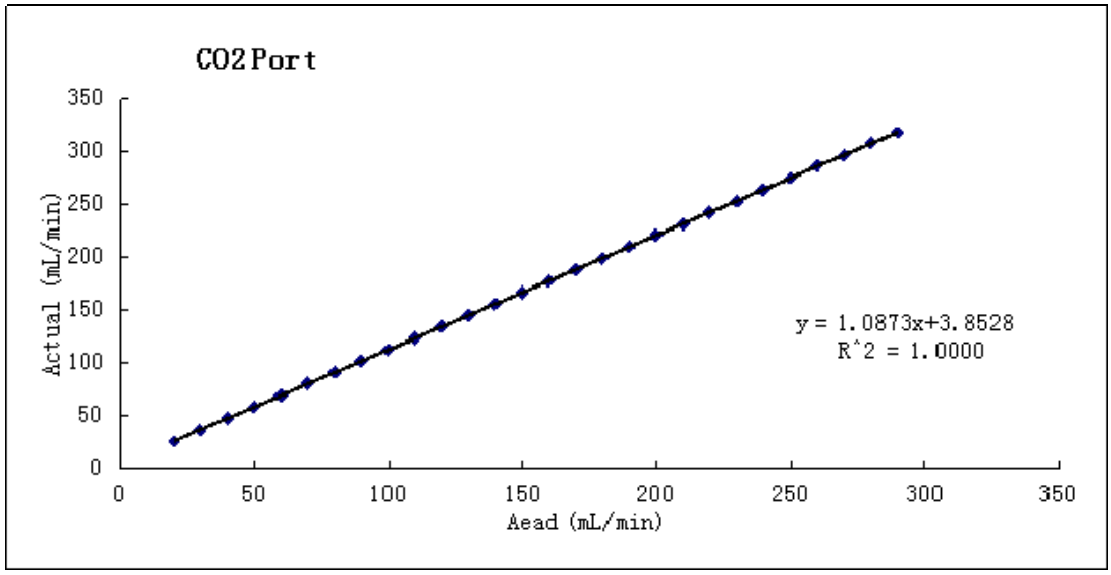

Fig. B-2 CO_2 MFC Calibration Curve

C: CH_4 MFC Calibration Data and Curve (Channel 3)

Table B-3 CH_4 MFC Calibration Data

Read (mL/min)	Actual at STP (mL/min)
19.7	27.1
29.8	38.8
39.8	50.5
49.9	62.1
59.9	73.8
69.8	85.2
79.8	95.8
89.8	108.4
99.8	119.9
109.8	129.0
119.8	142.4
129.8	154.4
139.8	165.8
149.8	177.4
159.8	188.5
169.9	200.1
179.9	211.4
189.8	222.8
199.8	234.1
209.8	245.3
219.8	257.0
229.8	268.1
239.8	278.8
249.8	291.1
259.8	303.0
269.8	315.8
279.8	326.5
289.8	336.4

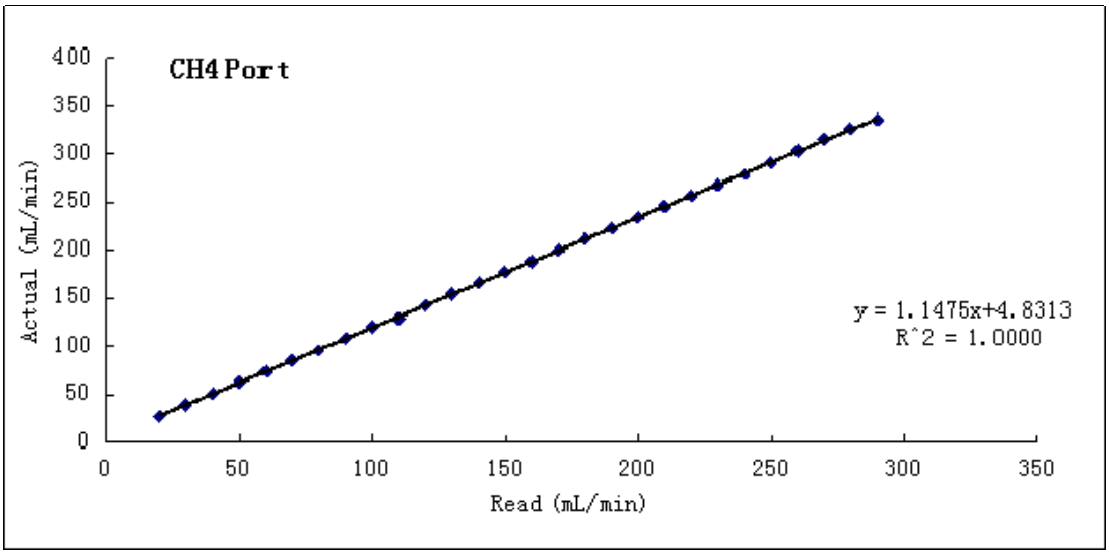

Fig. B-3 CH_4 MFC Calibration Curve

D: H_2 MFC Calibration Data and Curve (Channel 4)

Table B-4 H_2 MFC Calibration Data

Read (mL/min)	Actual at STP (mL/min)
10.0	14.7
13.9	20.9
19.9	29.9
24.0	35.9
30.0	44.8
34.0	50.8
39.9	59.6
43.9	65.5
49.9	74.4
53.9	80.3
60.0	89.1
63.9	95.0
69.9	104.0
73.9	109.8
79.9	118.8
83.9	124.7
89.9	133.7
93.9	139.6
99.9	148.7

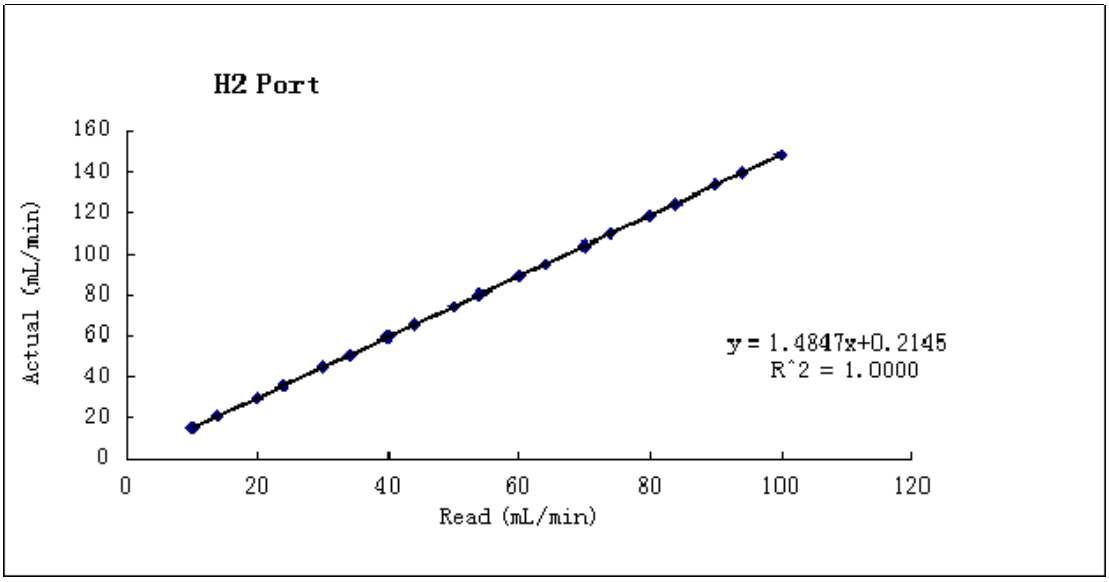

Fig. B-4 H_2 MFC Calibration Curve

B.2 GC Calibration Data and Curve

To calibrate the Gas Chromatography (GC), at least three times injection for each concentration was done. Then the average area was calculated to use in the calibration curve.

A: CO GC Calibration Data and Curve

CO gas was calibrated with N_2 gas as reference. Keep N_2 flow rate constant, then change the the CO flow rate by MFC in channel 4.

Table B-5 CO Calibration Data

X (Amount (mol %))	Y (Area)
27.3	10364.8
24.5	9146.6
21.4	7929.0
16.2	5933.5
33.7	12133.7

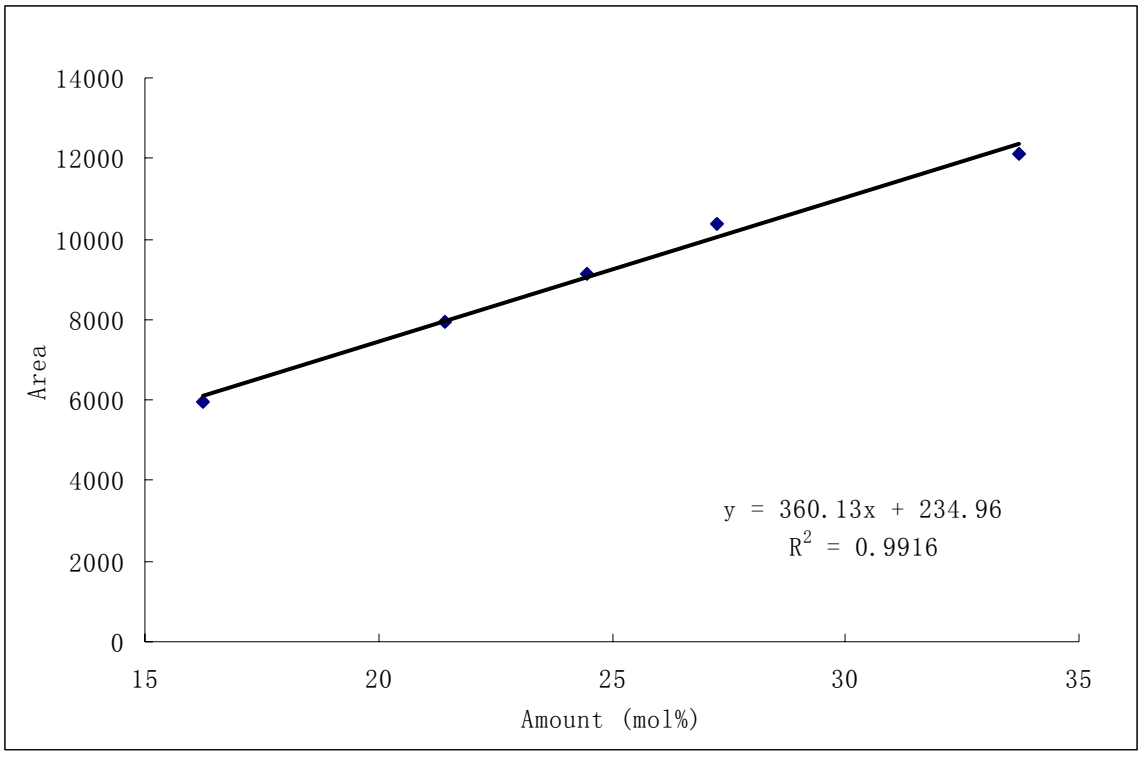

Fig.B-5 CO GC Calibration Curve

B: H_2 GC Calibration Data and Curve

H_2 gas was calibrated with N_2 gas as reference. Keep N_2 flow rate constant, then change the the CO flow rate by MFC in channel 4.

Table.B-6 H_2 Calibration Data

X (Amount (mol %))	Y (Area)
27.3	110.3
24.5	97.1
21.4	83.3
16.2	60.9
33.7	134.4

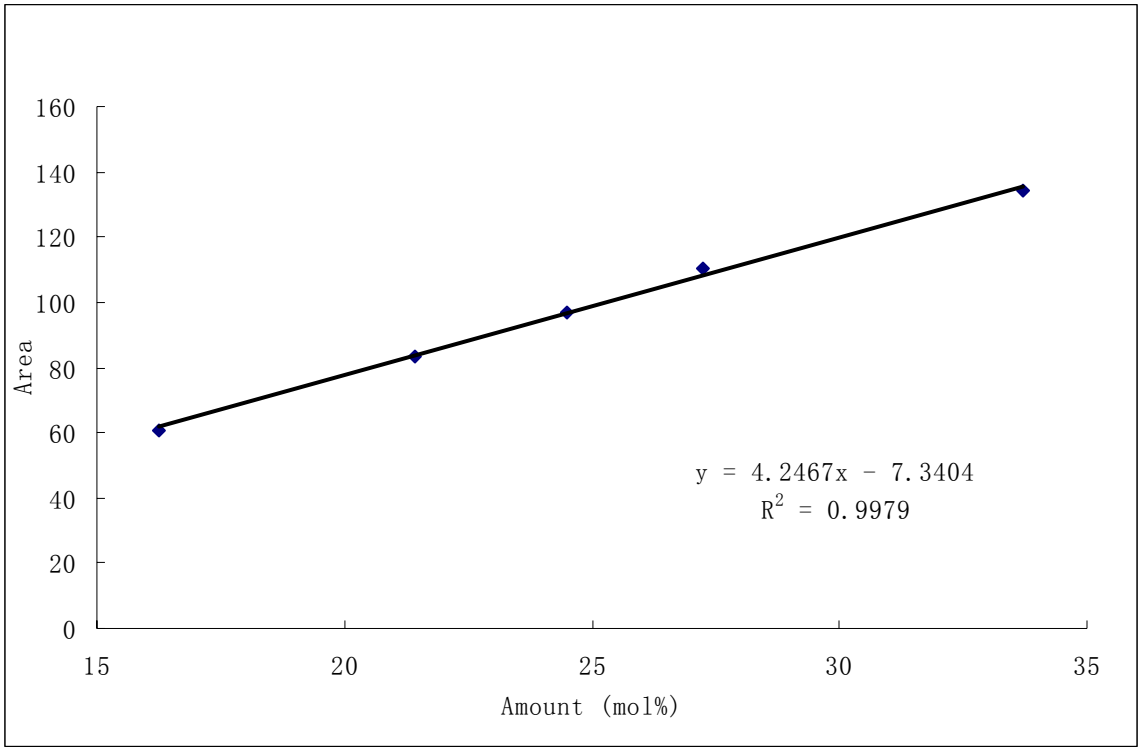

Fig. B-6 H_2 Calibration Curve

C: N_2 Calibration Data and Curve

Table B-7 N_2 Calibration Data

X (Amount (mol %))	Y (Area)
45.5	16445.5
51.0	18129.3
57.2	20038.9
67.5	23274.6
32.6	10903.2

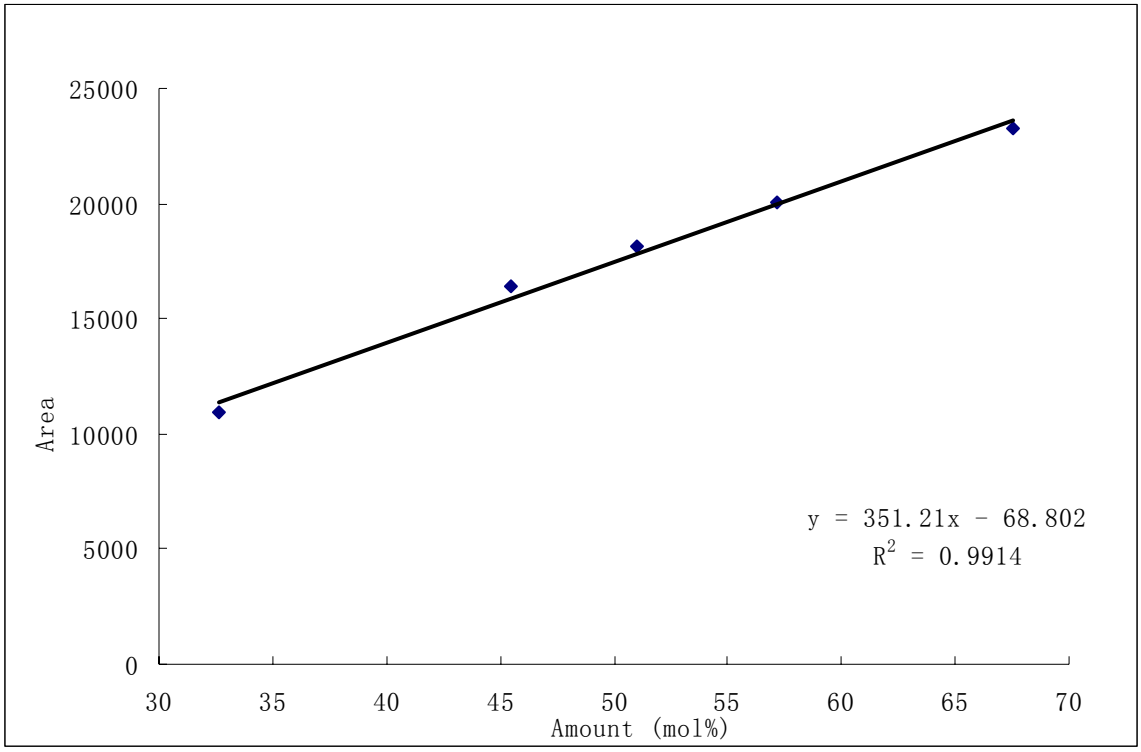

Fig. B-7 N_2 Calibration Curve

D: CO_2 Calibration Data and Curve

Table B-8 CO_2 Calibration Data

X (Amount (mol %))	Y(Area)
6.8	2632.6
8.9	4173.8
13.1	7162.6
33.4	24759.2
59.4	43272.8

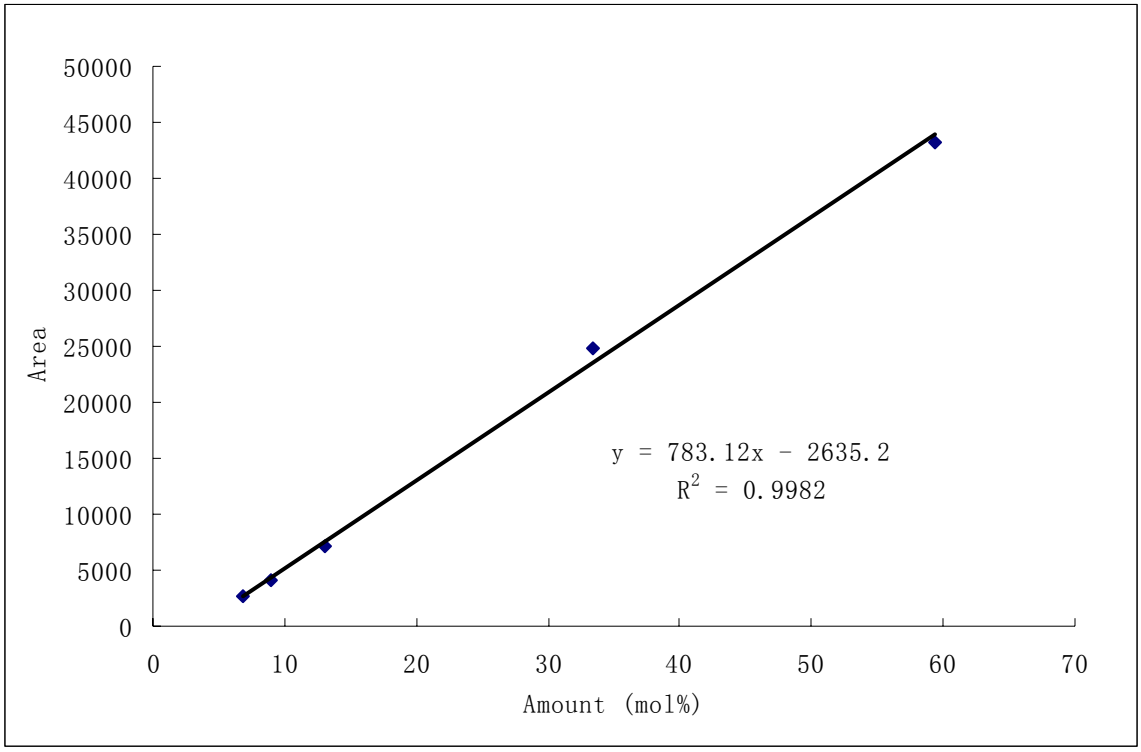

Figure B-8 CO_2 Calibration Curve

E: CH_4 Calibration Data and Curve

Table B-9 CH_4 Calibration Data

X (Amount (mol %))	Y (Area)
50.0	15074.6
41.1	12045.6
34.3	9899.3
26.9	7377.9
19.1	5129.2

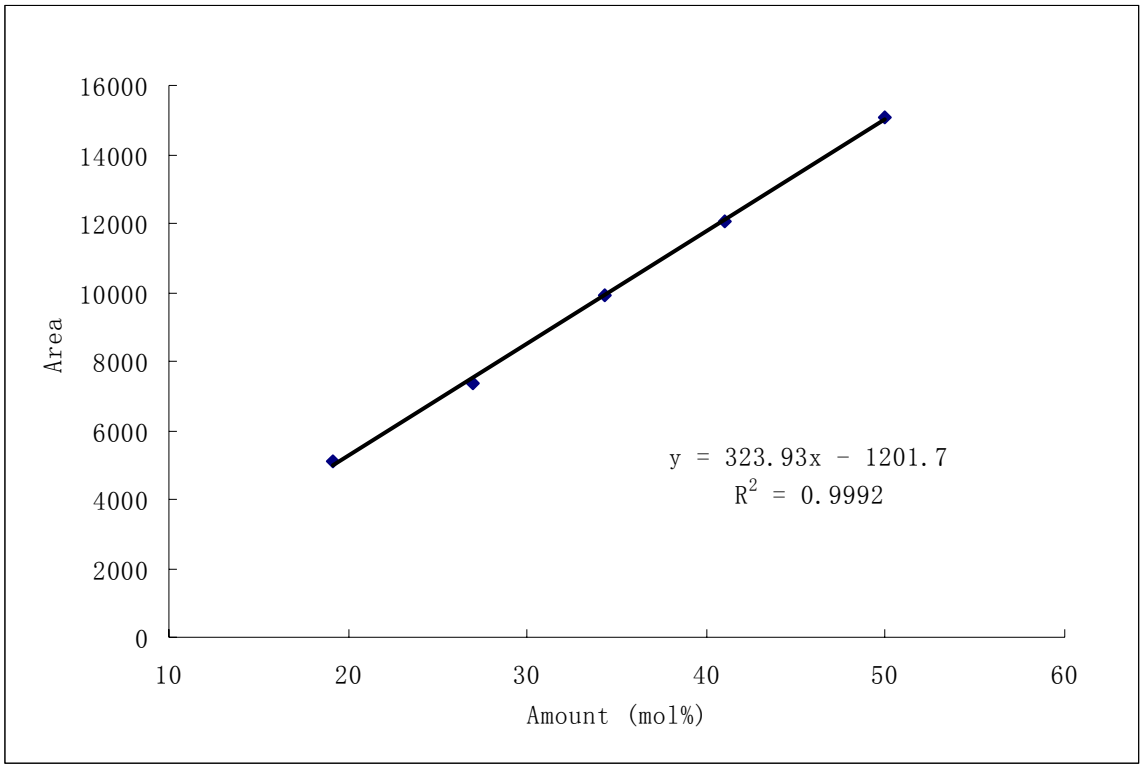

Figure B-9 CH_4 Calibration Curve

B.3. GC Error

GC error is calculated by testing a mixed gas, which contains 5 % H_2 and 95 % N_2. Then use H_2 % as reference to determine the error by comparing the actual value and calculated value. The ressults mean that the DATA GC generated are reliable.

Table 4-F Data of calculating GC error based on 5 % H_2 and 95 % N_2 mixed gas

H_2 % based on GC results	**Error (%)**
5.4	7.3
5.3	6.8
5.3	6.3
5.4	8.1
5.4	7.1
5.4	7.7
5.4	8.4
5.4	7.9
5.5	9.0
5.4	8.1
5.4	8.8
5.4	7.1
5.3	7.0
5.5	9.5
5.5	9.5
5.5	9.9
5.5	9.8
Average Error	**8.1**

Appendix C The Raw Data of Tests

Table C-1 Raw data of Compressive Strength Test

Catalyst Name	Compressive Load (N)									
BF-1-1/4(MgNiCo)-C	33.73	44.76	47.09	32.14	33.08	38.04	32.35	37.00	40.31	31.06
BF-2-1/4(MgNiCo)-C	29.30	33.89	45.00	44.18	35.08	17.33	34.21	33.76	33.05	29.22
BF-3-1/4(MgNiCo)	27.03	35.23	13.36	31.92	30.71	30.09	21.78	20.85	35.89	27.29
BF-4-1/4(MgNiCo)	31.64	37.51	15.08	33.90	42.56	25.72	31.39	21.88	28.37	21.35
BF-Buf-MgNiCo	22.93	33.75	19.55	23.64	11.07	19.69	14.61	15.20	20.85	16.68
BF-2-2(Mg0.5Ni0.5Co)	18.52	31.14	24.01	16.13	8.70	18.03	21.62	21.64	14.18	18.63
Virgin balls	15.51	30.14	29.16	17.28	35.46	32.36	10.56	20.45	10.31	15.66

Table C-2 Concentration of gases in effluent for the evaluation of repeat experiment: BF-4-0.25(MgNiCo)-C-1

Time (h)	N_2 (%)	CH_4 (%)	CO_2 (%)	H_2 (%)	CO (%)
1	22.5	8.2	5.5	28.7	35.2
20	22.5	8.4	5.6	28.5	35.1
40	22.6	8.6	5.7	28.2	34.9
60	22.7	8.7	5.8	28.0	34.9
80	22.8	8.9	5.9	27.8	34.7
100	22.8	9.2	6.0	27.6	34.4
120	23.0	9.5	6.1	27.5	33.9
140	23.1	9.8	6.3	27.2	33.7
160	23.2	9.9	6.4	27.1	33.6

Table C-3 Concentration of gases in effluent for the evaluation of repeat experiment: BF-4-0.25(MgNiCo)-C-2

Time (h)	N_2 (%)	CH_4 (%)	CO_2 (%)	H_2 (%)	CO (%)
1	22.1	7.5	5.3	29.6	35.4
20	22.7	8.7	5.8	28.3	34.5
40	23.3	9.6	6.2	27.0	34.0
60	23.7	10.1	6.5	25.9	33.7
80	23.9	10.4	6.6	25.4	33.6
100	23.9	10.6	6.7	25.5	33.3
120	24.1	10.9	7.0	25.2	32.8
140	24.2	11.1	7.1	25.0	32.7
160	24.6	11.9	7.6	24.1	31.8

Table C-4 Concentration of gases in effluent for the evaluation of catalyst selection raw data: BF-1-(MgNiCo)-Buffer

Time (h)	N_2 (%)	CH_4 (%)	CO_2 (%)	H_2 (%)	CO (%)
0	11.3	33.0	18.3	24.5	13.0
0.3	11.2	33.0	18.1	24.7	13.1
0.7	11.1	32.9	17.9	24.8	13.2
1.0	11.1	32.9	17.9	24.9	13.3
1.3	11.1	32.9	17.8	24.9	13.3
1.7	11.1	32.9	17.8	25.0	13.3
2.0	11.0	32.8	17.7	25.1	13.4
2.3	11.0	32.9	17.7	25.1	13.4
2.7	11.0	32.9	17.6	25.1	13.4
3.0	11.0	32.9	17.6	25.1	13.4
3.3	11.0	32.9	17.6	25.1	13.4
3.7	11.0	32.9	17.6	25.1	13.4
4.0	11.0	32.9	17.6	25.1	13.5
4.3	11.0	32.9	17.5	25.1	13.4
4.7	11.0	32.9	17.5	25.1	13.4
5.0	11.0	32.9	17.5	25.1	13.5

Table C-5 Concentration of gases in effluent for the evaluation of catalyst selection raw data: BF-2-Mg-MgNiCo

Time (h)	N_2 (%)	CH_4 (%)	CO_2 (%)	H_2 (%)	CO (%)
0	34.5	29.6	18.7	5.7	11.5
0.3	34.2	29.7	18.9	6.6	10.6
0.7	34.4	30.0	19.1	6.3	10.2
1.0	34.6	30.4	19.4	5.7	9.8
1.3	34.7	30.5	19.5	5.8	9.5
1.7	34.9	30.8	19.7	5.4	9.2
2.0	36.1	32.0	20.5	2.1	9.3
2.3	36.2	32.1	20.6	2.0	9.1
2.7	36.2	32.2	20.7	2.1	8.9
3.0	36.2	32.3	20.8	2.0	8.7
3.3	36.2	32.4	20.8	2.1	8.5
3.7	36.3	32.4	20.9	2.0	8.3
4.0	36.3	32.5	21.0	2.0	8.2
4.3	36.4	32.5	21.0	2.0	8.0
4.7	36.4	32.6	21.1	2.0	7.9
5.0	36.4	32.7	21.1	2.0	7.8

Table C-6 Concentration of gases in effluent for the evaluation of catalyst selection raw data: BF-1-(MgNiCo)

Time (h)	N_2 (%)	CH_4 (%)	CO_2 (%)	H_2 (%)	CO (%)
0	23.9	11.1	7.0	25.1	32.8
0.3	24.2	11.6	7.2	24.5	32.5
0.7	24.3	11.8	7.4	24.2	32.2
1.0	24.5	12.0	7.5	23.9	32.1
1.3	24.6	12.2	7.6	23.7	31.9
1.7	24.7	12.3	7.6	23.5	31.8
2.0	24.7	12.5	7.7	23.4	31.7
2.3	24.8	12.5	7.8	23.3	31.6
2.7	24.9	12.7	7.8	23.1	31.6
3.0	24.9	12.7	7.9	23.0	31.5
3.3	24.9	12.9	7.9	22.9	31.4
3.7	25.0	12.9	8.0	22.8	31.3
4.0	25.0	13.0	8.0	22.9	31.2
4.3	25.1	13.1	8.0	22.7	31.2
4.7	25.1	13.1	8.1	22.6	31.1
5.0	25.2	13.2	8.1	22.4	31.0

Table C-7 Concentration of gases in effluent for the evaluation of catalyst selection raw data: BF-2-0.5(MgNiCo)

Time (h)	N_2 (%)	CH_4 (%)	CO_2 (%)	H_2 (%)	CO (%)
0	23.2	10.2	6.5	26.4	33.6
0.3	23.1	10.1	6.5	26.6	33.8
0.7	23.1	10.1	6.5	26.6	33.7
1.0	23.2	10.1	6.5	26.5	33.7
1.3	23.2	10.1	6.5	26.6	33.7
1.7	23.2	10.1	6.5	26.5	33.6
2.0	23.2	10.2	6.5	26.4	33.7
2.3	23.2	10.2	6.5	26.4	33.6
2.7	23.2	10.2	6.5	26.4	33.6
3.0	23.3	10.2	6.6	26.3	33.6
3.3	23.3	10.3	6.6	26.2	33.6
3.7	23.3	10.3	6.6	26.2	33.6
4.0	23.3	10.3	6.6	26.2	33.5
4.3	23.3	10.3	6.6	26.2	33.5
4.7	23.3	10.4	6.6	26.2	33.5
5.0	23.4	10.4	6.7	26.0	33.5

Table C-8 Concentration of gases in effluent for the evaluation of catalyst selection raw data: BF-4-0.25(MgNiCo)

Time (h)	N_2 (%)	CH_4 (%)	CO_2 (%)	H_2 (%)	CO (%)
0	22.4	9.2	6.0	28.3	34.0
0.3	22.4	9.2	6.0	28.3	34.0
0.7	22.5	9.3	6.1	28.2	34.0
1.0	22.5	9.3	6.1	28.1	33.9
1.3	22.5	9.4	6.1	28.1	33.9
1.7	22.6	9.4	6.1	28.0	34.0
2.0	22.5	9.4	6.1	28.1	33.8
2.3	22.6	9.4	6.1	28.0	33.9
2.7	22.6	9.5	6.2	27.9	33.8
3.0	22.6	9.5	6.2	27.9	33.8
3.3	22.6	9.5	6.2	27.8	33.8
3.7	22.6	9.5	6.2	27.9	33.8
4.0	22.6	9.6	6.2	27.9	33.7
4.3	22.7	9.6	6.2	27.7	33.8
4.7	22.7	9.6	6.2	27.7	33.7
5.0	22.7	9.6	6.2	27.8	33.7

Table C-9 Concentration of gases in effluent for the evaluation of catalyst selection raw data: BF-4-0.25(MgNiCo)-C

Time (h)	N_2 (%)	CH_4 (%)	CO_2 (%)	H_2 (%)	CO (%)
0	22.1	7.5	5.3	29.6	35.4
0.3	22.1	7.5	5.3	29.7	35.4
0.7	22.1	7.5	5.3	29.8	35.3
1.0	22.2	7.5	5.3	29.7	35.4
1.3	22.1	7.5	5.3	29.7	35.3
1.7	22.1	7.5	5.3	29.8	35.3
2.0	22.2	7.6	5.3	29.7	35.3
2.3	22.2	7.6	5.3	29.6	35.3
2.7	22.2	7.6	5.3	29.6	35.3
3.0	22.1	7.6	5.3	29.8	35.2
3.3	22.2	7.6	5.3	29.6	35.2
3.7	22.2	7.6	5.3	29.7	35.2
4.0	22.2	7.7	5.3	29.6	35.2
4.3	22.2	7.7	5.3	29.6	35.2
4.7	22.2	7.7	5.3	29.5	35.2
5.0	22.2	7.7	5.4	29.4	35.3

Table C-10 Concentration of gases in effluent for the evaluation of effect of impregnation steps on catalyst reactivity raw data: BF-1-(MgNiCo)

Time (h)	N_2 (%)	CH_4 (%)	CO_2 (%)	H_2 (%)	CO (%)
1	23.8	11.6	7.2	25.0	32.4
20	26.6	16.6	9.9	18.9	28.1
40	33.6	29.6	19.5	7.1	10.3

Table C-11 Concentration of gases in effluent for the evaluation of Effect of impregnation steps on catalyst reactivity raw data: BF-4-0.25(MgNiCo)

Time (h)	N_2 (%)	CH_4 (%)	CO_2 (%)	H_2 (%)	CO (%)
1	23.1	10.1	6.5	26.6	33.8
20	24.0	11.4	7.1	24.9	32.7
40	25.1	13.3	8.1	22.4	31.0
60	26.9	16.4	9.8	18.5	28.3
80	29.3	20.5	12.3	14.2	23.7

Table C-12 Concentration of gases in effluent for the evaluation of effect of impregnation steps on catalyst reactivity raw data: BF-4-0.25(MgNiCo)

Time (h)	N_2 (%)	CH_4 (%)	CO_2 (%)	H_2 (%)	CO (%)
1	22.4	9.2	6.0	28.3	34.0
20	23.0	10.2	6.5	27.0	33.3
40	24.1	11.8	7.4	24.5	32.3
60	24.4	12.1	7.4	23.8	32.3
80	24.8	12.6	7.7	23.0	31.9
100	25.2	13.4	8.2	22.1	31.1
120	25.4	13.9	8.5	21.9	30.3
140	25.7	14.5	9.0	21.2	29.6
160	26.2	15.3	9.4	20.3	28.8
180	26.4	15.5	9.5	20.0	28.5

Table C-13 Concentration of gases in effluent for the evaluation of effect of calcination steps on catalyst reactivity raw data: BF-4-0.25(MgNiCo)-C

Time (h)	N_2 (%)	CH_4 (%)	CO_2 (%)	H_2 (%)	CO (%)
1	22.1	7.5	5.3	29.6	35.4
20	22.7	8.7	5.8	28.3	34.5
40	23.3	9.6	6.2	27.0	34.0
60	23.7	10.1	6.5	25.9	33.7
80	23.9	10.4	6.6	25.4	33.6
100	23.9	10.6	6.7	25.5	33.3
120	24.1	10.9	7.0	25.2	32.8
140	24.2	11.1	7.1	25.0	32.7
160	24.6	11.9	7.6	24.1	31.8
180	24.8	12.2	7.8	23.9	31.4

Table C-14 Concentration of gases in effluent for the evaluation of effect of calcination steps on catalyst reactivity raw data: BF-4-0.25(MgNiCo)

Time (h)	N_2 (%)	CH_4 (%)	CO_2 (%)	H_2 (%)	CO (%)
1	22.4	9.2	6.0	28.3	34.0
20	23.0	10.2	6.5	27.0	33.3
40	24.1	11.8	7.4	24.5	32.3
60	24.4	12.1	7.4	23.8	32.3
80	24.8	12.6	7.7	23.0	31.9
100	25.2	13.4	8.2	22.1	31.1
120	25.4	13.9	8.5	21.9	30.3
140	25.7	14.5	9.0	21.2	29.6
160	26.2	15.3	9.4	20.3	28.8
180	26.4	15.5	9.5	20.0	28.5